Conversion of Carbohydrates in Low Melting Mixtures

and

Melanoma Inhibitory Activity (MIA) Protein Inhibitors for the Treatment of Malignant Melanoma

Dissertation

Zur Erlangung des Doktorgrades der Naturwissenschaften
(Dr. rer. nat.)
an der Naturwissenschaftlichen Fakultät IV
- Chemie und Pharmazie -
der Universität Regensburg

vorgelegt von
Carolin Ruß
aus Schweinfurt

2012

The experimental part of this work was carried out between June 2008 and March 2012 under the supervision of Prof. Dr. Burkhard König at the Institute of Organic Chemistry, University of Regensburg.

The PhD thesis was submitted on: 11.06.2012

The colloquium took place on: 13.07.2012

Board of Examiners:

Prof. Dr. Bernhard Dick	(chairman)
Prof. Dr. Burkhard König	(1st referee)
Prof. Dr. Achim Göpferich	(2nd referee)
Prof. Dr. Joachim Wegener	(examiner)

Meiner Familie

in Liebe und Dankbarkeit

"I REALIZED THAT THE PURPOSE OF WRITING IS TO INFLATE WEAK IDEAS, OBSCURE POOR REASONING, AND INHIBIT CLARITY. WITH A LITTLE PRACTICE, WRITING CAN BE AN INTIMIDATING AND IMPENETRABLE FOG!"

(BILL WATERSON, *CALVIN & HOBBES*)

Contents

I. CONVERSION OF CARBOHYDRATES IN LOW MELTING MIXTURES

1. Low melting mixtures – the “greener” ionic liquids?

There is pressing need to replace hazardous and harmful solvents with “green” or “sustainable” media. Natural compounds have recently been used to produce deep eutectic solvents, sugar melts, or ionic liquids. This review presents physicochemical data of these reaction media and highlights recent advances in their use in organic synthesis and biotransformations.

C. Ruß, B. König, *Green Chem.*, **2012**, *submitted*.

Introduction

What makes a solvent green? The prevalent opinion is that the ideal green solvent is safe for both the human beings and the environment and its use and manufacture are sustainable.[1, 2]

Ionic liquids (ILs) are an intensively investigated class of alternative reaction media. They are defined as salts with a melting point below the boiling temperature of water (100 °C).[3] From all of their exceptional properties like low flammability, stability against air and moisture, excellent solvation potential, low water content, chemical and thermal stability, high heat capacity, density and conductivity, their negligibly low vapour pressure is the most prominent feature why they are considered as green. However, one property still in question - their impact on the environment – is intensively discussed.[4, 5] Ideally, the components of a green solvent expose a low acute toxicity and are rapidly degraded in the environment. The current consensus is that ionic liquids cannot be generalised as either green or toxic, but that their environmental impact is strongly dependent on the kind of cation and anion used to produce the IL.[5] For this reason, reaction media entirely composed of biomaterials have been developed which unite the outstanding physicochemical properties of ILs with the advantage of biodegradable and non-toxic starting materials. Additional advantages over ILs are their facile preparation and the use of readily available and inexpensive starting materials.

This review will focus on the application of these solvents made from renewable resources in organic syntheses. Some examples of biotransformations will be portrayed and also the physicochemical properties will be highlighted. As this is a fast growing and widespread field, we are not trying to be comprehensive, but try to give a general trend of this research area.

Classification of low melting mixtures and their synthesis

A central role in the class of "bio-based" solvents plays (2-hydroxyethyl)trimethylammonium chloride, or simply choline chloride (ChCl). The quaternary ammonium salt choline is considered as a member of vitamin B family, supports a multitude of metabolic processes, and serves as a dietary supplement of

animal feeds.[6] It is commercially produced by a simple gas phase reaction between trimethylamine, ethyleneoxide, and HCl.[6]

The foundation for solvents based on renewable resources was laid in 2003 when Abbott *et al*. reported on low melting mixtures of urea and ChCl which are liquid at room temperature, terming them "deep eutectic solvents" (DES).[7] A DES is defined as a mixture of hydrogen bond donor (HBD) systems with simple halide salts which produce liquids.[8] Their physicochemical properties resemble those of ionic liquids. Abbott's fundamental work inspired other researchers to exploit the unusual properties of this system. In the last years, different (uncharged) hydrogen bond donors of natural and synthetic origin were used in combination with choline chloride.[8-12] As in the case of ILs, the melting point of the mixtures is not predictable, but some general trends can be derived. Abbott hypothesised that the melting point depression is caused by charge delocalisation due to hydrogen bonding between the halide anion and the hydrogen bond donor.[7] In ionic liquids, the melting point is dependent on the charge distribution in the ions: the melting points tend to be lower when the charge is strongly delocalised or when the cations and / or anions are asymmetrical.[3] A similar effect was observed for melts with quaternary ammonium salts: with increasing asymmetry of the cation, the melting point decreases.[7] Furthermore, the freezing points are influenced by the hydrogen bond strength of the different negatively charged counterions of the choline salts in urea mixtures.[7] The preparation of deep eutectic solvents is very simple: the mixed components are stirred under heating (~ 80 °C) until a homogeneous, clear liquid has been formed.[8, 12]

The exchange of the halide anion for organic anions like carboxylates was a recent advancement to obtain ionic liquids based completely on biomaterials. This concept was firstly introduced by Nockemann *et al.* in 2007.[13] They synthesised ionic liquids by a metathesis reaction of choline chloride and the sodium salts of the non-nutritive artificial sweeteners acesulfame and saccharin, followed by purification using ion-exchange chromatography. Also in 2007, Fukaya *et al.* developed room temperature ionic liquids composed of biomaterials, and termed them "bio ionic liquids".[14] These so-called "bio-ILs" were prepared by two-step anion exchange reactions of choline hydroxide with different carboxylates. Simple alkanoic acids were used as counterions

by Petkovic *et al.* in 2009.[15] They prepared ionic liquids by titration of cholinium hydrogen carbonate with the corresponding acid. Recently, Liu *et al.* introduced room temperature ionic liquids using amino acids as anions and choline as cation.[16] They also used choline hydroxide as starting material which was added dropwise to an aqueous solution of eighteen different amino acids.

Sugar melts, low melting eutectic mixtures of sugar, urea, and salt, were described by Imperato *et al*.[17-19] The stable melts, which consist merely of neutral components, are prepared by heating up the grinded compounds until a clear liquid has formed. The obtained eutectic mixtures exhibit melting points above 60 °C. Even simpler eutectic mixtures termed "natural deep eutectic solvents" (NADES) were published by Choi *et al*. in 2011.[20] They presented 30 defined combinations of ChCl, organic acids, amino acids and sugars giving viscous liquids at room temperature. These media might play a role as water-free natural ionic liquids in cells, *e.g*. for dissolving metabolites or as solvent for biochemical reactions.

A) Overview of the physicochemical properties

1.1 Used components and melting points

Similar to ILs, the melting points of eutectic mixtures are not yet predictable. The liquid character of the salt mixtures is attributed to a reduction of Coulomb forces. They decrease with a large volume (or buried charge) and asymmetric charge distribution of the molecular ions. The melting points (T_m), freezing points (T_f) or glass transition temperatures (T_g) are summarised below (Table 1-9). In those cases, when two different melting points were determined, both values are given. Interestingly, the melting points of DES and ILs made from the same components, *e.g.* benzoic acid (Table 1, entry 3) and benzoate (Table 7, entry 17) or tartaric acid (Table 2, entry 4) and H-tartrate (Table 7, entry 16) deviate strongly from each other; mostly, the melting points of the DESs are lower than the melting points of the ILs.

1.1.1 Deep eutectic solvents based on choline chloride

Table 1 Deep eutectic solvents based on choline chloride (ChCl) and monocarboxylic acids. HBD: hydrogen bond donor, ChCl : HBD ratio in (mol:mol).

Entry	Compound	Structure	ChCl : HBD ratio	T (°C)		Ref.
1	Valeric acid	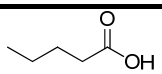	1:2	T_f	22	21
2	Levulinic acid	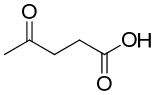	1:2	T_m	Liquid at rt	12
3	Benzoic acid	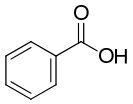	1:2	T_f	95	9
4	Phenylacetic acid	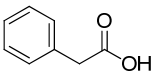	1:2	T_f	25	9
5	Mandelic acid	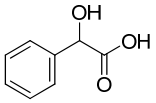	1:2	T_f	33	21
6	4-Hydroxybenzoic acid	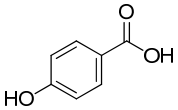	2:1	T_m	87	12
			1:2	T_f	97	21
7	Gallic acid	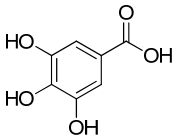	2:1	T_m	77	12
8	*trans*-Cinnamic acid	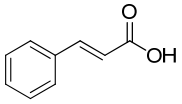	1:1	T_m	93	12
				T_f	101	21
9	*p*-Coumaric acid	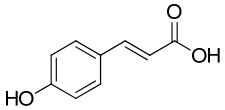	2:1	T_m	67	12
10	Caffeic acid	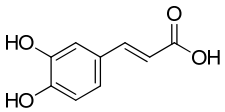	2:1	T_m	67	12

Table 2 Deep eutectic solvents based on choline chloride and dicarboxylic acids.

HBD: hydrogen bond donor, ChCl : HBD ratio in (mol:mol).

Entry	Compound	Structure	ChCl : HBD ratio	T (°C)	Ref.
1	Oxalic acid	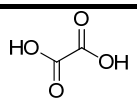	1:1	T_f 34	9
2	Malonic acid	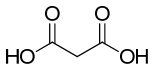	1:1	T_f 10	9
3	Glutamic acid	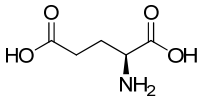	1:2	T_f 13	21
4	L-(+) Tartaric acid	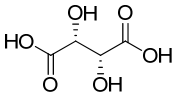	2:1	T_m 47	12
5	Itaconic acid	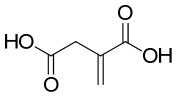	1:1 2:1	T_m 57	12
6	Succinic acid	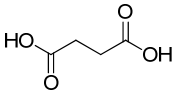	1:1	T_f 71	9
7	Adipic acid	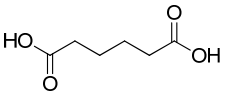	1:1	T_f 85	9
8	Suberic acid	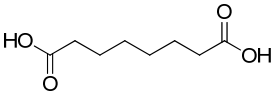	1:1	T_m 93	12

Table 3 Deep eutectic solvents based on choline chloride and tricarboxylic acids.

HBD: hydrogen bond donor, ChCl : HBD ratio in (mol:mol).

Entry	Compound	Structure	ChCl : HBD ratio	T_f (°C)	Ref.
1	Citric acid	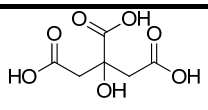	2:1	69	9
2	Tricarballylic acid	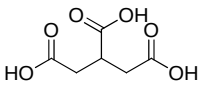	2:1	90	9

Table 4 Deep eutectic solvents based on choline chloride and alcohols.

HBD: hydrogen bond donor, ChCl : HBD ratio in (mol:mol).

Entry	Compound	Structure	ChCl : HBD ratio		T (°C)	Ref.
1	Glycerol	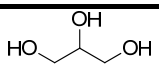	1:2	T_f	-40	[8]
2	Ethylene glycol	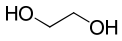	1:2	T_f	-20	[21]
3	Mannitol	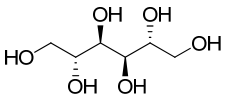	1:1	T_f	108	[21]
4	D-Fructose	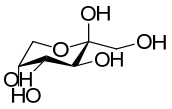	1:2	T_f	5	[21]
5	D-Glucose	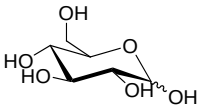	1:2	T_f	14	[21]
6	Vanilline	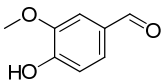	1:2	T_f	17	[21]
7	Xylitol	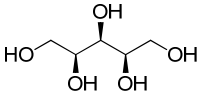	1:1	T_m	Liquid at rt	[12]
8	D-Sorbitol	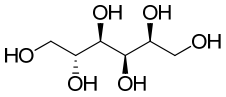	1:1	T_m	Liquid at rt	[12]
9	D-Isosorbide	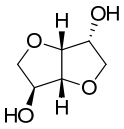	1:2	T_m	Liquid at rt	[12]

Table 5 Deep eutectic solvents based on choline chloride and urea derivatives.

HBD: hydrogen bond donor, ChCl : HBD ratio in (mol:mol).

Entry	Compound	Structure	ChCl : HBD ratio	T_f (°C)	Ref.
1	Urea	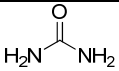	1:2	12	[7]
2	1,3-Dimethylurea (DMU)	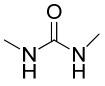	1:2	70	[7]

Table 6 Other natural ammonium salts used in eutectic mixtures.

Entry	Ammonium salt (AS)	Structure	HBD	Ratio (AS:HBD)	T_m	Ref.
1	L-Carnitine	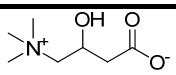	Urea	2:3 (wt:wt)	74	[22]
2	Betaine hydrochloride	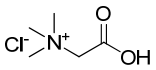	Urea	15:85 (mol:mol)	27	[23]
3	Betaine hydrochloride	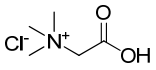	Glycerol		rt	[24]

1.1.2 Ionic liquids using choline as cation and natural products as counterions

Table 7 Ionic liquids based on the cholinium cation and carboxylates (entry 1-17) and artificial sweeteners (entry 18 and 19). Expectedly, the molar ratio of anion to cation is 1:1.

[a] n. d. not detected

Entry	Compound	Structure	T_m (°C)	T_g (°C)	Ref.
1	Acetate		51	n. d. [a]	[14]
			80	n. d. [a]	[15]
2	Propionate		n. d.[a]	-74	[14], [15]
3	Butanoate	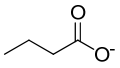	45		[15]
4	Valeric acid	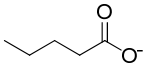	31		[15]
5	Hexanoate	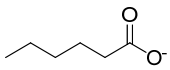	52		[15]
6	Octanoate	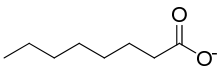	26		[15]
7	Decanoate	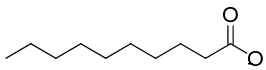	50		[15]
8	Isobutyrate		35		[15]
9	Pivalate		57		[15]
10	Glycolate	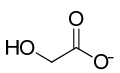	38	-67	[14]
11	Tiglate	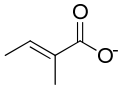	n. d.[a]	-62	[14]

12	H-Succinate	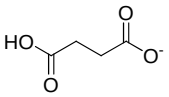	n. d.[a]	-52	[14]
13	H-Maleate	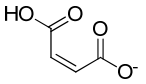	25	-72	[14]
14	H-Fumarate	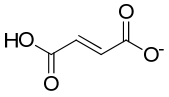	80	n. d.[a]	[14]
15	H-Malate	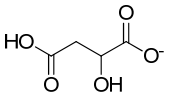	99	-40	[14]
16	H-Tartrate	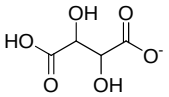	131	-6	[14]
17	Benzoate	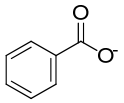	47	-51	[14]
18	Acesulfamate	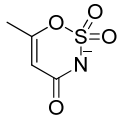	69	n. d.[a]	[13]
19	Saccharinate	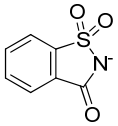	25	n. d.[a]	[13]

Table 8 Ionic liquids based on the cholinium cation and amino acids as counterions (molar ratio 1:1).

Entry	Counterion	T_g (°C)	Ref.	Entry	Counterion	T_g (°C)	Ref.
1	Glycine	-61	[16]	10	Tryptophane	-12	[16]
2	Alanine	-56	[16]	11	Proline	-44	[16]
3	Serine	-55	[16]	12	Aspartic acid	-22	[16]
4	Threonine	-39	[16]	13	Glutamic acid	-18	[16]
5	Valine	-74	[16]	14	Asparagine	-14	[16]
6	Leucine	-47	[16]	15	Glutamine	-40	[16]
7	Isoleucine	-47	[16]	16	Lysine	-48	[16]
8	Methionine	-61	[16]	17	Histidine	-40	[16]
9	Phenylalanine	-60	[16]	18	Arginine	-10	[16]

1.1.3 Low melting sugar mixtures

Table 9 Melting points and composition of low melting sugar mixtures.

DMU: 1,3-dimethylurea; sugar: urea : salt ratio (weight %).

Entry	Carbohydrate	Structure	Urea	Salt	Ratio[a]	T_m	Ref.
1	Citric acid	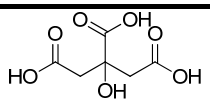	DMU	-	40:60	65	[18]
2	Sorbitol	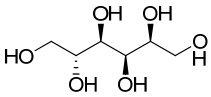	DMU	NH_4Cl	70:20:10	67	[18]
3	Maltose	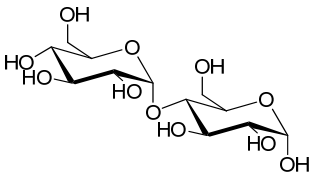	DMU	NH_4Cl	50:40:10	84	[18]
4	Mannitol	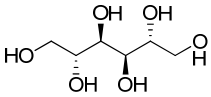	DMU	NH_4Cl	50:40:10	89	[18]
5	Lactose	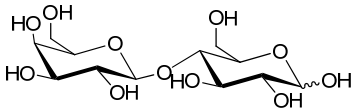	DMU	NH_4Cl	50:40:10	88	[18]
6	Mannose	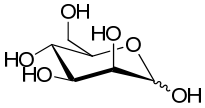	DMU	-	30:70	75	[18]
7	Fructose	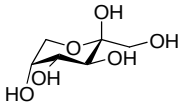	DMU	-	40:60	80	[18]
8	Fructose	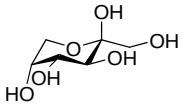	Urea	NaCl	70:20:10	73	[18]
9	Fructose	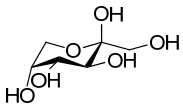	Urea	-	40:60	65	[17]
10	Glucose	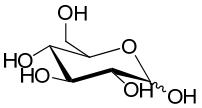	Urea	NaCl	60:30:10	78	[18]
11	Glucose	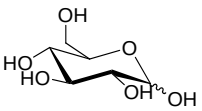	Urea	$CaCl_2$	50:40:10	75	[17]
12	Glucose	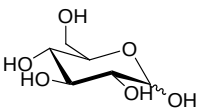		-	50:50	75	[25]

13	Galactose	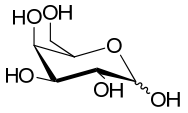	Urea	NH_4Cl	30:70:10	80	25
14	*N*-Acetyl-D-glucosamin	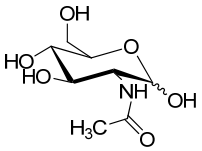	Urea	NH_4Cl	30:70:10	80	25
15	L-Rhamnose	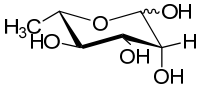	Urea	NH_4Cl	30:70:10	80	25
16	2-Deoxy- D-glucose	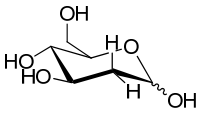	Urea	NH_4Cl	30:70:10	80	25

1.2 Polarity

Solvent polarity is an important factor in chemistry as it can significantly influence the course of the reaction.[26] Different scales exist to estimate the polarity of a solvent. One of the most commonly used empirical polarity scales is the $E_T(30)$ scale, introduced by Reichardt.[27] The polarity is calculated from the wavelength (nm) of maximum absorbance of the standard solvatochromic betaine dye no. 30 (Reichardt's dye) in solvents of different polarity at room temperature (25 °C) and normal pressure (1 bar) using the eqn. (1). As $E_T(30)$ is rather sensitive to hydrogen bonding solvents, Nile red or $E_T(33)$ are used instead.[27] Nile red data is here reported as $E_T(NR)$, calculated from eqn. (2).

$$E_T(30) \text{ / kcal mol}^{-1} = hc\nu_{max}N_A = 28\,591 / \lambda_{max,\,30} \quad (1)$$

$$E_T(NR) \text{ / kcal mol}^{-1} = hc\nu_{max}N_A = 28\,591 / \lambda_{max,\,NR} \quad (2)$$

(h= Planck's constant, c= speed of light,
ν_{max}= wave number of absorption maximum,
N_A= Avogadro's constant)

A normalised scale (E_T^N) was introduced to obtain dimensionless values, using water (E_T^N = 1.00) and tetramethylsilane (E_T^N = 0.00) as reference solvents, resulting in eqn. (3).

$$E_T^N = \frac{[E_T(solvent) - E_T(TMS)]}{[E_T(water) - E_T(TMS)]} \quad (3)$$

Table 10 summarises $E_T(30)$, E_T^N, and $E_T(NR)$ values of some common molecular solvents, ILs, sugar melts, and DES.

Table 10 Overview of determined $E_T(30)$, E_T^N, and $E_T(NR)$ (for the dye Nile Red) values of some common molecular solvents, ILs, sugar melts, and DES.

[Emim]: 1-Ethyl-3-methylimidazolium, [Bmim]: 1-butyl-3-methylimidazolium.

Solvent	$E_T(30)$/kcal mol^{-1}	E_T^N	$E_T(NR)$	Ref.
Water	63.1	1.000	48.21	[18], [27]
Glycerol	57.0	0.812	-	[27]
Ethylene glycol	56.1	0.784	50.6	[18]
	56.3	0.790	-	[27]
Ethanol	51.9	0.654	-	[27]
2-Propanol	48.5	0.549	52.94	[18]
	48.4	0.546	-	[27]
Dimethylsulfoxide	45.0	0.441	52.07	[18]
	45.1	0.444	-	[27]
Dimethylformamide	43.6	0.398	52.84	[18]
	43.2	0.386	-	[27]
[Bmim][acetate]	50.5	0.611	-	[28]
[Bmim][propionate]	49.1	0.568	-	[28]
[Bmim][H-maleate]	47.6	0.522	-	[28]
Citric acid-DMU	70.8	1.238	49.72	[18]
Sorbitol-DMU-NH_4Cl	68.1	1.154	50.16	[18]
Maltose-DMU-NH_4Cl	67.8	1.145	50.60	[18]
Fructose-urea-NaCl	66.5	1.105	52.55	[18]
Mannitol-DMU-NH_4Cl	65.8	1.083	52.94	[18]
Glucose-urea-NaCl	64.4	1.040	50.78	[18]
Lactose-DMU-NH_4Cl	53.9	0.716	52.55	[18]
Mannose-DMU	53.9	0.716	51.79	[18]
Carnitine-urea	-	-	49.89	[22]
Glycerol-ChCl	58.58	0.86	-	[8]
	-	0.84		[29]
Ethylene glycol-ChCl	-	0.80	-	[29]
Urea-ChCl	-	0.84	-	[29]

The polarities of the sugar melts (E_T(NR) = 50-52) and the DES (E_T^N = 0.80-0.86) are comparable to those of short chain alcohols (*e.g.* ethylene glycol, 2-propanol) and other polar, aprotic solvents (*e.g.* DMSO, DMF) (E_T(NR) = 51-53 kcal mol^{-1}, E_T^N = 0.39-0.81)., and follow a similar trend as common ionic liquids.[30]

1.3 Viscosity

Viscosity describes the internal friction of a moving fluid or, in other words, the resistance of a substance to flow. Usually, the dynamic viscosity η for ILs are reported in centipoise (cP) which corresponds to milli pascal-second (mPa s) in SI units. While viscosities of ILs range from around 10 cP to values beyond 500 cP,[3] the viscosities of the low melting mixtures shown in Table 11, range from 50 to 5000 cP for the mixtures of choline chloride with carboxylic acids,[9] from 650 to 8500 cP for the ionic liquids of choline with carboxylates,[14] and from 121 to 5640 cP for choline-amino acid liquids and are higher than those of ILs.[16] In comparison with the viscosities of different common solvents like dichloromethane (0.413 cP), DMSO (1.987 cP), ethylene glycol (16.1 cP), and glycerol (934 cP), the viscosity of low melting mixtures is up to three orders of magnitude higher. Viscosity has a remarkable influence on the course of a chemical reaction: high viscosities can decrease the reaction rate in case of diffusion-controlled chemical reactions. In engineering, low viscosities are preferred as operational costs for *e.g.* stirring, mixing, and pumping can be reduced in practice.

All listed low melting mixtures display rather high viscosities. As in ionic liquids, the viscosity in the low melting mixtures increases with increasing size or molecular weight of the anion. Furthermore, strong intermolecular interactions promote high viscosities.

Table 11 Viscosities of some common organic solvents, regular ionic liquids, "bio ILs", and sugar-urea-melts. Ionic species are enclosed in brackets; amino acids were abbreviated using the three letter code. [Ch]: choline, [Emim]: 1-Ethyl-3-methylimidazolium, [Bmim]: 1-butyl-3-methylimidazolium, [BMmorf]: 4-benzyl-4-methylmorpholinium.

Solvent	η (cP) at rt	Ref.
CH_2Cl_2	0.413	31
MeOH	0.544	31
Water	0.890	31
DMSO	1.987	31
Ethylene glycol	16.1	31
Glycerol	934	31
[Ch][maleate]	650	14
[BMmorf][maleate]	11.54	32
[Emim] [maleate]	383	14
[Ch][saccharinate]	328 (at 70 °C)	13
[Ch][acesulfamate]	1072	13
[Ch][glu]	2308	16
[Bmim][glu]	83	33
[Ch][gly]	121	16
[Bmim][gly]	67	33
[Emim][gly]	61	34
[Ch][ser]	402	16
[Emim][ser]	411	34
[Ch][pro]	500	16
[Emim][pro]	426	34
Fructose-DMU	35.3	35
Citric acid-DMU	289.6	35
Maltose-DMU-NH_4Cl	1732.7	35

1.4 Density

Typical values for the density of ILs range from 1.12 to 2.4 g cm^{-1} and are therefore higher than those of organic solvents and water.[3] The values of ILs are comparable to the densities of choline based ionic liquids and deep eutectic solvents (Table 12).

Table 12 Densities of different choline based DES and ILs.

Solvent	Molar ratio	Density ϱ [g cm^{-3}]	Ref.
[Ch][propionate]	1:1	1.23	[36]
[Ch][tiglate]	1:1	1.23	[36]
[Ch][H-maleate]	1:1	1.38	[36]
[Ch][saccharinate]	1:1	1.383	[13]
[Ch][acesulfamate]	1:1	1.284	[13]
ChCl-urea	1:2	1.25	[10, 37]
ChCl-ethylene glycol	1:2	1.12	[37]
ChCl-glycerol	1:2	1.18	[37]
ChCl-malonic acid	1:1	1.25	[37]

1.5 Molar heat capacities and conductivity

Molar heat capacities C_p of DESs are important to assess their potential for heat transfer applications. They were measured for pure choline chloride melts with urea, ethylene glycol and glycerol in the temperature range from 303.2 to 353.2 K and were determined to be between 181 and 254 J mol^{-1} K^{-1}.[38] Furthermore, C_p values increase with increasing temperature and increasing mole fraction of DES. Similar behaviour has previously been observed for other ionic liquids.[39]

High conductivities, shown in Table 13, were observed in DES (comparable to ionic liquids)[40, 41] and DES are therefore a highly investigated medium for electrochemical applications.[42-59]

Table 13 Conductivity of some DES and ILs

Solvent system	Conductivity σ (mS cm^{-1})	Ref.
ChCl-carboxylic acids	0.1 to 10	9
ChCl-urea	0.199	10
ChCl-ethylenglycol	7.61	11
ChCl-glycerol	1.047	11
[Ch][saccharinate]	0.21	13
[Ch][acesulfamate]	0.45	13

B) Reactions in low melting mixtures

Deep eutectic solvents and sweet eutectic mixtures are an environmentally benign alternative to hazardous (organic) solvents and might replace them in part. Their application in organic synthesis has notable advantages. As most of the components are soluble in water, addition of water to the reaction mixture dissolves the reaction medium. The organic products either form a separate layer or precipitate and can be filtered off. Furthermore, solvent and catalyst may be reused for another reaction cycle.

2.1 Reactions in DES

A variety of organic reactions were performed in deep eutectics solvents, mainly focused on the choline chloride-urea (1:2) eutectic mixture (Figure 1).

In 2010, high yields and high purities were reported for the bromination of 1-aminoanthra-9,10-quinone with molecular bromine in short reaction times.[60] Moreover, the reaction time and temperature of the Perkin reaction can be remarkably reduced without the use of a catalyst, while simultaneously improving the yields.[61] Coumarins were synthesized *via* a Knoevenagel condensation in short reaction times and high yields starting from salicyl aldehydes and active methylene compounds.[62] Recently, it was shown that the reduction of epoxides and carbonyl compounds with sodium borohydride can be conducted regio- and chemoselectively in good to excellent yields.[63]

Bromination[60]

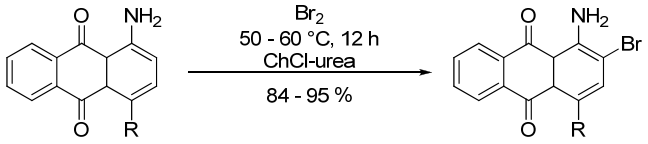

Perkin reaction[61]

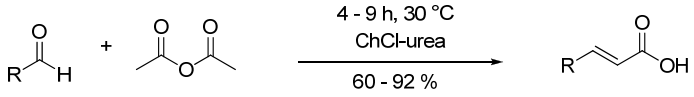

Knoevenagel condensation[62]

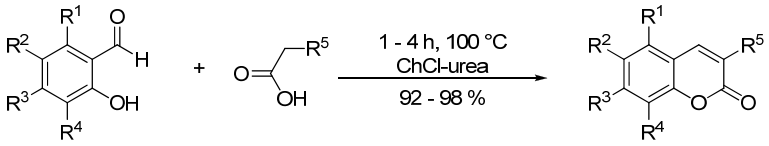

Reduction of epoxides and carbonyl compounds[63]

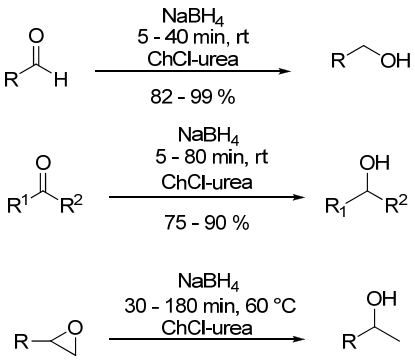

Figure 1 Some organic reactions in DES (Choline chloride (ChCl)-urea mixtures).

2.2 Reactions in low melting (carbohydrate) mixtures

"Sweet" low melting mixtures based on simple sugars or sugar alcohols and urea (derivatives) were introduced as reaction media for a variety of organic C-C-coupling reactions (Figure 2). The Diels-Alder reaction of cyclopentadiene with methyl acrylate was performed in high yields and *endo*/*exo* ratios comparable to those using ionic liquids and *sc*CO_2.[17, 64] Metal-catalysed reactions like Suzuki,[18, 22] Heck,[22] and Sonogashira reaction,[22] and the Huisgen 1,3-dipolar cycloaddition[22] were also successfully conducted in high yields. By exchanging the sugar melts by a carnitine-urea melt, reduced yields in the Heck reaction, a lower *endo*/*exo* ratio in the Diels-Alder reaction, but similar yields in the Huisgen 1,3-dipolar cycloaddition were observed.[22] Although the melts consist of chiral components, no asymmetric induction was observed in the catalytic hydrogenation of acetamido α-cinnamate.[18] Quinazoline

derivatives were synthesised in high yields *via* a one-pot three-component coupling reaction of 2-aminoaryl ketones, aldehydes, and ammonium acetate using maltose-DMU-NH_4Cl.[65]

The use of the sweet solutions is still limited due to their relatively high melting points. Another drawback of the melts is that their components are not chemically inert. However, a virtue can be made out of necessity. The reactivity of the sugars was utilised to convert efficiently carbohydrates into different glycosyl ureas.[25] Furthermore, 5-hydroxymethylfurfural, an important organic intermediate, was produced in such melts,[66, 67] as well as the glucosylated derivative 5-(α-D-glucosyloxymethyl)furfural (not shown below).[68]

Inspired by these investigations, low melting mixtures of L-(+)-tartaric acid and urea derivatives were used to synthesise racemic dihydropyrimidinones *via* a Biginelli reaction. Remarkably, the melt fulfils the triple role of being solvent, catalyst, and reactant.[69]

Diels-Alder[17, 22]

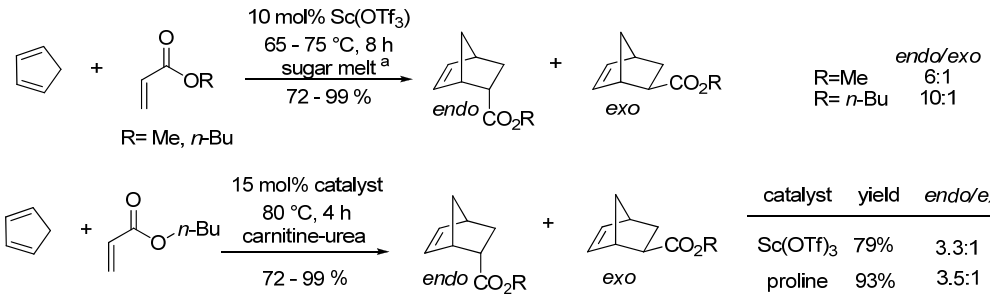

Suzuki coupling[18]

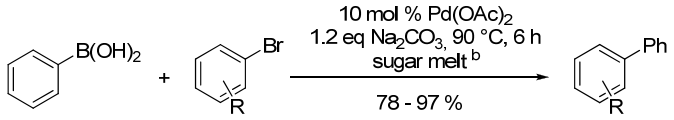

Heck reaction[22]

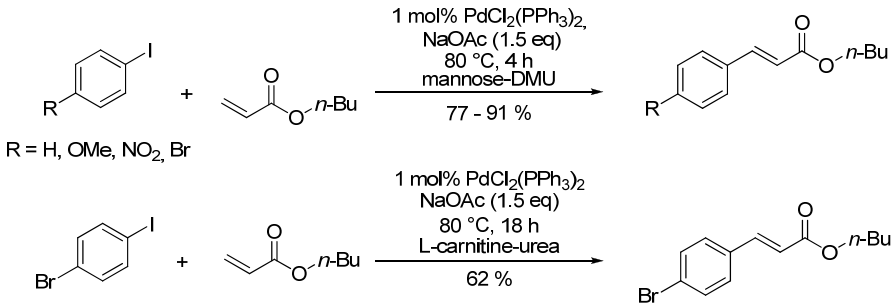

Sonogashira reaction[22]

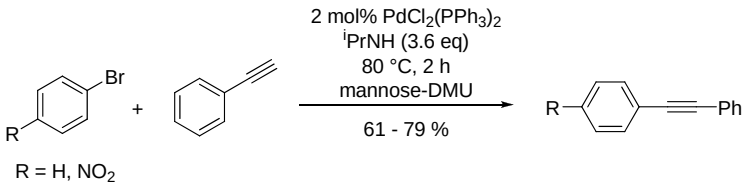

Huisgen 1,3 dipolar reaction[22]

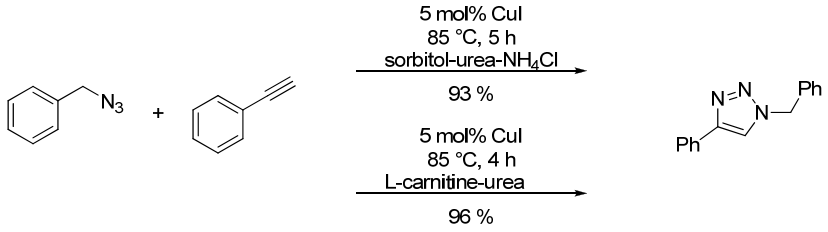

Catalytic hydrogenation[18]

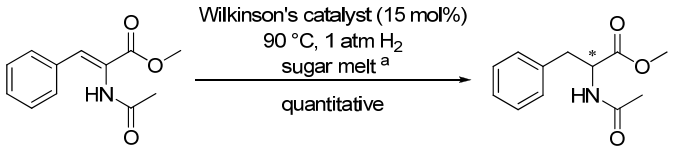

Synthesis of glycosylureas[25]

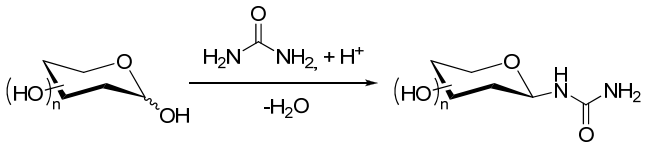

Catalyst free quinazoline multicomponent synthesis[65]

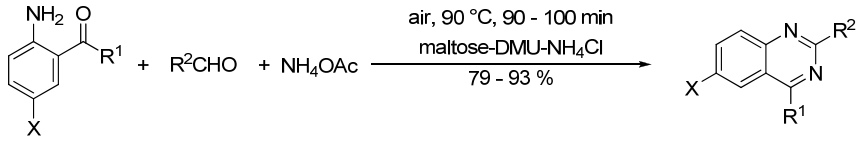

Biginelli reaction[69]

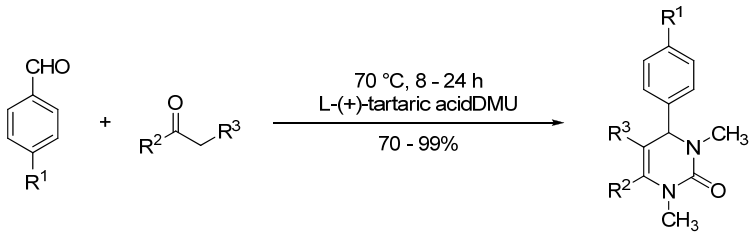

Figure 2 Organic reactions in low melting carbohydrate mixtures.

[a] Carbohydrate melts used as reaction media: fructose-DMU (70:30), maltose-DMU-NH_4Cl (50:40:10), lactose-DMU-NH_4Cl (60:30:10), mannitol-DMU-NH_4Cl (50:40:10), glucose-urea-$CaCl_2$ (50:40:10), sorbitol-DMU-NH_4Cl (70:20:10), citric acid-DMU (40:60).
[b] Carbohydrate melts used as solvent: fructose-urea-NaCl (70:20:10), maltose-DMU-NH_4Cl (50:40:10), mannose-DMU (30:70), lactose-DMU-NH_4Cl (60:30:10), mannitol-DMU-NH_4Cl (5:4:1), sorbitol-DMU-NH_4Cl (7:2:1), glucose-urea-NH_4Cl (6:3:1).

2.3 Biocatalytic reactions

Enzymes catalyse a broad spectrum of organic reactions like hydrolyses, oxidations, reductions, addition-elimination reactions, halogenations etc. chemo-, regio- and enantioselectively.[70] Their natural medium is water. However, hydrophobic reactants and products are sparely soluble in water. Although enzymes display the highest catalytic activity in water, the biocatalysts can work in non-aqueous media, such as organic solvents or ionic liquids. The most prominent advantage of non-aqueous media is that thermodynamic equilibria can be shifted from hydrolysis to synthesis. Accordingly, hydrolases can be used to form ester or amide bonds. Furthermore, side reactions, like hydrolysis or protein degradation, which often occur in aqueous solutions, might be suppressed in non-aqueous media. ILs have been applied as non-aqueous media in biotransformations and the field has recently been summarised by several reviews.[71-73] Enzymes generally show comparable or higher activities in ionic liquids than in conventional organic solvents and in some cases, they also exhibit enhanced thermal and operational stabilities and give higher regio- or enantioselectivities.[72] It is believed that enzymes can retain a residual hydration shell in non-polar solvents which stabilises the native fold.[74]

Due to their similar physicochemical properties, it was thus evident to investigate deep eutectic solvents as reaction media for biotransformations. Gorke *et al*. was the first to use enzymes in DES and to assess the activity of different hydrolases in choline chloride-urea mixtures.[29] Despite high concentrations of urea, which is a strong hydrogen bond donor and denatures proteins, and the presence of halides, which might inactivate or inhibit the proteins, the enzymes showed good catalytic activity. Furthermore, the conversion of styrene oxide to the corresponding diol with epoxide hydrolase was 20-fold enhanced using choline chloride-urea as co-solvent (Figure 3).[29] The hydrolysis of epoxides has been studied in more detail by Lindberg *et al*.[75] They investigated the effect of different DES (1:2 mixture of ChCl with urea, ethylene glycol, or glycerol) as co-solvents on the hydrolysis of chiral (1,2)-*trans*-2-methylstyrene oxide enantiomers by potato EH StEH1 hydrolase. By applying DES as co-solvents, higher reactant concentrations could be achieved and the regioselectivity could be influenced. Zhao *et al*. studied the protease-catalysed transesterification activities in choline

chloride-glycerol mixtures (1:2).[76] *N*-Acetyl-1-phenylalanine propyl ester was produced from the corresponding ethyl ester in 1-propanol with 98% selectivity and this reaction was favoured over the hydrolysis to the carboxylic acid. The same group developed a new species of eutectic mixture, a combination of the ionic liquid choline acetate with glycerol as hydrogen bond donor, thus achieving a lower viscosity.[77] *Candida antarctica* lipase B catalysed highly selectively (>99%) the transesterification of ethyl sorbate with 1-propanol in DES, as well as the transesterification of a mixture of triglycerides with methanol to biodiesel.

The combination of DES and the enzyme lipase from *Rhizopus oryzae* as biocatalyst was used to synthesise (racemic) dihydropyrimidines by a Biginelli reaction (Figure 3).[78]

Epoxide hydrolysis[29]

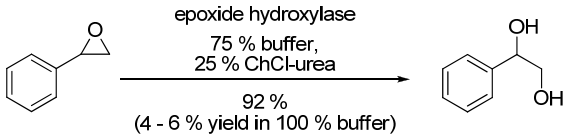

Biginelli in DES with lipase[78]

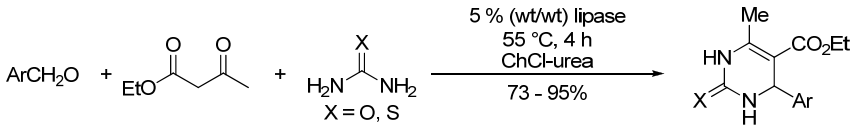

Figure 3 Some biotransformations in DES.

2.4 Other applications

ILs can even dissolve a wide variety of molecules and materials of low solubility. Different deep eutectic solvents (ChCl-urea, ChCl-malonic acid) increase the solubility of poorly soluble compounds (*e.g.* benzoic acid, griseofulvin, danazol, itraconazol) 5- to 20 000-fold compared to their solubility in water.[79] In NADES, an enhanced solubility of the flavonoid rutin, which is only slightly soluble in water, was observed.[20] The solubility was 50- to 100-fold higher in glucose/fructose or aconitic acid/ChCl mixtures than in water.[20]

Deep eutectic solvents are also versatile tools for the synthesis of inorganic materials and play a structure directing role as templates for the framework formation of metal phosphates,[80] oxalatophosphates,[81] aluminophosphates,[82] carboxymethyl-phosphonates,[83] oxalatophosphonates,[84] polyoxometalate-based hybrids,[85] zeolites,[86] or metal-organic frameworks.[87] Their structure directing role was also observed for

nucleic acids which can form several secondary structures that reversibly denature on heating in a water-free DES. Four distinct nucleic acid structures can exist in DESs or room-temperature ILs.[88]

Furthermore, monodispersed concave tetrahexahedral Pt nanocrystals were prepared by electrochemical shape-controlled synthesis in deep eutectic solvents[44]. Using this new synthetic method, the size and shape of the nanocrystals can be controlled without addition of seeds, surfactants, or other chemicals.

In addition, ionic liquids derived from choline were also used to dissolve biopolymers. Choline acetate was reported to dissolve approx. 2-6 wt% of microcrystalline cellulose within 5-10 min at 110 °C.[89] In another example, high solubilities of lignin and xylan were observed in liquids produced from choline and amino acids; they were also used for the selective extraction of lignin from lignocellulose.[16] Cholinium alkanoates were shown to efficiently and specifically dissolve suberin domains from cork biopolymers.[90]

Conclusion and Outlook

The application and characterisation of low melting mixtures, i. e. deep eutectic solvents, sugar-urea-salt mixtures, and ionic liquids from biomaterials, are still in the early stage of development. Since the first publication on DES in 2003, the number of related articles has been growing nearly exponentially. Even while writing this review, new articles on the physicochemical properties of these alternative media, their application in synthesis, electrochemistry, or the structure directing role of biopolymers have been published, underpinning their importance and great potential. Basically, their properties and the fields of application overlap with those of regular ionic liquids. Their apparent advantage over ionic liquids, however is their easy access from inexpensive, non-toxic and completely biodegradable and biocompatible materials.[15] Considering the variety of anions and cations nature provides, an enormous range of combinations could be synthesised to produce environmentally benign solvents, with tailor-made of properties.

2. Efficient preparation of β–D-glucosyl and β–D-mannosyl ureas and other *N*-glucosides in carbohydrate melts

Sugar melts or solvent-free systems have been used to react simple unprotected hexoses at the C-1 atom with urea and urea derivatives to sugar-ureides by acid catalysis in short reaction times. In one step, β-D-glucosyl- and β-D-mannosyl urea **2a**/**b** were obtained in high yields. D-Galactose **6**, *N*-acetyl-D-glucosamine **7**, L-rhamnose **8**, and 2-deoxy-D-glucose **9** were converted likewise to the glycosyl ureas. Additionally, urea-related nucleophiles were investigated as melt components. *N*,*N*′-Ethylene urea **15**, *N*,*N*′-allylurea **16** and ethyl carbamate **18** were β-selectively converted with D-glucose in good yields giving the corresponding *N*-glycosides. Under these conditions, however, the condensation product with *N*-octylurea **17** was not accessible.

C. Ruß, F. Ilgen, C. Reil, C. Luff, A. Haji Begli, B. König
"Efficient preparation of β-D-glucosyl and β-D-mannosyl ureas and other *N*-glucosides in carbohydrate melts" *Green Chem.*, **2011**, *13*, 156-161

C. Ruß optimised and extended the application of urea addition which was discovered by F. Ilgen and C. Reil. C. Luff performed the experiments under the supervision of C. Ruß regarding *N*,*N*'-allyl urea as project within her final thesis for her studies as a teacher.

Introduction

In the 21st century, the utilization of renewable raw material will gain significant importance in the industrial conversion of chemicals. This fact is a consequence of diminishing fossil fuel reserves which will urge to develop new methodologies to make use of sustainable sources for chemical production in the near future.[91] Since biomass is renewable, abundant and distributed widely in nature, it is a promising alternative for the sustainable supply of valuable intermediates and platform chemicals to the chemical industry.[92]

Carbohydrates form the main part of biomass with more than 75 wt%.[93] They can be used directly for chemical conversion or after hydrolysis of poly- and oligosaccharides to monosaccharides like D-glucose and D-fructose. Substitution at the most oxidized site in monosaccharides, the anomeric centre, gives access to the important and prominent group of the glycosides. *O*-,[94] *S*-,[95] *C*-[96, 97] and *N*-glycosides[98] are examples for this group of C-1 substituted monosaccharides. A representative of the *N*-glycosides is the stable class of glycosyl ureas. Glycosyl ureas are widely used in a mixture with phenol and water as an adhesive with excellent properties. This formulation is important for the forest product industry which is interested in reducing the phenol content in adhesives for construction material and furniture due to the toxicity of phenol.[99] Glycosyl thymines can be prepared from glycosyl ureas as described by Sano *et al*.[100] Another important application of glycosyl ureas is the use as lyophilization stabilizers for enzymes.[101] Recently, Shoji *et al.* introduced a glycosyl urea based lectin adsorbent with high and controllable adsorption capacity, which can be manufactured conveniently.[102] Structurally similar *N*-acyl-*N*′-β-glucopyranosyl ureas were identified as nanomolar inhibitors of rabbit muscle glycogen phosphorylase and might be applied in the therapy of type 2 diabetes mellitus.[103, 104] The *N*-Aryl-*N*′-β-glucopyranosyl ureas exhibited weaker binding to the glycogen phosphorylase than the acyl derivatives.[103, 105] The condensation product between aldoses and urea is obtained from acid catalysed reactions in water or water mixtures and was first described for D-glucose by Schoorl *et al.* as early as 1900.[106, 107] After minor modifications in the original procedure, the synthesis of glycosyl ureas was improved by Benn and Jones yielding 32% after 42 h with sulphuric acid as catalyst.[108] The best results so far

were obtained by M. Sano *et al.* using the ion exchanger Amberlite IR-120 (H-form) to obtain β-D-glycosyl urea in 53% chemical yield after 4 d at 75-80 °C.[100] Higher yields could not be achieved without significantly longer reaction times (7-14 d).[99] Modern and more versatile methods use the reaction of glycosyl isocyanates with amines to prepare glycosyl ureas. These and other important synthetic approaches towards carbohydrate-based ureas were reviewed by Spanu et Ulgheri.[109] A simple synthesis of α-glycosyl ureas was developed by Bianchi *et al*.[110]

The reported methods for the preparation of β-D-glycosyl and β-D-mannosyl ureas suffer from moderate yields and long reaction times. An ideal method for the conversion of biomass into platform chemicals, however, is the use of highly concentrated systems featuring a high substrate concentration and high chemical yields. Such systems should allow efficient conversions in short reaction times.

Here, we report the application of carbohydrate urea melts developed in our working group[17, 18, 22, 67, 111, 112] with diverse Brønsted and Lewis acids as catalyst in aldose concentrations as high as 3 mol/L. Using such carbohydrate melt systems, the reaction times are reduced, while the yields could be significantly increased compared to the reported systems (up to 78%). Apart from β-D-glucosyl urea **2a**, β-D-mannosyl urea **2b** was prepared in the highest yields reported (up to 81%) so far in the literature (Scheme 1). Glycosyl urea formation was also observed for D-galactose **6**, N-acetyl-D-glucosamin **7**, L-rhamnose **8**, and 2-deoxy-D-glucose **9**. Moreover, we showed that *N*,*N*'-ethylene urea **14**, *N*,*N*'-allylurea **15** and ethyl carbamate substitute in the melt at the C-1 position of D-glucose.

Results and Discussion

Formation of β–D-glucosyl urea in carbohydrate melt

The acid catalysed condensation of D-glucose with urea in aqueous media applying long reaction times was described by both Benn *et al*.[108] and Sano *et al*.[100] The stereochemistry at the anomeric centre was determined based on ^{1}H-NMR coupling constants of the two axial protons in C-1 and C-2 position by Helm to be the β-form.[99] Typically, the anomeric effect favours the α-configuration in sugars with electronegative substituents in C-1 position.[113] Nitrogen has a lower electronegativity

compared to oxygen and halogens and thus contributes less to the anomeric stabilisation of glycosyl ureas. Polar solvents are known to reduce the stabilisation at the anomeric centre. Both effects and the steric hindrance account for the preferred β-glycoside configuration.

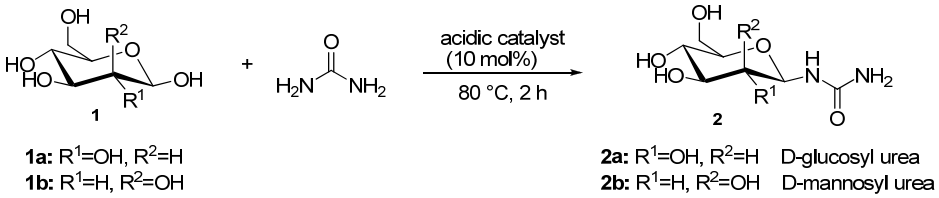

Scheme 1 Acid catalysed formation of β-form condensation products **2a** and **b** in the melt.

First results for the condensation reaction were obtained using montmorillonite as catalyst in a D-glucose/urea/NH_4Cl melt (3:7:1, wt:wt:wt). Montmorillonite, a phyllosilicate with Brønsted and Lewis acid character, was chosen as a catalyst because it is mild, non-toxic and could be recycled after the reaction since it is a heterogeneous catalyst. After 48 h reaction time at 80 °C, the reaction was analysed by ^{13}C-NMR showing a high conversion and a high selectivity. The resonance signal for **1a** at the anomeric centre (92.3 ppm, d_6-DMSO) disappeared completely and the only carbonyl resonance signal detected at 158.0 ppm (d_6-DMSO) indicated the selective formation of one isomer. The sample was analysed by mass spectrometry to confirm that urea was selectively mono glycosylated. The high coupling constant in the ^{1}H-spectrum confirmed the β-configuration of the glycoside (Scheme 1).

After the initial experiment, several other catalysts were tested. The product yield was determined by HPLC using sucrose as internal standard (Table 14).

Table 14 Chemical yields for β-D-glycosyl urea **2a** preparation in carbohydrate melts (2 h).

catalyst	yield [%][a]
Amberlyst 15	81
$FeCl_3$	27
$ZnCl_2$	14
p-TsOH	37
Montmorillonite	14
Without catalyst	14

[a]Yields determined by HPLC

The highest yield for the glycoside **2a** was 81% with Amberlyst 15 after 2 h at 80 °C determined by HPLC. *para*-toluene sulfonic acid (*p*-TsOH) and $FeCl_3$ yielded 37% and 27% of **2a**, respectively. Montmorillonite and $ZnCl_2$ displayed no catalytic reactivity. Additionally, the HPLC measurements showed that after 30 minutes at least 60% of D-glucose **1a** was converted, after 2 h about 8% sugar **1a** could be detected, even in the absence of a catalyst. The discrepancy between the low yields and the high D-glucose consumption is mostly due to the formation of a second product, detected as a single peak next to the product peak in the HPLC chromatogram. The integrals of the HPLC signals were compared, which is possible for the nearly quantitative ELSD detector due to uniform responses. After 15 minutes reaction time with Amberlyst 15, the amount of intermediate **3** was 10 % less than the amount of glucosyl urea **2a**, whereas after 2 h only 7% of **3** were present. The 6-7-fold amount of the second product compared to glucosyl urea **2a** was found without catalyst after 15 minutes and after 6 h still a 4-fold excess. Further LC-MS analysis proved that the unknown product exhibits a molecular weight of 240 g/mol which might correspond to the intermediate **3** (Scheme 2), obtained by nucleophilic addition of urea at C-1.

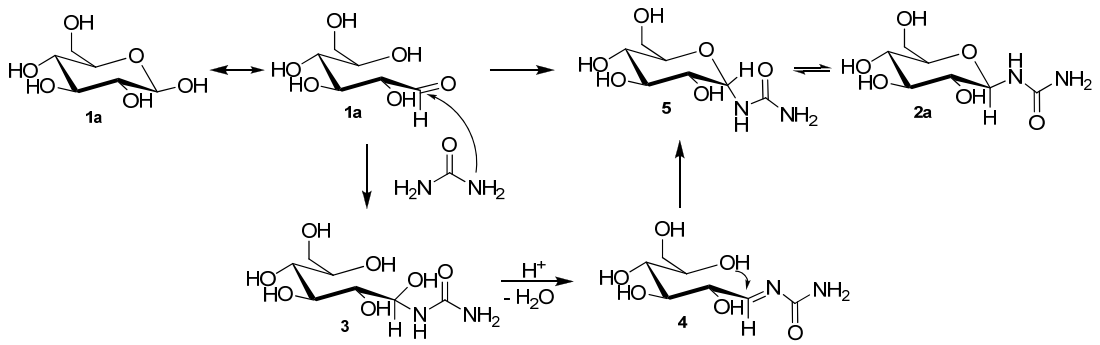

Scheme 2 A suggested reaction mechanism for the reaction of D-glucose **1a** with urea *via* intermediate **3** in a sugar-urea-salt melt under acidic conditions.

Formation of β-D-mannosyl urea in carbohydrate melt

Based on the successful conversion of D-glucose **1a** the epimer D-mannose **1b** was tried to show the general applicability of acid catalysed condensation with urea in high concentration carbohydrate melts for different sugars (Scheme 1). Badawi reported an inefficient procedure in water with sulphuric acid as catalyst and reaction times of up to 7 days. [114] The yield of β-D-mannosyl urea **2b** after 7 days was 12% after

recrystallisation from MeOH. β-Configuration at the anomeric centre was established by optical rotation of the derivatives after periodate reaction, which was compared with the values of derivatives of β-D-glucosyl urea **2a**.

In an initial study, a melt consisting of D-mannose/urea/NH_4Cl (3:7:1, wt:wt:wt) was stirred with Amberlyst 15 as catalyst and the purified product was analysed by NMR and mass spectrometry. ^{13}C-NMR and NOE experiments confirmed the expected β-anomer as the reaction product and the mass spectrometric analysis indicated that selective mono condensation had taken place. Again, the reduced electronegativity of the C-1 substituent and the bulkiness of the urea moiety are the probable reasons for the observed stereochemistry. Quantification of the sugar ureide **2b** by HPLC showed that optimum yields with selected catalysts were achieved after 1 h reaction time at 80 °C.

The best yields of condensation product **2b** were obtained with $FeCl_3$ (81%), Amberlyst 15 (75%), and *p*-TsOH (64%). Montmorillonite and $ZnCl_2$ were also applied, but showed less catalytic activity and the determined yields remained below those of the other catalysts. In contrast to the condensation with monosaccharide **1a**, only one product was found by HPLC. With 1 h and 2 h, respectively, for both β-D-mannosyl **2b** and β-D-glycosyl urea **2a**, the reaction times could be significantly reduced compared to literature.

A fructose/urea melt was reacted under acidic conditions (Amberlyst 15) at 80 °C for 24 h forming a mixture of condensation products which could not be separated. We assume that the fructose/urea condensation products are present in the furanose- and pyranose- as well as in the α- and β-form.

Reactions of further monosaccharides in the carbohydrate-urea melts

To investigate the effects of stereochemistry on the reaction pathway and to enlarge the scope of application, four additional sugar/urea/NH_4Cl melts (3:7:1, wt:wt:wt) were examined for their reaction under acidic conditions. In the depicted conformations (Scheme 3), D-galactose **6** has an axial OH-group in 4-position, *N*-acetyl-D-glucosamine **7** is substituted with a bulky and electron-withdrawing group at 2-position, L-rhamnose **8** shows an axial OH-group at 2-position like D-mannose, and in 2-deoxy-D-glucose **9**, the OH-group in 2-position is replaced by a hydrogen atom (Scheme 3).

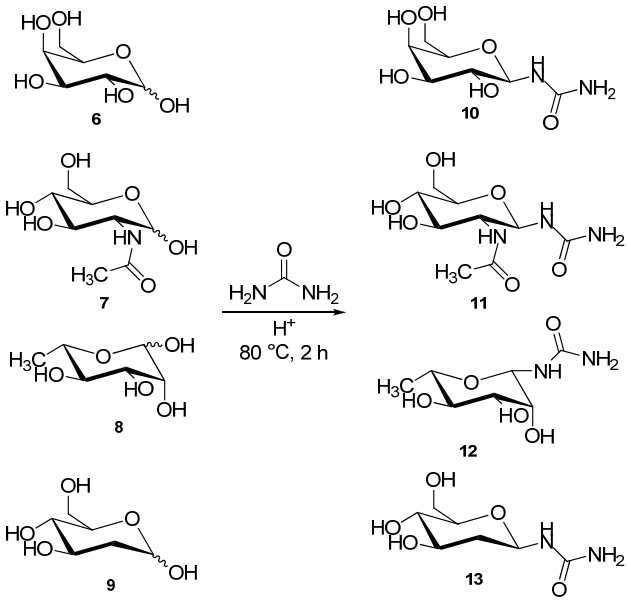

Scheme 3 Glycosyl ureas **10**-**13** from the acid catalysed reaction of monosaccharides **6**-**9** in melts.

After stirring the melts with the acidic Amberlyst 15 at 80 °C for 2 h, reaction control by ^{13}C-NMR showed that the twelve signals of the corresponding starting materials were reduced to six signals. As in the case of glucosyl- and mannosyl urea, the resonance signal for the anomeric centre had disappeared and a new carbonyl resonance was detected at 160 ppm (D_2O). Apparently, one anomer was selectively formed, presumably the β-anomer. HPLC-MS measurements confirmed for all monosaccharides that only one product was obtained, according to the mass of the

glycosyl urea. Additionally, we observed that more than 90% of the starting material was converted. Neither in the samples with catalyst nor in samples without catalyst, an intermediate (*cf.* D-glucose, **3**) was found.

Reactions of D-glucose with urea derivatives under solvent-free and acidic conditions

After exploring the efficient condensation of the monosaccharides **1a**/**b** and **6-9** with urea, different urea derivatives and nucleophiles with similar structures to urea were tested as melt components to form *N*-glucosides (Scheme 4).

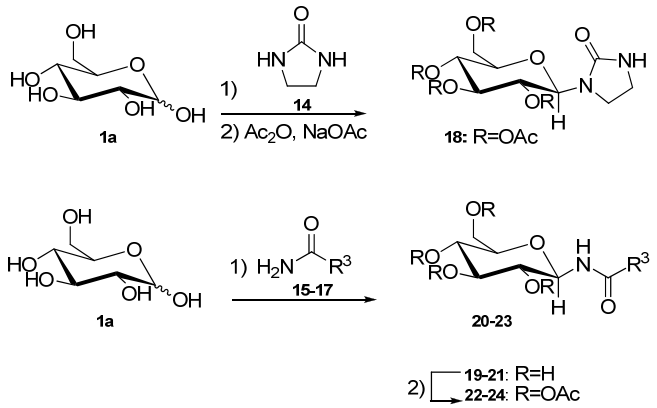

Scheme 4 Acid catalysed formation of condensation products 19-24 in melts.

Therefore, the lowest melting point (eutectic point) of mixtures of sugar **1a** and one of the additive compounds **14-17** (Table 15) was determined. However, only the cyclic *N*,*N*′-ethylene urea **14** showed a melting point depression and a clear melt was formed. In all other cases, the sugar could only be suspended in an excess of the melted component.

The addition of Amberlyst 15 to a 1:1 (wt:wt) mixture of cyclic *N*,*N*′-ethylene urea **14** with D-glucose **1a** followed by stirring the melt for 6 h at 75 °C afforded 27% of pure *N*-D-glucosyl-*N*′-ethylene urea tetraacetate **18** after acetylation and purification by column chromatography or recrystallisation. A corresponding mixture of the cyclic urea **14** with D-fructose showed the formation of the dehydratisation product HMF after stirring at 85 °C over night with Amberlyst 15.

Table 15 Different urea derivatives (**14**-**17**), which were reacted with D-glucose **1a**; reaction time, temperature and yield of the product (after peracetylation).

Product	R^3	Reaction time (h)	Temperature (°C)	Yield (%)
18	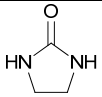 **14**	6	75	27
19, 22	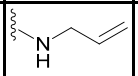 **15**	2	85	60
20, 23	 **16**	2-24	110	-
21, 24	 **17**	4	70	73

Although D-glucose **1a** and *N*-allyl urea **15** do not form a clear melt, the addition of Amberlyst 15 to a suspension of D-glucose/*N*-allyl urea (2:1, mol:mol) at 85 °C catalysed the condensation of the urea derivative with the C-1 position of compound **1a**. After 2 h reaction time, sugar **1a** was completely consumed and about 50% of the unprotected product *N*-D-glucosyl-*N'*-allyl urea **19** was formed (NMR estimation). Due to the amphiphilic character of the molecule, only analytical amounts of the unprotected form could be isolated. From the large ^{1}H-NMR coupling constant (J = 9.1 Hz) between the H-atom at the anomeric centre (C-1) with the H-atom on the adjacent carbon (C-2) in the unprotected sugar, we inferred that both H-atoms have axial-axial configuration, thus the β-form is favoured. HPLC measurements confirmed the highest yield after 2 h. Acetylation of crude **19** and purification by column chromatography afforded 60% of pure product **22**.

Sugar-based surfactants would be obtained by the condensation of long-chain alkyl ureas to saccharides. Procedures for the direct condensation of aldohexoses with such urea derivatives in solution are already published.[115, 116] Another strategy without protecting groups involves the use of D-glucosylamines and alkyl isocyanates.[116, 117]

Under solvent-free conditions, a number of products occurred in a suspension of melted *N*-octylurea **16** and D-glucose **1a**, with varying acidic catalysts. The low reactivity of the long-chain alkyl ureas might be explained by the intermolecular

hydrogen bonding between alkyl ureas.[118, 119] Furthermore, many products were generated presumably due to Maillard-like reactions or caramelisation of the sugar at such high reaction temperatures.

Finally, an *N*-glucoside of ethyl carbamate **17** with D-glucose **1a** was synthesised. Carbamates are structurally related to ureas, also called carbamides. They are established as protecting groups for amine groups and can be cleaved by various chemical and also enzymatic methods. Tetraacetyl-D-glucosylethylurethane was firstly reported by Helferich *et al*. and synthesised by the reaction of tetraacetyl-D-glucosamine and ethyl chloroformate in dry pyridine.[120] Another method developed by Sarap *et al*. involves the synthesis of tetra-*O*-acetyl-β-D-glucosyl isocyanate and its conversion with ethanol.[121] In an initial screening of acid catalysts, $FeCl_3$ was identified as the catalyst with the highest conversion. In a suspension of ethyl carbamate **17** and D-glucose **1a** (2:1, mol:mol) with 10 mol% of the catalyst after 5 h reaction time at 70 °C, 73% of product **24** were found after acetylation and purification. Only analytical amounts of the unprotected *N*-D-glucosyl-ethyl carbamate **21** could be isolated by our means. In this case, the β-anomer is the only obtained isomer again, which was confirmed by the large coupling constant (J= 9.3 Hz) in the ^{1}H-NMR spectrum.

Conclusion

In conclusion, we have shown that carbohydrate-urea melts are suitable reaction media to synthesise *N*-glycosides efficiently in high yields (up to 81%) under mild reaction conditions and high concentrations. The readily available starting materials consist mainly of renewables and cheap bulk chemicals. In a one-step reaction and without the need of protecting groups, the β-anomer was formed selectively. Our data imply that the reaction of D-glucose may proceed *via* an intermediate *O,N*-hemiacetal formed by the addition of the nucleophile to C-1. D-Glucose, D-mannose, D-galactose, *N*-acetyl-D-glucosamin, L-rhamnose, and 2-deoxy-D-glucose were converted likewise and the scope of the melt condensation reaction includes *N*-substituted ureas and carbamates. The here reported glycosyl urea synthesis is superior to previously reported procedures as it is very simple and efficient.

Experimental

General. All chemicals were used for syntheses as received without further purification. *N*-octylurea **16** was prepared according to Kehm.[122] IR spectra were recorded with a Bio-Rad FT-IR-FTS 155 spectrometer. Melting points were determined by an Optimelt MPA 100 apparatus from Stanford Research Systems.

NMR Spectra were recorded on a Bruker Avance 600 (T= 300 K). The spectra are referenced against the internal NMR-solvent standard and chemical shifts are reported in ppm.

HPLC measurements

Glucosyl urea **2a**: The HPLC measurements were conducted with a Phenomenex Luna 3u HILIC 200 Å, 150 x 2.00 mm column, LC system Agilent 1100, Varian PL-ELS 2100 Ice (30 °C) as detector, and run with MeCN/H_2O/100 mM NaOAc 90:5:5 as eluent. The column temperature was 40 °C, the injection volume 0.1 μL, while a flow rate of 0.3 mL/min and sucrose as internal standard was used. The system was run with ChemStation for LC 3D Systems Rev. B.03.02 as software.

Mannosyl urea **2b**: The HPLC measurements were conducted with a Phenomenex Luna 3u HILIC 200 Å, 150 x 2.00 mm column, LC system Agilent 1100, Varian PL-ELS 2100 Ice (30 °C) as detector, and run with MeCN/H_2O/100 mM NaOAc 90:5:5 as eluent. The column temperature was 25 °C, the injection volume 0.5 μL, while a flow rate of 0.3 mL/min and sucrose as internal standard was used. The system was run with ChemStation for LC 3D Systems Rev. B.03.02 as software.

Typical procedure for the preparation of β-D-glucosyl urea (2a)

D-Glucose (0.6 g, 3.3 mmol), urea (1.4 g, 26.7 mmol) and NH_4Cl (0.2 g, 3.7 mmol) were molten in a 25 mL reaction flask at 80 °C until a clear melt was formed. Amberlyst (0.2 g) was added and the reaction was stirred for 2 h at that temperature. After the reaction was finished, water was added to the still warm melt and the catalyst was filtered off. After the removal of the water, the brownish solid was twice recrystallised from MeOH to give pure β-D-glucosyl urea as white crystals (0.47 g, 64%). (For characterisation data see lit. [99]).

β-D-Mannosyl urea (2b)

D-Mannose (0.6 g, 3.3 mmol), urea (1.4 g, 26.7 mmol) and NH_4Cl (0.2 g, 3.7 mmol) were molten in a 25 mL reaction flask at 80 °C until a clear melt was formed. Amberlyst 15 (0.2 g) was added and the reaction was stirred for 1 h at that temperature. After the reaction was finished, water was added to the still warm melt and the catalyst was filtered off. After the removal of the water, the brownish solid was twice recrystallised from MeOH to give a mixture of β-D-mannosyl urea and urea. Urea was degraded by urease in an aqueous solution, the urease was filtered off and after freeze-drying, pure β-D-mannosyl urea was obtained as a white powder (0.53 g, 72%).

^{1}H-NMR (600 MHz, DMSO-d_6): δ [ppm] = 2.97-3.03 (m, 1 H), 3.24-3.34 (m, 2 H), 3.36-3.43 (m, 1 H), 3.50-3.52 (m, 1 H), 3.59-3.65 (m, 1 H), 4.41 (t, J = 6,0 Hz, 1 OH), 4.67 d (d, J = 5,0 Hz, 1 OH), 4.76 (d, J = 5,4 Hz, 1 OH), 4.80 (m, 1 H), 4.83 (d, J = 5,4 Hz, 1 OH), 5.84 (s, NH2), 6.47 (s, NH); **^{13}C-NMR (150 MHz, DMSO-d_6)**: δ [ppm] = 61.41, 66.88, 71.22, 74.39, 78.30, 78.46, 157.53; FT-IR (ATR): v [cm-1] = 3334, 3244, 2942, 2358, 1663, 1614, 1528, 1446, 1411, 1377, 1200, 1140, 1076, 1047, 1024, 958, 863, 801,614, 539: **MP:** 178 °C; **LSI-MS** (glycerol): m/z (%) = 223.1 (100) [MH^+], 315.3 (43) [MH^+ + glycerol]; **LSI-MS:** calcd.: 223.0930, found: 223.0933.

NOE spectrum for β-D-mannosyl urea (2b)

The H-1/H-5 and H-1/H-3 NOE contacts in the β-conformation are clearly observed.

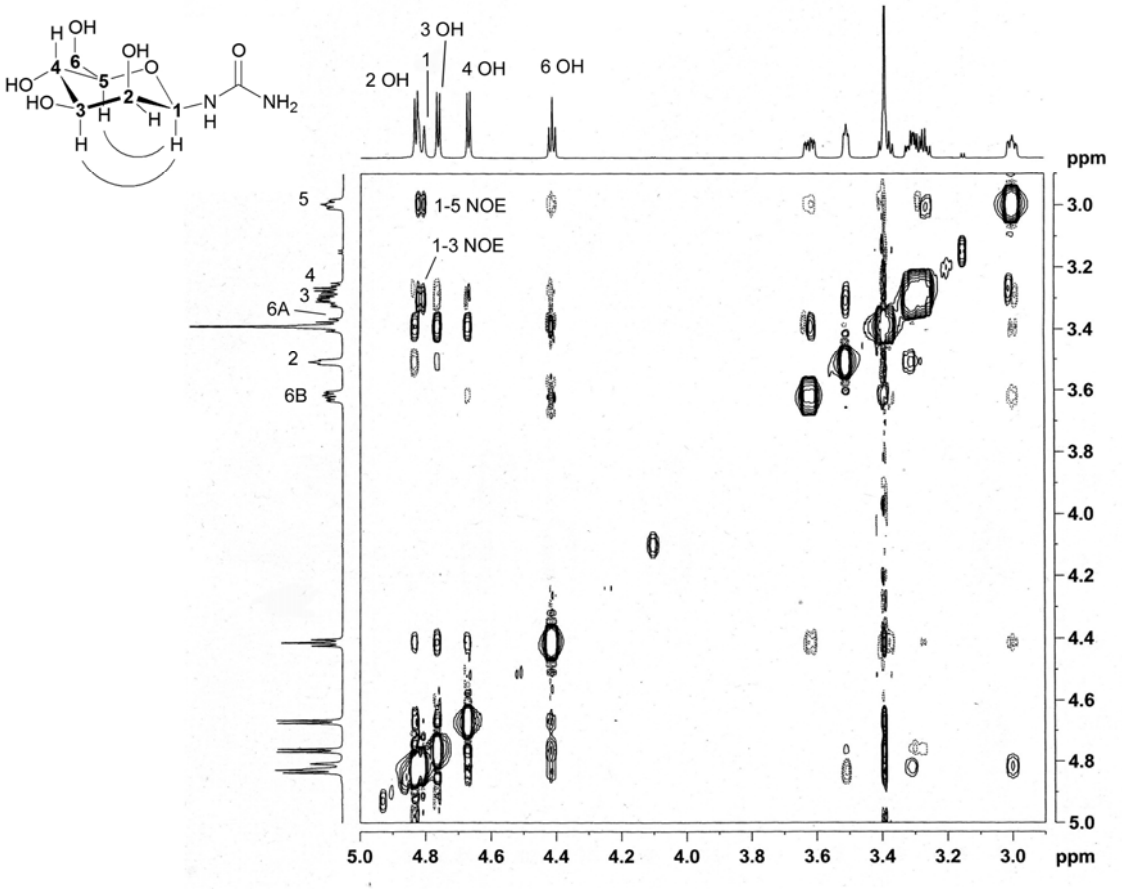

Typical procedure for the preparation of β-D-glycosyl ureas (10-14)

Monosaccharide **7-10** (0.6 g, 3.3 mmol), urea (1.4 g, 26.7 mmol) and NH_4Cl (0.2 g, 3.7 mmol) were molten in a 25 mL reaction flask at 80 °C until a clear melt was formed. Amberlyst (0.2 g) was added and the reaction was stirred for 2 h at that temperature. After the reaction was finished, D_2O/H_2O was added to the still warm melt and reaction mixtures were directly used for further measurements.

D-Galactosyl urea (10)

^{13}C-NMR (75 MHz, D_2O): δ [ppm] = 61.1, 68.8, 69.6, 73.5, 76.3, 81.4, 160.7.

ESI-MS: m/z (%) = 445.1 [2 MH^+] (100), 223.1 [MH^+] (46).

***N*-Acetyl-D-glucosaminyl urea (11)**

^{13}C-NMR (75 MHz, D_2O): δ [ppm] = 22.1, 54.3, 60.71, 69.7, 74.3, 77.2, 80.2, 160.4, 174.9.

ESI-MS: m/z (%) = 264.1 [MH^+] (100), 527.2 [2 MH^+] (53).

L-Rhamnosyl urea (12)

^{13}C-NMR (75 MHz, D_2O): δ [ppm] = 16.8, 70.6, 71.8, 73.2, 73.3, 78.7, 160.0.

ESI-MS: m/z (%) = 413.1 [2 MH^+] (100), 207.1 [MH^+] (35).

2-Deoxy- D-glucosyl urea (13)

^{13}C-NMR (75 MHz, D_2O): δ [ppm] =37.4, 61.0, 70.8, 71.1, 77.2, 77.6, 160.2.

ESI-MS: m/z (%) = 207.1 [MH^+] (100), 413.1 [2 MH^+] (66).

Preparation of *N*-D-Glucosyl-*N'*-ethylene urea-tetraacetate (18)

A melt of D-glucose (0.5 g, 2.8 mmol) and *N*,*N'*-ethylene urea (0.5 g, 5.8 mmol) was stirred with 50 mg of Amberlyst 15 for 6 h at 75 °C. After addition of water, filtering off the catalyst and freeze-drying, the white solid was heated to 90 °C in a mixture of Ac_2O (2.2 mL, 23.3 mmol) and NaOAc (0.4 g, 4.9 mmol) for 1.5 h. Then, the solution was poured into saturated $NaHCO_3$ solution and the aqueous phase was extracted three times with CH_2Cl_2. The combined organic layers were washed twice with water. A colourless solid was obtained after recrystallisation from EtOAc/PE (4:1) (0.3 g, 27%).
^{1}H-NMR (300 MHz, D_2O): δ [ppm] = 2.00, 2.02, 2.03, 2.06 (4x s, 12 H), 3.33-3.47 (m, 2 H), 3.56-3.61 (m, 2 H), 3.77-3.83 (m, 1 H), 4.04-4.10 (m, 1 H), 4.21-4.26 (m, 1 H), 5.01-5.17 (m, 4 H), 5.26-5.32 (m, 1 H). **^{13}C-NMR (75 MHz, D_2O)**: δ [ppm] = 20.7, 20.7, 20.8, 20.9, 38.2, 39.7, 60.0, 68.3, 68.3, 73.5, 73.6, 80.6, 161.7, 169.7, 170.0, 170.8. **FT-IR (ATR)**: ν [cm^{-1}] = 2896, 1738, 1673, 1486, 1434, 1369, 1214, 1127, 1034, 900, 842, 765, 697, 599, 495, 461, 436. **MP:** 154 °C, **ESI-MS:** m/z (%) = 434.0 [MNH_4^+] (100), 417.0 [MH^+] (76).

Preparation of *N*-D-glycosyl-*N'*-allyl urea (19)

A slurry of D-glucose (5.0 g, 0.03 mol) and *N*,*N'*-allyl urea (5.5 g, 0.05 mol) was stirred with 2 g of Amberlyst 15 for 6 h at 85 °C. After addition of water, the solid catalyst was filtered off and the aqueous solution decolourised with charcoal and freeze-dried. The sample was subsequently subjected to Soxhlet extraction with EtOAc over three days, in which the solvent was exchanged after 24 h. Finally, a colourless powder precipitated from the EtOAc layer which was the product (54 mg, 0.7%).
^{1}H-NMR (300 MHz, D_2O): δ [ppm] = 3.32-3.91 (m, 8 H), 4.83 (d, J=9.06 Hz, 1 H), 5.11-5.22 (m, 2 H), 5.94 (m, 1 H); **^{13}C-NMR (75 MHz, D_2O)**: δ [ppm] = 41.93, 60.74, 69.48,

72.01, 73.20, 76.62, 77.11, 81.15, 114.88, 135.00, 159.58; **FT-IR (ATR)**: ν [cm^{-1}] = 3300, 2920, 1639, 1557, 1420, 1363, 1272, 1073, 1012, 921, 559; **MP:** 136 °C (decomp.); **ESI-MS:** m/z (%) = 525.2 [2 MH+] (100) 263.1 [MH^+] (32), **GC-MS (SiMe$_3$)**: m/z (%) = 479.0 [MH^+-$SiMe_3$] (100), 496.1 [MNH_4^+] (64).

Preparation of *N*-D-glycosyl-*N'*-allyl urea-tetraacetate (22)

A slurry of D-glucose (1.0 g, 5.5 mmol) and *N*,*N'*-allyl urea (1.1 g, 11.1 mmol) was stirred with 0.4 g Amberlyst 15 for 2 h at 85 °C. After addition of 6 mL Ac_2O (63 mmol) and 0.9 g sodium acetate (11 mmol), the mixture was heated to 90 °C for 2 h. The reaction was stopped by pouring the cool solution into saturated $NaHCO_3$ solution. Then, the aqueous phase was extracted three times with EtOAc, the combined organic layers were washed with water, dried over $MgSO_4$ and evaporated. The crude product was purified by flash chromatography (EtOAc:PE = 2:1) affording a colourless solid (1.4 g, 60%).

^{1}H-NMR (300 MHz, $CDCl_3$): δ [ppm] = 1.99, 2.00, 2.03, 2.05 (s, 12 H), 3.84 (m, 2 H), 4.06 (dd, J_1=1.92 Hz, J_2=12.35 Hz, 1H), 4.30 (dd, J_1=4.39 Hz, J_2=12.35 Hz, 1H), 4.86-5.31 (m, 6H), 5.70 (d, J=9.39 Hz), 5.75-5.90 (m, 1H); **^{13}C-NMR (75 Hz, $CDCl_3$)**: δ [ppm] = 20.69, 20.85, 42.86, 68.46, 70.66, 73.08, 73.24, 80.24, 116.10, 134.87, 156.58, 169.79, 170.03, 170.81, 171.08; **FT-IR**: ν [cm^{-1}] = 3319, 2948, 1739, 1637, 1580, 1434, 1373, 1210, 1096, 1030, 907, 674, 599, 490, 464; **MP:** 131 °C **ESI-MS**: m/z (%) = 448 [MNH_4^+] (100), 431 [MH^+] (78).

Preparation of *N*-D-glycosyl-*O*-ethyl carbamate (21)

A slurry of D-glucose (0.4 g, 2.2 mmol) and *N*-ethyl carbamate (0.4 g, 4.5 mmol) was stirred with 20 mol% $FeCl_3$*$6H_2O$ for 2.5 h at 80 °C and the excess of carbamate was removed by ultrasonic extraction with EtOAc (3×10 mL) and an extraction time of one hour. The residual solid was solved in a small amount of MeOH and dropped into ice-cooled Et_2O. Finally, the Et_2O phase was evaporated and a colourless solid was obtained (18 mg, 3 %).

^{1}H-NMR (300 MHz, DMSO-d_6): δ [ppm] = 1.16 (t, J=7.14 Hz, 3 H), 9.97-3.63 (m, 8 H), 3.99 (q, J=7.04 Hz, 2 H), 4.43-5.18 (m, 3 H), 7.73 (d, J=9.33 Hz, 1 H); **^{13}C-NMR (75 MHz, DMSO-d_6)**: δ [ppm] = 14.53, 59.68, 60.80, 69.77, 71.83, 77.39, 78.18, 82.22, 155.94; **^{1}H-NMR (300 MHz, D_2O)**: δ [ppm] = 1.14 (t, J=7.14 Hz, 3 H), 3.22-3.79 (m, 6 H),

4.05 (q, J=6.95 Hz, 2 H), 5.32 (d, J=5.49 Hz, 1 H); **^{13}C-NMR (75 MHz, D_2O)**: δ [ppm] = 13.73, 60.58, 62.41, 69.26, 71.76, 76.48, 77.27, 81.75, 158.48; **FT-IR**: ν [cm^{-1}] = 3122, 3037, 2817, 2674, 2361, 2323, 1607, 1558, 1402, 1253, 1180, 1120, 421; **MP:** 182 °C (decomp.); **ESI-MS**: m/z (%) = 269.1 [MNH_4^+] (100), 252.1 [MH^+].

Preparation of *N*-D-glycosyl-*O*-ethyl carbamate-tetraacetate (24)

A slurry of D-glucose (0.4 g, 2.2 mmol) and *N*-ethyl carbamate (0.4 g, 4.5 mmol) was stirred with 10 mol% $FeCl_3$*$6H_2O$ for 4.5 h at 70 °C in a 10 mL reaction tube. After addition of water, $FeCl_3$ was precipitated with aqueous NH_3, filtered off and the remaining was solution freeze-dried. Then, NaOAc (0.5 g 2.2 mmol) and 3 mL Ac_2O were added and the mixture was stirred at 90°C for 1.5 h in a round bottom flask. The content of the flask was poured into 20 mL of ice water which was extracted three times with CH_2Cl_2.The combined organic phases were washed with saturated $NaHCO_3$ solution and water, dried over $MgSO_4$ and the solvent was evaporated. After recrystallisation from Et_2O/PE, a colourless solid was obtained (yield: 73%).

^{1}H-NMR (300 MHz, DMSO-d_6): δ [ppm] = 1.18-1.26 (m, 3 H), 1.97, 1.99, 2.02, 2.04 (4x s, 12 H), 3.77 (m, 1 H), 4.03-4.15 (m, 3 H), 4.25-4.29 (m, 1 H), 4.85-5.28 (m, 3 H), 6.02 (d, J=9.62 Hz, 1 H); **^{13}C-NMR (75 MHz, DMSO-d_6)**: δ [ppm] = 14.4, 20.6, 20.7, 20.8, 22.1, 61.8, 68.2, 70.3, 72.9, 73.3, 80.8, 155.7, 169.6, 170.0, 170.7; **FT-IR**: ν [cm^{-1}] =2961, 1736, 1531, 1434, 1367, 1211, 1094, 1029, 908, 782, 599, 554, 484; **MP:** 105 °C (lit.: 104 °C)[120] **ESI-MS**: m/z (%) = 437.0 [MNH_4^+] (100), 420.0 [MH^+] (70).

3. Solvent-free preparation of 5-(α-D-glucosyloxymethyl) furfural from isomaltulose- choline chloride melts and Synthesis of *N*-(2,3,4,6,1',3',4'-hepta-*O*-acetyl-L-isomaltulosyl)urea

5-(α-D-Glucosyloxymethyl)furfural **2**, a versatile building block from renewable resources, was prepared from isomaltulose **1**-choline chloride melts by acid catalysis. In this solvent-free process, moderate yields were achieved under mild reaction conditions.

C. Ruß, C. Luff, A. Haji Begli, B. König

"Solvent-free preparation of 5-(α-D-glucosyloxymethyl)furfural from isomaltulose - choline chloride melts" *Synth. Commun.*, **2012**, *42*, 1-5.

C. Ruß supervised and carried out the experiments of GMF synthesis together with C. Luff within her final thesis for her studies as a teacher.

Introduction

Building blocks from renewable resources will gain importance due to the limited natural resources of fossil starting materials for organic synthesis. As carbohydrates amount to 75% of the annually renewable biomass,[123] they could provide organic carbon for a variety of intermediate chemicals.[124]

5-Hydroxymethylfurfural (HMF) is one of the top value added chemicals from biomass.[125] Hexoses, for example, are converted to HMF upon acid catalysed dehydration. In comparison between different monosaccharides, D-fructose provides the highest yields.[126] 5-(α-D-Glucosyloxymethyl)furfural (GMF) **2** is formed by thermal decomposition of isomaltulose (= palatinose) **1**[127] and was also isolated from steamed Radix Rehmanniae and from Amelanchier fruits. [128, 129] It is also generated when heating HMF with glucose in 1,4-dioxane.[130] Originally, it was synthesised in the group of Lichtenthaler in high yields starting from isomaltulose **1** using DMSO as solvent.[131, 132] The mixture was heated to 120 °C for 4 h with a strongly acidic, sulfonic acid type ion exchange resin. Resulting mixtures consisted of GMF **2** (65-70%), isomaltulose dimers (10%), HMF, glucose (5-10%), and starting material (10%) determined by HPLC. The starting material isomaltulose **1** is commercially produced from sucrose in an enzymatically catalysed 1,6-glycosyl shift.[133] The fructosyl moiety of isomaltulose **1** was dehydrated to a furfural derivative, while the glucosyl residue was stable.

GMF **2** was used as building block for a variety of derivatisation reactions to obtain the furancarboxylic acid, GMF-nitrile, the GMF-amine *via* reductive amination, or aldol-type reaction products.[131]

Ionic liquids or deep eutectic solvents are considered as alternatives to hazardous solvents.[134] In our working group, sugar-urea-salt mixtures were developed as alternative solvents for organic reactions.[17-19] Furthermore, glycosyl ureas could be synthesised in high yields in these melts.[135] Ilgen *et al*. used carbohydrate–choline chloride melts to produce HMF from the carbohydrate content.[67] Likewise, Han *et al*. converted inulin to HMF in choline chloride/citric acid or choline chloride/oxalic acid melts.[136]

Adopting the concept of dehydration of hexoses in choline chloride melts, we now report the preparation of GMF **2** in an isomaltulose **1**–choline chloride melt by different acidic catalysts under mild reaction conditions in good yields (Scheme 5).

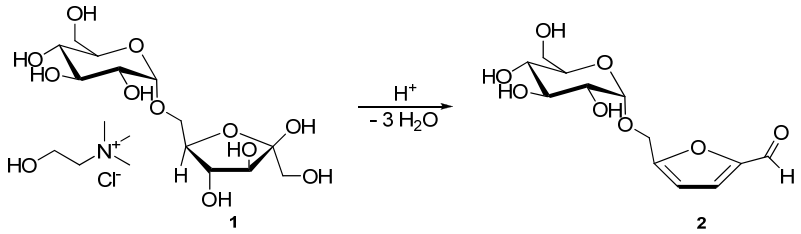

Scheme 5 Dehydration of isomaltulose **1** to α-GMF **2** under acidic conditions.

Advantages of such sugar melts are the omission of solvents like DMSO, the low vapour pressure of the liquid, and the exclusive use of non-toxic, renewable compounds.

Results and Discussion

The sugar–choline chloride mixture with the lowest melting point contained both compounds in a 1:1 ratio (wt/wt) which corresponds to a carbohydrate concentration of 1.7 mol/L in the melt. Though the water content of the melts is low (approx. 2%), a pre-drying at 90 °C and 10 mbar vacuum was necessary to remove most of the water. Water causes the hydrolysis of GMF **2** to D-glucose and HMF. Furthermore, the reaction was performed under vacuum to remove water which is generated during the dehydration reaction to suppress the decomposition.

The catalytic activity was evaluated for different acids at three different temperatures (90 °C, 100 °C, 110 °C) and at regular time intervals (15, 30, 60, 90 min). Amberlyst 15 is an inexpensive and strongly acidic ion exchange resin. It can easily be handled and removed by simple filtration. Montmorillonite is also a non-toxic, non-corroding solid ion exchanger. *para*-toluenesulfonic acid (*p*-TsOH) is a water-soluble, strong organic acid. $FeCl_3$ is a hygroscopic and strong Lewis acid. $ZnCl_2$ is also hygroscopic with a moderate Lewis acidity.

The content of isomaltulose **1**, GMF **2**, D-glucose, and HMF in the samples was quantified by HPLC. Optimum GMF yields were obtained after 15 min at 100 °C, similar to those at 90 °C (with a difference of at most 3%, Table 16). At 110 °C, less GMF **2** was found; simultaneously the HMF content increased. Generally, more HMF was formed, when the temperature was raised. The HMF yields were between 6% with Montmorillonite and 60% with $FeCl_3$ as catalyst at 100 °C. However, with longer reaction times, the yields dropped due to the formation of HMF polymers and humins, which is known to occur in concentrated solutions.[137]

D-Glucose was mainly found in the samples which were not pre-dried before addition of the catalyst, however only in amounts between 12 and 14%. Additionally, it was found in all the samples with Amberlyst 15 (3-6%) and $FeCl_3$ (2-3%). The starting material palatinose was only detected in the samples with Montmorillonite and $ZnCl_2$ when no pre-drying was applied (7 and 84%, respectively).

Table 16 GMF **2** yields for different catalysts under optimised conditions (temperature and time).

Entry	Catalyst	T (°C)	t (min)	Yield (%)
1	$ZnCl_2$	100	60	52
2	Montmorillonite	100	15	46
3	Amberlyst	100	15	34
4	*p*-TsOH	100	15	35
5	$FeCl_3$	100	15	27

Reaction of isomaltulose with urea

Isomaltulose **1**, or 6-*O*-α-D-glucopyranosyl-D-fructose, formed also a low melting mixture with urea and the same reaction conditions as for the aldoses, like glucose and mannose (chapter 2), were applied. The most electrophilic carbon atom is that at the anomeric carbon atom of the fructosyl moiety. As the 6-OH group is locked at the D-glucose part, only two furanoid forms are predominant in solution: β-*f*-form : α-*f*-form : acyclic form = approx. 25% : 72% : 3%.[138]

An isomaltulose **1**-urea melt (3:7:1 wt/wt) was allowed to react with Amberlyst for 2 h at 80 °C (Scheme 6). First analysis of the crude reaction mixture by ^{13}C-NMR showed the presence of isomaltulose and the typical peak at about 160 ppm next to the urea peak, indicating the formation of a glycosyl urea. After acetylation and column chromatography, pure isomaltulosylurea heptaacetate (α-anomer) was isolated in 11% yield and fully characterised. The correct assignment of the signals of the (2*R*)-configured furanosid was only possible by two-dimensional NMR spectra. Furthermore, we inferred from TLC, LC-MS and NMR that the β-anomer was formed in 15% yield.

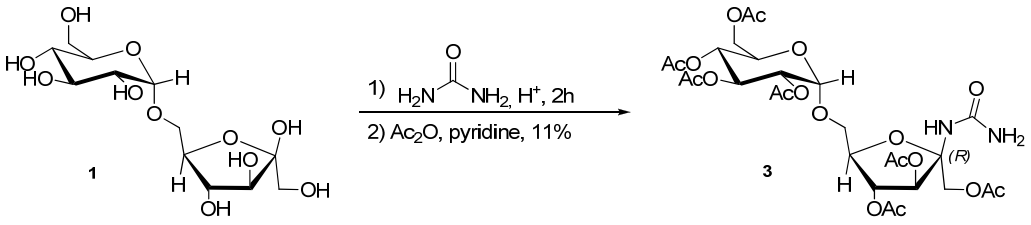

Scheme 6 Reaction of isomaltulose **1** with urea to *N*-(2,3,4,6,1',3',4'-hepta-*O*-acetyl-L-isomaltulosyl) urea **3** under acidic conditions.

Conclusion

In summary, we have converted isomaltulose to GMF **2** in the presence of catalysts without any solvent, but in highly concentrated (50 wt% of sugar), environmentally benign sugar – choline chloride melts. Highest yields were obtained for $ZnCl_2$ as catalyst. However, in view of the shorter reaction times required, the handiness, and the recyclability, the use Montmorillonite would be preferable. The isolated GMF **2** yields are currently still lower than in the comparable DMSO solution process. However, the reported direct conversion in neat melt without added organic solvents may be of interest as an alternative very simple and non-toxic process for GMF synthesis.

In addition, we reported for the first time that acidic conditions catalyse the addition of urea to the C-2 atom of the fructosyl moiety of isomaltulose in low melting sugar-urea mixtures.

Experimental

General. Commercial reagents and starting materials were purchased from Aldrich, Fluka or Acros and used without further purification. Isomaltulose and pure GMF as reference were kind gifts of the Suedzucker AG. Flash chromatography was performed on silica gel (Merck silica gel Si 60 40-63 μm); products were detected by TLC on aluminium plates coated with silica gel (Merck silica gel 60 F_{254}, thickness 0.2 mm) and visualised with 10% H_2SO_4 or $KMnO_4$ staining solution. Melting points were determined with Optimelt MPA 100 and are uncorrected. NMR spectra were recorded with Bruker Avance 300 (^{1}H: 300.1 MHz; ^{13}C: 75.5 MHz; T = 300 K), Bruker Avance 400 (^{1}H: 400.1 MHz; ^{13}C: 100.6 MHz; T = 300 K) and Bruker Avance 600 Kryo (^{1}H: 600.2 MHz; ^{13}C: 150.9 MHz; T=298 K) instruments. Chemical shifts are reported in δ/ppm relative to the external standards and coupling constants J are given in Hz. Abbreviations for the characterisation of the signals: s = singlet, d = doublet, t = triplet, m = multiplet, bs = broad signal, dd = double doublet. The relative number of protons is determined by integration. Error of reported values: chemical shift: 0.01 ppm (^{1}H NMR), 0.1 ppm (^{13}C NMR), coupling constant: 0.1 Hz. The used solvent for each spectrum is reported.

Mass spectra were recorded on a ThermoQuest Finnigan TSQ 7000 LC/MS spectrometer (low resolution), high resolution spectra (HRMS) on an Agilent Tech 6540 UHD Accurate Mass Q-TOF LC/MS and with Finnigan MAT TSQ 7000 (ESI) spectromter, IR spectra with a Bio-Rad FT-IR-FTS 155 spectrometer and UV/VIS spectra with a Cary BIO 50 UV/VIS/NIR spectrometer (Varian). Optical rotation was determined with Krüss optronic P8000T.

General procedure for the preparation of GMF 2

In a 10 mL Schlenk tube, a pestled mixture of isomaltulose (0.5 g, 1.5 mmol) and choline chloride (0.5 g, 3.6 mmol) were melted and dried at 90 °C under reduced pressure (10 mbar) for 2 h. Then, 10 mol% of catalyst ($ZnCl_2$, p-TsOH or $FeCl_3$) or 250 mg of heterogeneous catalyst (Montmorillonite or Amberlyst 15) were added. All analytical data were in accordance with those in the literature.[131]

Preparation of the HPLC samples

The complete reaction batch was dissolved in 30 mL of millipore water. The HPLC measurements were conducted with a Phenomenex Luna 3u HILIC 200 Å, 150 x 2.00 mm column, LC system Agilent 1100, Varian PL-ELS 2100 Ice (30 °C) as detector, and run with MeCN/H_2O/100 mM NaOAc 90:5:5 as eluent. The column temperature was 40 °C, the injection volume 0.1 µL, while a flow rate of 0.3 mL/min and sucrose as internal standard was used. The system was run with ChemStation for LC 3D Systems Rev. B.03.02 as software.

Retention times in analytical HPLC:

R_t (HMF, DAD) = 1.55 min, R_t (GMF, DAD) = 2.19 min, R_t (Glucose, ELSD) = 3.82 min, R_t (Isomaltulose, ELSD) = 6.51 min.

***N*-(2,3,4,6,1',3',4'-Hepta-*O*-acetyl-L-isomaltulosyl) urea 3**

Isomaltulose (1.2 g, 3.5 mmol), urea (1.4 g, 26.7 mmol), and NH_4Cl (0.2 g, 3.7 mmol) were heated in a 10 mL reaction flask at 80 °C until a clear melt was formed. Amberlyst 15 (200 mg) was added and the reaction mixture was stirred for 2 h at that temperature. Methanol was added, solids filtered off, and the solvent evaporated. Then, 6 mL (5.8 g, 74.3 mmol) of pyridine and 6 mL of Ac_2O (6 mL, 6.5 g, 63.5 mmol) were added to the mixture and the mixture was first stirred for 1 h in an ultra-sound bath, then over night at room temperature without sonication. The reaction was stopped by pouring the solution into saturated $NaHCO_3$ solution. The aqueous phase was extracted three times with CH_2Cl_2. The combined organic layers were washed twice with 2N HCl, twice with water, and were finally dried over $MgSO_4$ and evaporated. The crude product was purified by column chromatography (SiO_2, CH_2Cl_2/MeOH 95:5), R_f =0.11 (α-anomer) (0.36 mg, 15%), R_f =0.03 (β-anomer) (0.23 mg, 10%).

β -Anomer

^{1}H-NMR (600 MHz, $CDCl_3$): δ [ppm] = 2.02-2.13 (7×s, 7×3H, OAc), 3.63 ((pseudo-dd, ^{2}J(H-6'^{a}, H-6'^{b}) = 9.45 Hz, ^{3}J(H-6'^{a}, H-5) = 1.29 Hz, 1H, H-6'^{a}), 3.97 (dd, ^{3}J(H-5, H-6'^{b}) = 1.28 Hz, ^{2}J(H-6'^{a}, H-6'^{b}) = 10.80 Hz, 1H, H-6'^{b}), 3.99-4.02 (m, 1H, H-5'), 4.13 (dd, ^{3}J(H-6^{a}, H-5) = 1.88 Hz, ^{2}J(H-6'^{a}, H-6'^{b}) = 12.27 Hz, 1H, H-6^{a}), 4.26-4.30 (m, 2H, H-6^{b}, H-4), 4.48 (bs, 2H, H-1'), 4.91 (dd, ^{2}J(H-2, H-1) = 3.90 Hz, ^{2}J(H-2, H-3) = 10.32 Hz, 1H, H-2), 5.10 (d, ^{2}J(H-1, H-2) = 3.90 Hz, 1H, H-1), 5.15-5.18 (m, 2H, H-5, NH), 5.38-5.43 (m, 3H, H3, H3', NH), 5.57 (dd, ^{2}J(H-4, H-3) = 7.35 Hz, ^{2}J(H-4, H-5) = 7.24 Hz, 1H, H-4); **^{13}C-NMR (75 Hz, $CDCl_3$)**: δ [ppm] = 20.5, 20.6, 20.6, 20.6, 20.7, 20.7, 20.8 (CH_3-Ac), 61.4 (C-6), 64.6 (C-1'), 66.6 (C-6'), 67.4 (C-5), 67.8 (C-4), 70.1 (C-3), 71.0 (C-2), 73.4 (C-4'), 77.1 (C-3'), 77.5 (C-5'), 90.3 (C-2'), 96.1 (C-1), 157.5 (C=O, urea), 169.3, 169.8, 170.1, 170.2, 170.3, 170.6, 170.6 (C=O, OAc); **FT-IR (ATR)**: ν [cm^{-1}] = 1739, 1690, 1590, 1524, 1436, 1367, 1211, 1031, 958, 897, 775, 635, 598; **MP:** 84-86 °C; **ESI-MS**: m/z (%) = 696.3 (MNH_4^+, 100), 679.2 (MH^+, 78); $[\alpha]_D^{20}$ = +82.397 (c 1.011, chloroform).

NOE spectrum for β- *N*-(2,3,4,6,1',3',4'-Hepta-*O*-acetyl-L-isomaltulosyl) urea 3

The H-1'/H-3' NOE contacts in the β -conformation are observed.

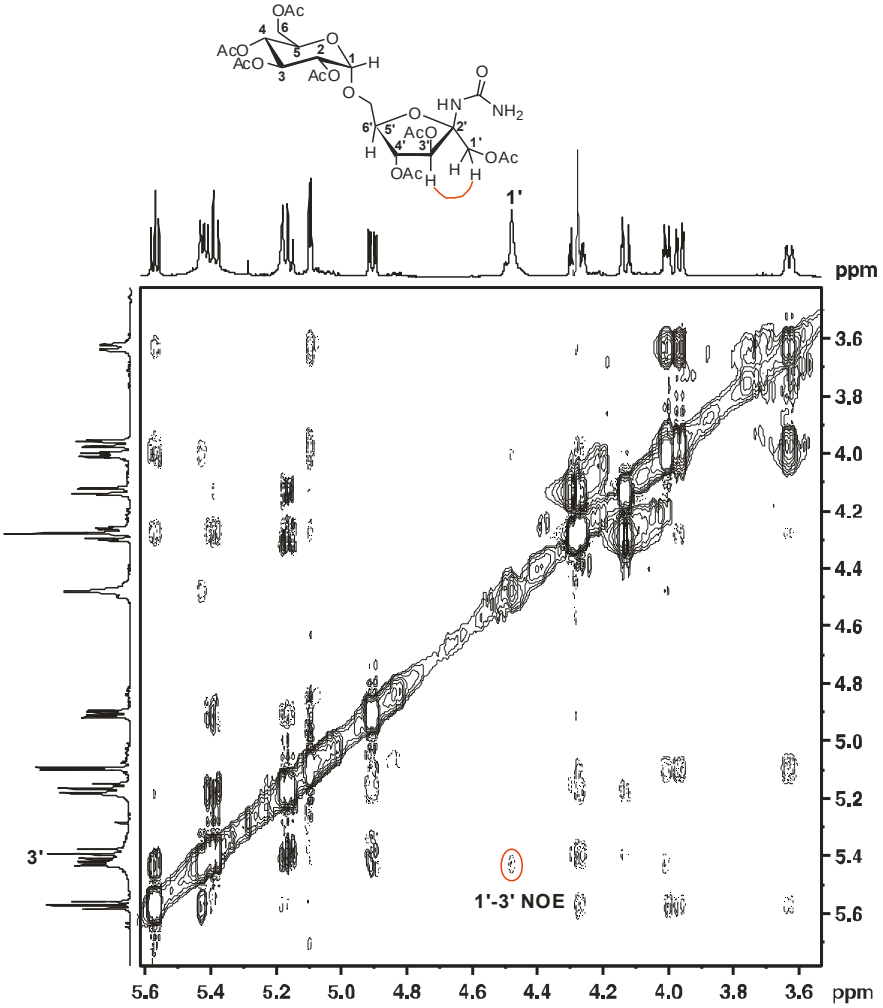

α-Anomer

^{1}H-NMR (400 MHz, $CDCl_3$): δ [ppm] = 2.00-2.10 (7×s, 7×3H, OAc), 3.64-3.67 (m, 1H, H-6'^{a}), 3.85-3.89 (m, 1H, H-6'^{b}), 4.06-4.13 (m, 2H, H-5, H6^{a}), 4.24-4.27 (m, 2H, H-1',H-6^{b}), 4.35-4.41 (m, 2H, H-1', H-5'), 4.86 (dd, 1H, H-2), 5.04-5.13 (m, 4H, H-1, H-3', H-4', NH), 5.34-5.43 (m, 1H, H-3), 5.72 (bs, 1H, H-4); **^{13}C-NMR (75 Hz, $CDCl_3$)**: δ [ppm] = 20.7-20.8 (CH_3-Ac), 61.7 (C-6), 62.7 (C-1'), 67.5 (C-5), 67.6 (C-6'), 68.4 (C-4'), 70.1 (C-3), 70.8 (C-2), 77.0 (C-3'), 79.8 (C-5'), 79.8 (C-4), 91.7 (C-2'), 95.9 (C-1), 157.8 (C=O, urea), 169.6-, 170.8 (C=O, OAc); **FT-IR (ATR)**: ν [cm^{-1}] = 1740, 1695, 1546, 1435, 1367, 1216, 1031, 898, 770, 600; **MP:** 84-86 °C; **ESI-MS**: m/z (%) = 696.3 (MNH_4^+, 100), 679.3 (MH^+, 20). $[\alpha]_D^{20}$ = 98.523 (c 1.013, chloroform).

4. Condensation and dehydration reactions of L-sorbose in eco-friendly melt systems

L-Sorbose **1** was converted to 5-hydroxymethylfurfural **8** in choline chloride melts in moderate yields. A simplified synthesis of sorbosylurea tetraacetate **4** in two steps using urea melts was performed achieving average yields.

C. Ruß, A. Haji Begli, B. König

"Condensation and dehydration reactions of L-sorbose in eco-friendly melt systems" *Synth. Commun.*, **2012,** *accepted.*

Synthesis and characterisation were performed by C. Ruß

Introduction

In 2011, a review by Zebiri *et al*. criticises the fact that the use of L-sorbose in organic chemistry is exceedingly poor and they encourage the development of new synthetic methods.[139] For this reason, reactions of L-sorbose in the unconventional carbohydrate melts developed in our working group were examined.[17-19] Low melting mixtures allow the conversion of biomass at high concentration into valuable intermediates.

L-Sorbose is one of the rare natural L-sugars and is mainly used as starting material in the synthesis of vitamin C. Therefore, it is the most readily available L-sugar on large scale.[139, 140] As 5-epimer of D-fructose, its structural similarity would suggest a comparable reactivity. Both, fructose and sorbose form a mixture of two pyranoid **1** and two furanoid stereoisomers **3** (plus negligible amounts of acyclic form **2**) (Scheme 7). The composition is not only strongly dependent on the solvent employed, but also on the temperature.[141, 142] Simple derivatisation reactions with fructose often yield product mixtures.[140] In contrast to fructose, sorbose highly favours the α-pyranoid form in solution: in water, the α-pyranoid form amounts to 87-98 % in a temperature range of 25-85 °C.[141] The benefit of sorbose is that reactions to pyranosid derivatives are proceeding in a more uniform manner and allow better yields than in the case of fructose.

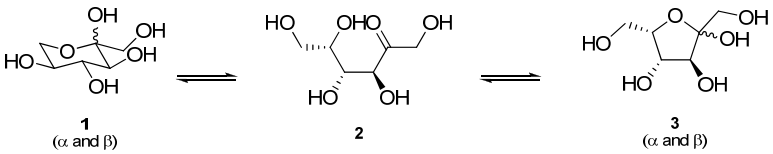

Scheme 7 Pyranose **1** and furanose **3** form and acyclic form of L-sorbose **2**.

We therefore investigated the reaction behaviour of L-sorbose in four carbohydrate melts: urea, dimethylurea, ethylene urea and choline chloride melts. Significant conversions were only observed in urea and choline chloride melts.

Results and Discussion

From our former investigations we know that glycosyl ureas are formed in carbohydrate-urea melts.[135] L-sorbose also forms stable melts with urea giving a melting point of 79-80 °C. Under acidic conditions, approx. 30% of the L-sorbose were mainly converted to sorbosyl urea **4** after 1.5 h reaction time at 80 °C (estimated by

^{13}C-NMR) (Scheme 8). Most of the starting material was recovered, but degradation to 5-hydroxymethyl furfural (5-HMF) and to brown humins was also observed, especially for longer reaction times and at higher temperatures. The isolated peracetylated sorbosyl urea **4** has (*2R)*-configuration (*α*-anomer) which was ascertained by NOESY experiments. A second fraction was an inseparable mixture presumably composed of sorbosyl acetate, the β-anomer sorbosyl urea **4**, and the sorbosylbiuret, inferred from ^{13}C-NMR spectra and ESI-MS measurements.

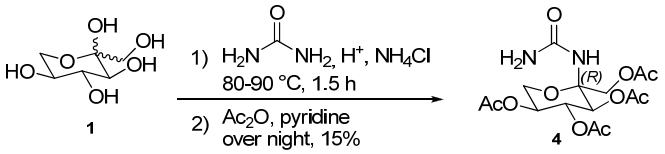

Scheme 8 Synthesis *N*-(1,3,4,5-tetra-*O*-acetyl-L-sorbopyranosyl)urea **4** in sorbose-urea melts under acidic conditions.

The synthesis of the peracetylated derivative **4** was reported by Tokuyama and Katsuhara in 1966 (Scheme 9).[143] They obtained the sorbopyranosyl urea **4** (both, *α*-anomer and β-anomer in 15% yield) by ammonolysis of the isocyanate **6** starting from 1,3,4,5-tetra-*O*-acetyl-L-sorbopyranosyl chloride **5**.

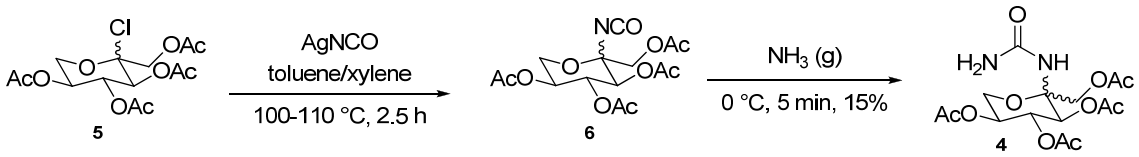

Scheme 9 Synthesis of *N*-(1,3,4,5-tetra-*O*-acetyl-L-sorbopyranosyl)urea **4** according to Tokuyama.[143]

Our previous investigations showed that choline chloride melts promote the production of 5-hydroxymethylfurfural **8** (5-HMF) from carbohydrates.[67] The production of 5-HMF from L-sorbose has already been patented in 1948 by Haworth (yield: 23%)[144] and was later investigated in organic solvents catalysed by lanthanide(III)ions (61.4%)[145], and subcritical water by Asghari *et al.* (50%).[146] Other reaction conditions to make 5-HMF from different sugars were recently reviewed.[147, 148] As expected, the only product from a choline chloride-sorbose melts was 5-HMF **8** (Scheme 10). After 1.5 h at 80 °C under acidic conditions using Amberlyst 15 as catalyst, the starting material was completely consumed and 24% of 5-HMF were obtained.

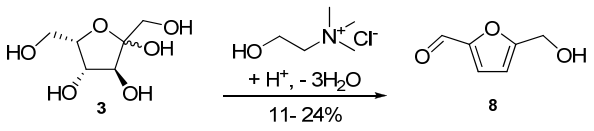

Scheme 10 Synthesis of HMF **8** from L-sorbose **3** in a choline chloride melt.

Under the same reaction conditions used by Ilgen *et al.* (100 °C, 0.5 h, 10% *p*-TsOH),[67] L-sorbose yielded only 11% of HMF while 67% were received starting from D-fructose. The lower 5-HMF yields starting from L-sorbose were previously observed by Seri *et al*.[145] and by Asghari *et al*.[146] They suggested that the different configurations of the hydroxyl groups at the C-3 and the C-4 atom in L-sorbose impair the dehydration reaction leading to lower yields.

Conclusion

In summary, new reactions of L-sorbose were investigated using low melting carbohydrate mixtures as eco-friendly reaction medium. We showed that the important intermediate 5-HMF can be produced from L-sorbose in choline chloride melts under acidic conditions.

Furthermore, a new, time-saving synthesis of sorbosylurea tetraacetate **4** is reported here. Using urea melts, we successfully simplified the literature known four step synthetic route to a two step procedure starting from unprotected L-sorbose, without the need of expensive reagents and inconvenient reaction conditions. For the first time, the structure of the selectively formed α-pyranose form was proven by two-dimensional NMR techniques. We introduced two new solvent-free systems here based on non-toxic and renewable resources for the conversion of L-sorbose.

Experimental

General. Commercial reagents and starting materials were purchased from Aldrich, Fluka or Acros and used without further purification. Flash chromatography was performed on silica gel (Merck silica gel Si 60 40-63 μm); products were detected by TLC on aluminium plates coated with silica gel (Merck silica gel 60 F_{254}, thickness 0.2 mm) and visualised with 10% H_2SO_4 or $KMnO_4$ staining solution. Melting points were determined with Optimelt MPA 100 and are uncorrected. NMR spectra were recorded with Bruker Avance 300 (^{1}H: 300.1 MHz; ^{13}C: 75.5 MHz; *T*=300 K), Bruker Avance 400 (^{1}H: 400.1 MHz; ^{13}C: 100.6 MHz; *T*=300 K) and Bruker Avance 600 Kryo (^{1}H: 600.2 MHz; ^{13}C: 150.9 MHz; *T*=298 K) instruments. Chemical shifts are reported in δ/ppm relative to the external standards and coupling constants *J* are given in Hz. Abbreviations for the characterisation of the signals: s = singlet, d = doublet, t = triplet, m = multiplet, bs = broad signal, dd = double doublet. The relative number of protons is determined by integration. Error of reported values: chemical shift 0.01 ppm (^{1}H NMR), 0.1 ppm (^{13}C NMR), coupling constant 0.1 Hz. The used solvent for each spectrum is reported.

Mass spectra were recorded on a ThermoQuest Finnigan TSQ 7000 LC/MS spectrometer (low resolution), high resolution spectra (HRMS) on an Agilent Tech 6540 UHD Accurate Mass Q-TOF LC/MS and with Finnigan MAT TSQ 7000 (ESI) spectromter, IR spectra with a Bio-Rad FT-IR-FTS 155 spectrometer and UV/VIS spectra with a Cary BIO 50 UV/VIS/NIR spectrometer (Varian). Optical rotation was determined with Krüss optronic P8000T.

_N_-(1,3,4,5-Tetra-_O_-acetyl-L-sorbopyranosyl)urea (7)

L-Sorbose (0.6 g, 3.3 mmol), urea (1.4 g, 26.7 mmol) and NH_4Cl (0.2 g, 3.7 mmol) were heated in a 10 mL reaction flask at 80 °C until a clear melt was formed. Amberlyst 15 (150 mg) was added and the reaction was stirred for 1.5 h at that temperature. Methanol was added, solids filtered off and the solvent evaporated. Then, 6 mL (5.8 g, 74.3 mmol) of pyridine and 3.5 mL of Ac_2O (3.8 g, 37.0 mmol) were added to the mixture and the mixture was first stirred for 1 h in the ultra-sound bath and then over night at room temperature without sonication. The reaction was stopped by pouring

the solution into saturated $NaHCO_3$ solution. The aqueous phase was extracted three times with CH_2Cl_2. The combined organic layers were washed twice with 2N HCl, twice with water and were finally dried over $MgSO_4$ and evaporated. The pure product was crystallised from ethyl acetate affording a colourless powder (0.215 g, 0.55 mmol, 16%).

^{1}H-NMR (300 MHz, $CDCl_3$): δ [ppm] = 2.02, 2.04, 2.08, 2.10 (s, 12 H, OAc), 3.75 (dd, 1 H, H-6), 4.01 (dd, 1H, ^{3}J(H-5, H-6') = 5.91 Hz, H-6'), 4.03 (dd, 1H, ^{2}J(H-1, H-1') = 12.36 Hz, 166.24 Hz, H-1), 4.58 (dd, J_1=12.33 Hz, J_2=166.24 Hz, 1H, H-1'), 5.00-5.09 (m, 1H, H-5), 5.24 -5.40 (m, 5H, H-3, H-4, urea); **^{13}C-NMR (75 Hz, $CDCl_3$)**: δ [ppm] = 20.5, 20.6, 20.5, 20.7 (CH_3-Ac), 59.9 (C-5), 62.0 (C-1), 68.3 (C-4), 69.0 (C-5), 70.4 (C-3), 85.3 (C-2), 156.6 (urea), 168.6, 169.8, 170.1, 170.2 (C=O, Ac);

^{1}H-NMR (600 MHz, $CDCl_3$): δ [ppm] = 2.01, 2.04, 2.07, 2.10 (4×s, 4×3H, OAc), 3.74 ("dd", ^{2}J(H-6^{ax}, H-6^{eq}) = 10.98 Hz, ^{3}J(H-6^{ax}, H-5) = 10.98 Hz, 1 H, H-6^{ax}), 4.00 (dd, ^{3}J(H-5, H-6') = 5.91 Hz, ^{2}J(H-6^{ax}, H-6^{eq}) = 11.07 Hz, 1H, H-6^{eq}), 4.04 (d, 1H, ^{2}J(H-1, H-1') = 12.37 Hz, H-1), 4.58 (d, ^{2}J(H-1, H-1') = 12.37 Hz, 1H, H-1'), 5.02-5.06 (m, 1H, H-5), 5.26 (d, ^{3}J(H-3, H-4) = 9.87 Hz, 1H, H-3), 5.35 -5.38 (m, 2H, H-4, urea); **^{13}C-NMR (75 Hz, $CDCl_3$)**: δ [ppm] = 20.5, 20.6, 20.6, 20.7 (CH_3-Ac), 59.8 (C-5), 62.0 (C-1), 68.3 (C-4), 69.0 (C-5), 70.4 (C-3), 85.3 (C-2), 156.7 (urea), 168.6, 169.8, 170.1, 170.2 (C=O, Ac); **FT-IR (ATR)**: ν [cm^{-1}] = 3487, 3458, 3341, 1753, 1744, 1697, 1665, 1620, 1614, 1591, 1564, 1547, 1535, 1441, 1433, 1377, 1371, 1275, 1229, 1211, 1138, 1103, 1061, 1032, 908; **MP:** 192 °C. **ESI-MS**: m/z (%) = 407.9 (MNH_4^+, 100), 431.9 (MH^+ +MeCN, 37), 390.9 (MH^+, 15). $[\alpha]_D^{20}$ = -37.395 (c 1.000, chloroform) (α-anomer) (literature [143]: $[\alpha]_D^{23.5}$ = -34.4 (c 0.973, chloroform).

NOE spectrum for *N*-(1,3,4,5-Tetra-*O*-acetyl-L-sorbopyranosyl)urea (7)

The NH/H-6^{ax} and NH/H-1 NOE contacts in the α-conformation are clearly observed.

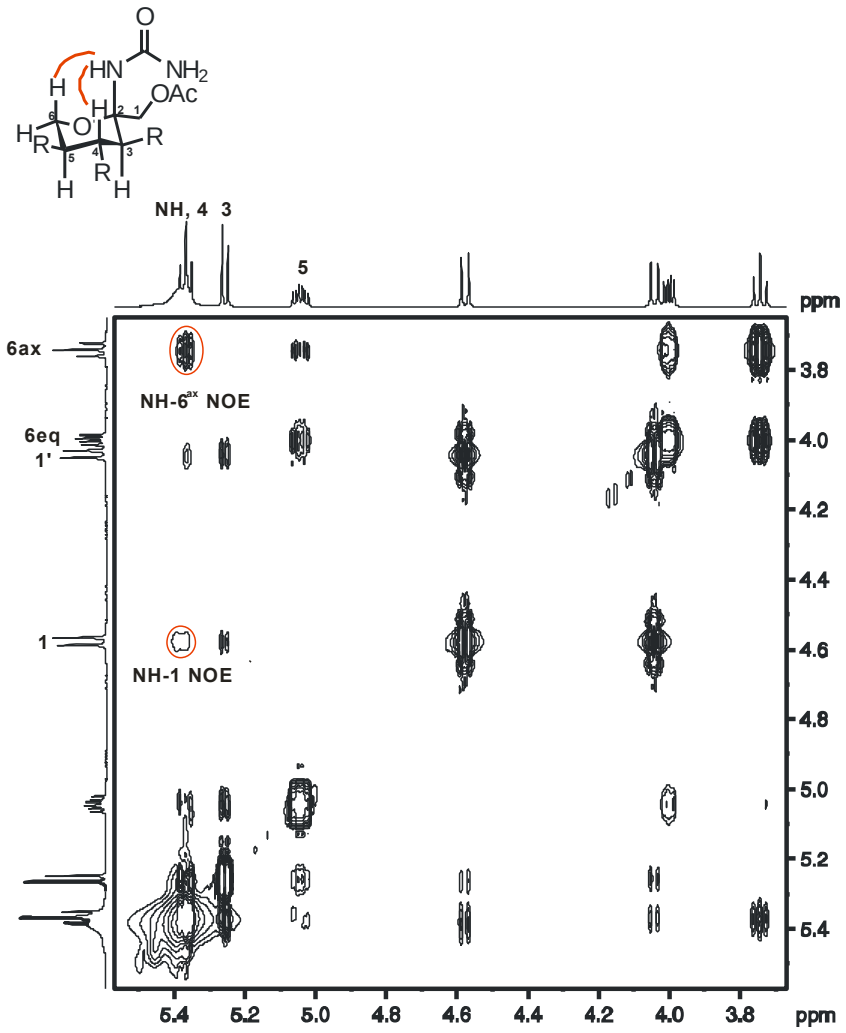

Synthesis of HMF

L-Sorbose (0.4 g, 2.2 mmol) and choline chloride (0.6 g, 4.3 mmol) were heated in a 10 mL reaction flask at 80 °C until a clear melt was formed. Amberlyst 15 (150 mg) was added and the reaction was stirred at that temperature. After 1.5 h, water was added, solids were filtered off and the solution was extracted three times with ethyl acetate. The organic layer was dried over Na_2SO_4 and the solvent was evaporated to obtain the product (0.103 g, 0.8 mmol, 24%). The ^{1}H-and ^{13}C-NMR data were concordant with those in literature.[149]

5. Base-, metal-, and photo catalysis in carbohydrate melts

To establish new methods in order to convert carbohydrates in the melt, the effect of different chemical catalysts on sugar melts should be investigated. As no new discoveries were received from basic, metal, and photo catalysis, the observations will shortly be summarised.

The effects of homogeneous and heterogeneous and inorganic and organic base catalysts (e.g. metal oxides and carbonates; triethylamine, DBU, (-)-sparteine) on glucose-urea-NaCl (6:3:1, wt:wt:wt) and glucose-choline chloride (2:3, wt:wt) melts were examined. Mainly, decomposition of the carbohydrate and the formation of complex mixtures due to Maillard reactions were observed. Using choline chloride melts, glucose underwent the Lobry-de Bruyn-van Ekenstein transformation, resulting in a mixture of glucose, mannose, and fructose.

Metal catalysts were applied to achieve selective oxidation of glucose to glucuronic acid. A variety of oxidations conditions (e.g. $KMnO_4$, Pt/O_2, $RuO_2/NaIO_4$) were tried in glucose-urea-NaCl (6:3:1, wt:wt:wt), mannose-DMU (3:7, wt:wt), and sorbitol-urea-NH_4Cl, melts (7:2:1, wt:wt:wt). The formation of oxidation product was not obtained; glucosyl urea, complex reaction mixtures or no conversion of the carbohydrate were observed instead.

To trigger radical or fragmentation reactions, four different low melting glucose mixtures with urea, dimethylurea, ethylene urea, or choline chloride as second component, were irradiated in the presence of photocatalysts (e.g. TiO_2, $Ru(bpy)_3]Cl_2$, fluorescein, riboflavinetetraacetate). Under these conditions, the starting material glucose was recovered accompanied by glucosyl urea if the catalyst was acidic

6. Süße Chemie zum Dahinschmelzen - Kohlenhydrat-basierte Medien als alternative Lösungsmittel und zur Umsetzung von Zuckern

Die Chemie der Zukunft wird notwendigerweise auf nachwachsende Rohstoffe als Ausgangsmaterial zurückgreifen müssen. Kostengünstige, kohlenhydratbasierte Schmelzen nutzen bereits nachwachsende Rohstoffe und stellen eine unkonventionelle Alternative zu erdölbasierten Medien dar. Physikalisch-chemische Eigenschaften, die Verwendung der Schmelzen als Lösungsmittel und die Umsetzung des Kohlenhydrat-Anteils werden vorgestellt.

C. Ruß, B. König

„Süße Chemie zum Dahinschmelzen“, GIT Labor Fachz., **2011**, *55*, (12), 836-837.

Einleitung

Ein seit Jahren bekanntes und in letzter Zeit immer akuter werdendes Problem ist die zunehmende Verknappung der fossilen Ressource Erdöl. Steigender Verbrauch bei schwindenden Reserven erfordert eine langfristige und nachhaltige Alternative. Auch die Synthesechemie basiert zum großen Teil auf Erdöl als Rohstoff. Deshalb sind erneuerbare und umweltfreundliche Produkte und Prozesse zwingend erforderlich.[150] Kohlenhydrate sind attraktive Ausgangsverbindungen für die Herstellung von Feinchemikalien, da sie eindeutig den größten Anteil an jährlich erzeugter Biomasse stellen. Im Gegensatz zu fossilen Kohlenwasserstoffen, die durch Synthese funktionalisiert werden, müssen die komplexen Naturstoffe de- oder umfunktionalisiert werden. Bis jetzt ist in diesem Bereich das Potential der Chemie nicht ausgeschöpft und noch viel Forschungsarbeit zu leisten. Dazu tragen die von uns entwickelten Zuckerschmelzen bei.

Physikalisch-chemische Eigenschaften der Zuckerschmelzen

Jeder Hobbykoch weiß, dass beim Erhitzen des Haushaltszuckers Saccharose Karamell entsteht, im schlimmsten Fall Kohlenstoff. Will man allgemein Zucker ohne Zersetzung schmelzen ist dies durch die Mischung mit einer zweiten Komponente möglich. Durch die zweite Komponente werden Wasserstoffbrücken zwischen Zuckermolekülen aufgebrochen und so die Schmelzpunkte beider Substanzen erniedrigt. Infolgedessen ist der Zucker bereits bei 65 - 85 °C ohne zusätzliches Lösungsmittel flüssig. Außerdem kann durch die Zugabe von Salzen, wie z.B. NaCl, $CaCl_2$ oder NH_4Cl der Schmelzpunkt der Mischung weiter abgesenkt werden. So liegt der Schmelzpunkt von Glucose bei ca. 150 °C, der von Harnstoff bei 133 °C. Die Mischung aus Glucose, Harnstoff, NaCl (6:3:1, Massenverhältnis) schmilzt dann bei 78 °C. Die Stabilität der Zuckerschmelzen ist bis 120 °C gewährleistet; oberhalb dieser Temperatur können Zuckerabbaureaktionen stattfinden. Außer Glucose können auch andere Zucker, Zuckeralkohole oder Zitronensäure verflüssigt werden. Eine Schmelze aus Sorbitol, Harnstoff, Ammoniumchlorid (7:2:1, Massenverhältnis) ist immerhin bis 220 °C stabil.[17] Als zweite Komponente wurden neben Harnstoff und dessen Derivaten auch Imidazol, Malonsäure oder Cholinchlorid erfolgreich eingesetzt. Deren unterschiedliches Säure-

Basen-Verhalten ändert auch den pH-Wert der Schmelze. Dadurch kann der pH-Wert in einem Bereich von pH 3 bis 10 eingestellt werden.[67] Werden Rohmaterialien verwendet, ergibt sich ein sehr geringer Wassergehalt von ca. 1.3%, der durch Trocknung im Vakuum auf 0.07% noch weiter reduziert werden kann. Zudem zeichnen sich die Schmelzen, wie auch ionische Flüssigkeiten, durch einen geringen Dampfdruck aus ($1.2 \cdot 10^{-1}$ mbar bei 70 °C).[18] Soll die Schmelze als alternatives Lösungsmittel verwendet werden, ist die Polarität des Mediums von Bedeutung. Deshalb wurde die Polarität der süßen Lösungsmittel im Vergleich zu konventionellen polaren organischen Lösungsmitteln durch solvatochrome Farbstoffe wie Nile Red und Reichardt's dye bestimmt. Derartige als Polaritätssonden eingesetzte Farbstoffe ändern ihre Farbe in Abhängigkeit von der Polarität des umgebenden Mediums. Da die Schmelzen in etwa so polar sind wie DMF, DMSO und Ethylenglykol, wurden darin verschiedene organische Reaktionen durchgeführt. So wurden die erforderlichen polaren Lösungsmittel in der Stille Reaktion, der Suzuki-Kupplung (Abb. 1a) oder Diels-Alder-Reaktion (Abb. 1b) durch die Schmelzen ersetzt. Nahezu quantitative Ausbeuten sprechen für den Erfolg des Konzepts.[17-19] Die Schmelzen haben außerdem den Vorteil, dass die Aufarbeitung vereinfacht wird. Nach Zugabe von Wasser setzt sich entweder eine organische Phase mit den Produkten ab oder die Produkte fallen bereits aus und können dann abfiltriert werden. Ein weiterer Aspekt macht die Zuckerschmelzen zu einem interessanten Medium: die Hauptbestandteile sind chiral. Daher kann man sich vorstellen, dass die Chiralität des Lösungsmittels einen Einfluss auf die Stereoselektivität von Reaktionen haben könnte. Jedoch wurde weder bei der Diels-Alder-Reaktion (Abb. 1b), noch bei der katalytischen Hydrierung von 1-Acetamidozimtsäure (Abb. 1c) eine nennenswerte Stereoinduktion festgestellt.[17, 18]

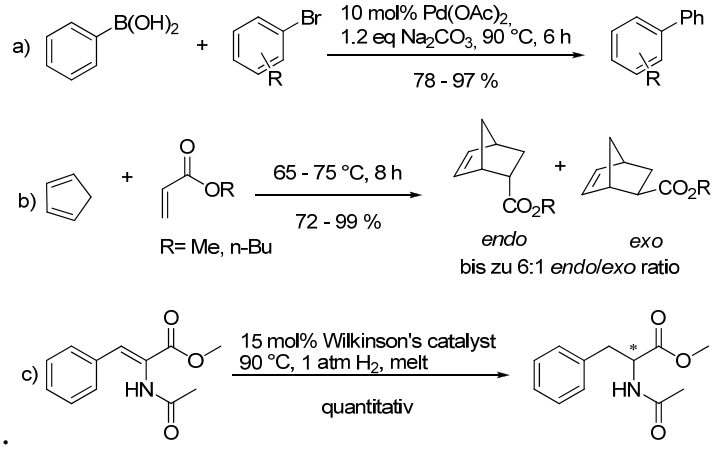

Abb. 1 Die niedrig schmelzenden Zucker-Harnstoff-Mischungen dienten als Lösungsmittel für a) die Suzuki-Kupplung, b) Diels-Alder-Reaktion und c) die katalytische Hydrierung von 1-Acetamidozimtsäure.

Konversion von Kohlenhydraten in der Schmelze

Die bemerkenswert hohen Zuckerkonzentrationen von ca. 1 - 3 mol/l in den Mischungen – das kann einem Zuckeranteil von bis zu 50% entsprechen – machen diese für die chemische Umsetzung der verflüssigten Kohlenhydrate in Feinchemikalien interessant.

Ein derzeit viel diskutierter Synthesebaustein ist 5-Hydroxymethylfurfural (5-HMF), da er aus verschiedenen Kohlenhydraten gewonnen werden kann.[147] Dieses wird auch als potentieller klimaneutraler Rohstoff für Treibstoffe und Chemikalien angesehen. Die Verbindung 5-HMF entsteht beim Erhitzen von Kohlenhydraten durch Abspaltung von drei Wassermolekülen und Ausbildung des heteroaromatischen Systems. Dieser Prozess wurde im Arbeitskreis König gezielt in einer Cholinchlorid-Kohlenhydrat Schmelze mit verschiedenen sauren Katalysatoren herbeigeführt.[67] Nach 30 Minuten Reaktionszeit bei 100 °C konnte mit D-Fructose und *para*-Toluolsulfonsäure eine gute Ausbeute von 67% erzielt werden (Abb. 2a). In einem ähnlichen Verfahren wurde 5-α-D-Glucosyloxymethylfurfural (GMF), die glucosylierte Variante von 5-HMF, aus Isomaltulose durch gezielte Dehydratisierung des Fructosylteils hergestellt (Abb. 2b).[68] Dabei wurden mit $ZnCl_2$ als Katalysator ebenfalls gute Ausbeuten von bis zu 52% erzielt. Klare Vorteile beider Methoden sind, dass auf problematische und teure

Lösemittel, wie z.B. DMSO, verzichtet werden kann und eine kontinuierliche Prozessführung in flüssiger, hochkonzentrierter Schmelze prinzipiell möglich ist.

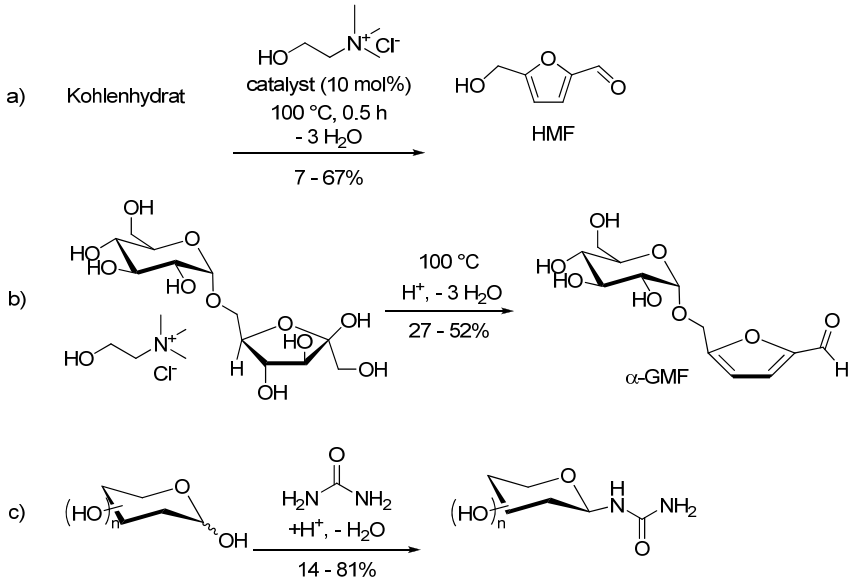

Abb. 2 a) Umsetzung von Kohlehydraten zu 5-HMF, b) Gewinnung von GMF aus Isomaltulose, c) Synthese von Glycosylharnstoffen in der Zucker-Harnstoff-Schmelze.

Des Weiteren wurden in der Schmelze in einer einstufigen Reaktion Glycosylharnstoffe hergestellt.[135] Dabei addiert Harnstoff unter Abgabe von Wasser am C-1 Atom des Saccharids und es wird selektiv das stabilere β-Anomer gebildet (Abb. 2c). Zum ersten Mal wurde Glucosylharnstoff im Jahr 1900 von Schoorl beschrieben[106] und findet seitdem breite Anwendung, z.B. als Spezialdünger oder als Teil biologisch aktiver Moleküle. Nach einer verbesserten Vorschrift konnte in wässriger Lösung nach vier Tagen Reaktionszeit bei 75-80 °C eine maximale Ausbeute von 53% erreicht werden. Benutzt man aber eine Zucker-Harnstoff-Schmelze, so kann bei 80 °C schon nach zwei Stunden Reaktionszeit in Gegenwart des heterogenen, sauren Katalysators Amberlyst 15 eine Ausbeute von 81% des gewünschten Produkts erzielt werden. Auf diese Weise lassen sich Monosaccharide, wie z.B. Mannose, Galactose und 2-Deoxyglucose zu verschiedenen Harnstoffderivaten umsetzen.

Nicht nur Kohlenhydrate lassen sich in der Schmelze umsetzen. In ähnlicher Weise können pharmazeutisch interessante Grundstrukturen mittels einer Mehrkomponentenreaktion durch säurekatalysierte Kondensation von Aldehyden und β-Ketoestern mit Harnstoff in exzellenten Ausbeuten synthetisiert werden.[151] Dabei

spielte die Weinsäure-Dimethylharnstoff-Schmelze eine dreifache Rolle: als Lösungsmittel, Katalysator und Reaktand.

Zusammenfassung

Mit den Zuckerschmelzen steht uns ein ungewöhnliches und vielseitiges Reaktionsmedium zur Verfügung. Die stabilen und nichtflüchtigen Mischungen haben die Vorteile, dass sie nicht toxisch sind, aus erneuerbaren Ressourcen gewonnen werden können, leicht verfügbar und biologisch abbaubar sind. Durch ihre hohe Polarität können sie konventionelle Lösungsmittel wie DMF oder DMSO ersetzen. Der hohe prozentuale Zuckeranteil macht sie außerdem für die milde, effiziente und lösungsmittelfreie Konversion von Kohlenhydraten attraktiv.

7. Conclusion

In the course of this project, acidic, basic, metal, and photo catalysts were applied to carbohydrate melts. We aimed to find chemical reactions converting carbohydrates in a selective and efficient way into fine chemicals in this screening process.

The present study revealed that under basic conditions carbohydrates isomerise *via* well-known keto-enediol intermediates which are in equilibrium. Besides, observed decomposition reactions were also unselective. The addition of amines led to random Maillard products. Caramelisation products occurred constantly, especially at high temperatures. Furthermore, we could show that carbohydrates were not converted by applying metal catalysis, with the focus on oxidation reactions, or photo catalysis. Often, glucosylurea was formed during the reaction.

Acid catalysed reactions provided the most promising results. In choline chloride melts, acids catalyse the elimination of water molecules which leads to furfural derivatives, important organic platform chemicals. We illustrated the synthesis of 5-hydroxmethylfurfural (5-HMF) from L-sorbose and 5-(α-D-glucosyloxymethyl)furfural (GMF) from isomaltulose.

In general, glycosylureas are produced in sugar-urea melts from different aldohexoses as well as from ketohexoses under acidic conditions. They are remarkably stable and are stereoselectively formed in high yields and short reaction times. Slightly acidic conditions are sufficient to make them the preferred product. Thus, we could improve existing syntheses of glycosylureas by implementing a method using environmentally benign bulk chemicals without the need of a solvent. Accordingly, reactions times were reduced and yields were increased.

Summing up, we concluded that sugars show similar reaction behaviour in melts as in solution.

8. Zusammenfassung

Im Verlauf dieses Projektes wurden Säure-, Basen-, Metall- und Photokatalysatoren hinsichtlich ihrer Wirkung auf Kohlenhydrat-Schmelzen untersucht. Unser Ziel war es in einem „Screening"-Verfahren chemische Reaktionen zu finden, in denen Kohlenhydrate, speziell Monosaccharide, selektiv und effizient zu Feinchemikalien umgesetzt werden.

Unter Basen-, Metall- und Photokatalyse verliefen die Reaktionen unselektiv, weswegen sie hier nur kurz zusammengefasst werden. Basische Reaktionsbedingungen führten zu einer Epimerisierung von Glucose, die im Gleichgewicht mit Mannose und Fructose (und anderen epimeren Hexosen) vorlag. Ebenfalls unter basischen Bedingungen auftretende Abbaureaktionen wurden auch in der Schmelze beobachtet, waren aber nicht selektiv. Eine Vielzahl von Maillardprodukten entstand nach der Zugabe von Aminen. Bei den meisten Reaktionsansätzen entwickelten sich Karamellisierungsprodukte, insbesondere bei hohen Temperaturen. Des Weiteren wurden die Kohlenhydrate in Anwesenheit von Metall- oder Photokatalysatoren oft nicht umgesetzt; häufig war Glucosylharnstoff das bevorzugte Produkt. Vielversprechende Ergebnisse wurden unter sauren Bedingungen erhalten. In Cholinchlorid-Schmelzen wurden säurekatalysiert nach Abspaltung von Wassermolekülen Furfural-Derivate, wichtige organische Bausteine, erhalten. Auf diese Weise wurde 5-Hydroxymethylfurfural (HMF) aus verschiedenen Kohlenhydraten und 5-(α-D-Glucosyloxymethyl)furfural (GMF) ausgehend von Isomaltulose hergestellt. In Zucker-Harnstoff-Schmelzen war die Bildung von Glycosylharnstoffen, ausgehend von Hexosen und auch Ketosen, nach sehr kurzen Reaktionszeiten in hohen Ausbeuten auffallend. Glucosylharnstoff war oft das Hauptprodukt bei versuchten Oxidationsreaktionen und Photoreaktionen. Schwach saure Bedingungen sind offenbar ausreichend, dass dieser das bevorzugt gebildete Produkt ist.

Zusammenfassend zeigten unsere Versuche, dass die Zucker in der Schmelze ein ähnliches Reaktionsverhalten aufweisen wie in Lösung.

II. MELANOMA INHIBITORY ACTIVITY (MIA) PROTEIN INHIBITORS FOR THE TREATMENT OF MALIGNANT MELANOMA

Introduction and Goals

Over the last three decades, the incidence of malignant melanoma, a very aggressive type of skin cancer, increased drastically.[152] The survival rate of this malignant tumor of transformed melanocytes is extraordinarily poor once the melanoma has metastasised.[152] The formation of metastases already occurs at early stages of the disease and is further accompanied by uncontrollable growth of the highly invasive tumor.

Currently, the main therapeutic strategies are surgical resection and systemic chemotherapy, but they are not always effective.[153] It is therefore of utmost importance to develop new strategies for the treatment of malignant melanoma. New strategies involve immunotherapy and molecular targeting, e.g. inhibition of mutated BRAF and RAF kinase family members.[152]

Since the identification of melanoma inhibitory activity (MIA) protein in the early 1990s, it was shown to play a key role in development, progression and metastasis of malignant melanoma cells and was therefore assessed as interesting target to regulate the formation of metastases.[154, 155] Importantly, MIA protein, an 11 kDa protein is only expressed in malignant melanoma cells and early-phase differentiating chondrocytes, but not in normal melanocytes.[156, 157] In tumor cells secreted MIA inhibits the attachment of melanoma cells to the extracellular matrix (ECM) components like fibronectin, laminin, and tenascin *in vivo*.[158-160] These ECM structures are responsible for cellular adhesion (cellular 'glue') and interconnect the cells. The blocking of these binding sites by MIA protein reduces the cell matrix contacts, and thus enables the cell to migrate, invade and, finally, metastasise.

The three-dimensional structure of MIA protein was determined by multidimensional nuclear magnetic resonance (NMR) spectroscopy and X-ray crystallography techniques.[161-165] Further studies revealed that self-assembly of MIA protein is crucial

for functional activity; the dimers are assembled by head-to-tail orientation.[165, 166] By inhibiting the dimerisation and/or by inducing the dissociation of functionally active MIA dimers by e.g. small molecules, tumor cell invasion and formation of metastases could be reduced. Moreover, side effects of conventional chemotherapy targeting all fast dividing cells should be reduced as MIA protein is only expressed in malignant melanoma and differentiating chondrocytes. Such antimetastatic agents (which inhibit the dimerisation of MIA protein) would be a powerful tool in treatment of malignant melanoma.

A heterogeneous transition metal-based fluorescence polarization (HTFP) assay has been established to selectively screen for MIA dimerisation inhibitors. In this screening assay a dodecapeptide with the sequence Ac-FHWRYPLPLPGQ-NH_2, designated as AR71, was identified as particularly potent. NMR spectroscopy revealed that AR71 binds to the dimerisation domain of MIA protein.[167, 168] Furthermore, the inhibitory potential of this dodecapeptide was confirmed in *in vitro* and *in vivo* studies. After daily *i.v.* injections of AR71 into a mouse melanoma model, strongly reduced numbers of metastases were observed in the mice.[167, 168] After testing both mutated and truncated peptide sequences derived from AR71, hexa-, tetra-, and even tripeptides, were shown to inhibit MIA dimerisation much better than AR71.[165] Therefore, we focused our investigations on the following sequences: WWW, WHW, WHF, and furthermore FHWH and FHWRYP.

The major drawback of peptidic drug candidates is that the mammalian system has developed efficient barriers to restrict the intrusion of foreign macromolecules.[169] As a consequence, drug molecules are removed from the systemic circulation by these protective mechanisms and a therapeutic effect might not be achieved due to low concentrations at the target. The first barrier comprises proteolytic enzymes that degrade the protein. They are widely distributed over the human body and show their highest activity and the highest occurrence particularly in the intestinal tract.[169] Secondly, proteins have to overcome different absorption barriers, most important of these barriers is the passing over biological membranes.[169] Moreover, proteins are rapidly removed from the circulation by the liver and kidneys. To summarise, peptides exhibit a low bioavailability due to their poor pharmacokinetic properties: small

proteins are rapidly renally cleared from the bloodstream. Their short *in vivo* half-lifes (< 30 min) usually entails a frequent application.[170] Although oral application is most convenient, a parenteral delivery, e.g. *i.v.* injection, is necessary for this substance class to avoid the gastrointestinal tract and achieve high plasma concentrations.[171]

Different strategies are proposed to increase the bioavailability by improving pharmacokinetic properties (absorption, distribution, metabolism, extraction, toxicology (ADMET)) of peptide and protein drugs. We pursued two strategies in this work: the modification of the molecular structure to enhance the stability against enzymatic degradation and to increase the permeability across biological membranes. The second approach utilises the versatile tool of drug formulation, in particular sustained release systems.[169, 172]

We therefore modified the chemical structure of the lead peptide systematically: the amide bond in the peptide backbone was *N*-methylated (chapter 9.1) and the amide moiety was replaced by a pseudo-isosteric group (peptoid, chapter 9.2). Additionally, head-to-tail-cyclisation (chapter 9.3) of the lead structures should give more information about the bioactive conformer and structure-activity-relationships. The functional activity of the synthesised compounds was determined by HTFP assay, Western Blot analysis, and Boyden chamber invasion assay.

Equally important, PEGylated peptides (chapter 10.1), a lipid implant (chapter 10.2) and hydrogels (chapter 10.3) for sustained release were developed and the *in vitro* release kinetics were investigated.

9. Melanoma inhibitory activity (MIA) protein inhibitors – Synthesis and biological testing

MIA protein is an important factor in the formation of metastases of the malignant melanoma. Highly potent MIA inhibitors would be a powerful tool in the treatment of this type of skin cancer. Known MIA protein inhibitors are small peptidic molecules. To increase their *in vivo* stability, *N*-methylated **1**-**3** and cyclic derivatives **7**-**11**, as well as peptoids **4**-**6**, were synthesised and tested by *in vitro* methods: the heterogeneous transition metal-based polarisation (HTFP) assay and Western Blot analysis.

All compounds assembled by solid phase synthesis were synthesised by C. Ruß. The bifunctional poly(ethylene glycol) linker was kindly provided by Dr. Florian Schmidt, University of Regensburg.

The test assays of the biological activity were performed by Dr. Alexander Riechers, Institute of Molecular Pathology, Regensburg.

Introduction

A common approach to obtain more stable and bioactive peptides is to gradually transform the peptide into derivatives with a less peptidic character, termed peptide mimetics or also peptidomimetics. They are defined as derivatives of a (biologically active) peptide whose structural features should be analogous to the original peptide sequence. Moreover, the functional activity should be preserved or improved.[173, 174] The interested reader is referred to a small selection of excellent review articles covering this topic.[173, 175]

With this study, we aimed to get further insight into the structure-activity relationship of MIA protein inhibitors; but more importantly, we wanted to increase the metabolic stability of the peptides. To this end, we transformed known effective MIA protein inhibitors into peptidomimetics.

Results and Discussion

9.1 *N*-methylation of peptide backbone

A simple and efficient method nature uses to increase the stability against proteases and the membrane permeability (due to a higher lipophilicity) is the *N*-methylation of the amide moiety in the backbone of peptides.[176, 177] An additional substituent at the *N*-atom influences not only the pharmacological properties, but also the conformation of the molecule. Steric hindrance creates more rigid molecules with less conformational freedom favouring an extended (trans) conformation.[178, 179]

Alkylation of primary amines with alkyl halides and dialkyl sulfates often generates undesired tertiary amines and/or (quarternary) ammonium salts, as the reaction product is more nucleophilic than the starting material and reacts preferentially with the alkylating agent.[180] To circumvent this problem, the *N*-methylated peptides were synthesised by an optimised solid-phase method published by Biron *et al.*[181] which is based on a three-step procedure developed by Miller and Scanlan (Scheme 11).[182] Succinctly, the free amino group is protected and activated by an *o*-nitrobenzenesulfonyl group (*o*-NBS) which is followed by direct methylation (pathway A) or Mitsunobu reaction (pathway B). After deprotection, the coupling step was performed twice to complete the coupling of the sterically hindered *N*-atom.

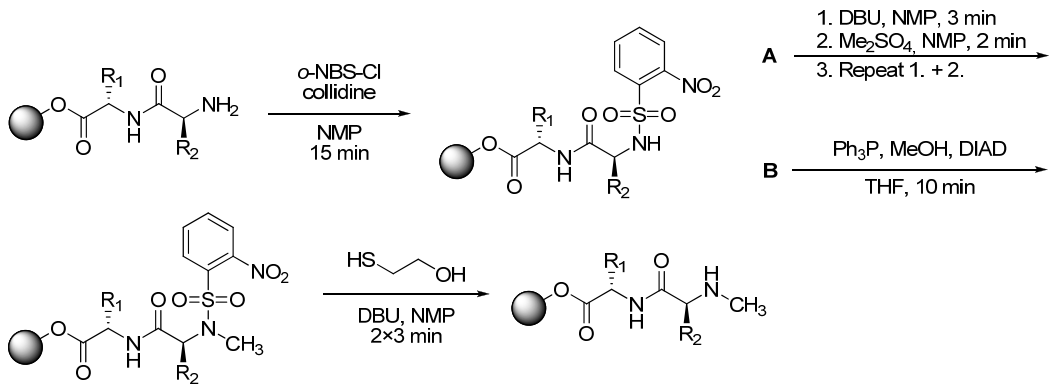

Scheme 11 Procedure of *N*-methylation on solid phase (according to literature[181]).

At first, an *N*-methyl scan of the tripeptides WHW, WHF, and WWW was carried out along the backbone of the peptides (Figure 4). Therefore, single amide bonds were systematically methylated at the *N*-atom. Accordingly, two derivatives per sequence were synthesised to cover all expedient sites of methylation.

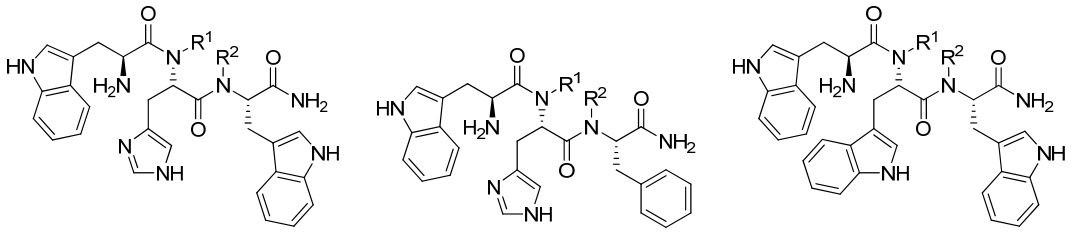

1a: R^1= H, R^2= CH_3, 52%
1b: R^1= CH_3, R^2= H, 42%
2a: R^1= H, R^2= CH_3, 41%
2b: R^1= CH_3, R^2= H, 35%
3a: R^1= H, R^2= CH_3, 21%
3b: R^1= CH_3, R^2= H, 27%

Figure 4 Structures and yields of the synthesised *N*-methylated MIA inhibitors **1**-**3**.

9.2 Peptoids (*N*-alkylated glycines)

Another way to replace the amide bond in the backbone is the transformation into peptoids (or *N*-alkylated glycines). This class of compounds is very versatile and easy to synthesise by a solid-phase submonomer synthesis protocol which will be described below (Scheme 12).[183] Peptoids are similar to retro-inverso peptidomimetics; the side chain which is normally attached to the α-C atom is shifted to the achiral amide nitrogen. Stereochemical information is lost as the backbone becomes also achiral. Another consequence is a gain of flexibility. Similar to *N*-methylation, the absent amide proton changes the stabilisation of the secondary structure of the peptoid oligomer by hydrogen bonding in comparison to the original peptide. Secondary structures, like α-helices, can then be induced by the introduction of chiral side chains.[184] These

structural changes further increase the hydrophobicity of the peptoid, thus improving permeability across cell membranes[185, 186] and enhancing protease resistance.[187, 188]

The most common synthesis approach to peptoids was developed by Zuckermann *et al*. in 1992 and is based on a submonomer solid-phase synthesis (Scheme 12).[183] Briefly, the oligomers are assembled from the *C*- to the *N*-terminus in two repetitive steps. The first step is a (DIC)-mediated acylation with chloro- or bromoacetic acid. In the second step, the halide is substituted by a primary amine.

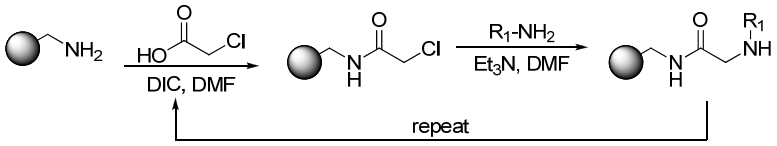

Scheme 12 Synthesis of peptoids by the submonomer method on solid phase (according to literature[183]).

The peptoids synthesised in this work had the same sequence of side chain residues as the original tripeptides WHW, WHF, and WWW (Figure 5). In addition to the compounds with free *N*-terminus, in a set of derivatives the *N*-terminus was acetylated to simulate the natural continuous amide bonds in the backbone of proteins.

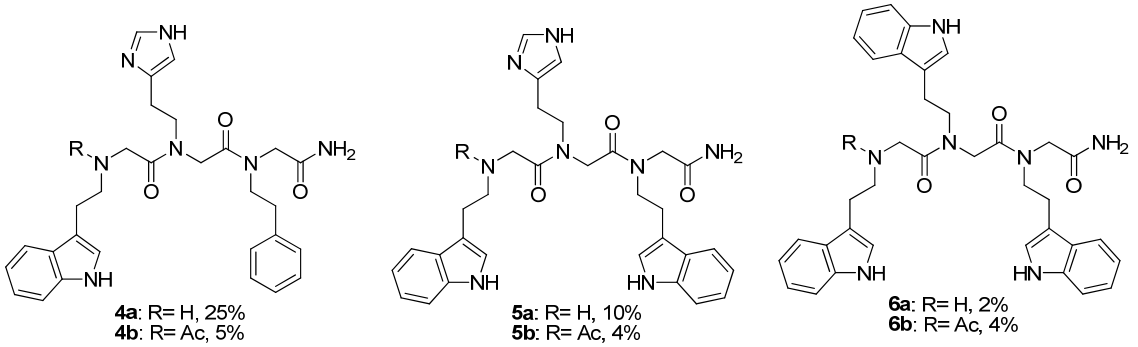

Figure 5 Structures and yields of peptoids **4**-**6**. **4a**-**6a**: free *N*-terminus, **4b**-**6b**: acetylated *N*-terminus.

9.3 Cyclisation

Naturally occurring macrocycles are a complex, and highly interesting substance class. They protrude by their numerous and diverse biological activities and favourable pharmacological properties. The peculiarity of cycles lies in the unusual structural combination of rigidity and flexibility. Ring formation results in a pre-organisation of functional groups in the molecule. One consequence is that the loss of entropy is reduced on binding to a biological target and the binding event is energetically more

favourable. Furthermore, pharmacological stability against proteolytic or metabolic degradation improves the bioavailability distinctly.[189] When the ring structure is pre-organised in such a way that it matches the bioactive conformation, a highly potent ligand with high affinities and selectivities can be achieved.[190]

These principles are also valid for cyclic peptides. The number of distinct conformations is notably reduced upon cyclisation of very flexible linear peptides.[191, 192] In addition, cyclic peptides are more resistant to exo- and endopeptidases. Although the macrocycles often do not abide to Lipinski's "rule of five" (which states that poor absorption or permeation of a drug is more likely when there are more than 5 H-bond donors, 10 H-bond acceptors, the molecular weight is greater than 500 Da and the calculated Log P is greater than 5)[193], they still expose drug like physico-chemical and pharmacological properties (like good solubility, lipophilicity, metabolic stability, bioavailability).[190] The use of cyclic peptides in therapy is still limited, but a growing field. The difficulty in designing cyclic peptide mimics is to retain the biological activity after changing the structure. It is therefore advantageous to know the role of each amino acid.[194]

Synthetically, linear peptides can be connected at four different sites: head-to-tail, side chain-to-tail, head-to-side chain, and side chain-to-side chain.[191] Generally, intramolecular cyclisations work out best under high dilution, thus intermolecular reactions (like oligo- and polymerisation) are less prone to occur. To exploit the practical advantages of solid phase synthesis, we followed the strategy to use the trifunctional amino acid aspartic acid as anchor to the resin in the first step. Furthermore, the *C*-terminus must be protected orthogonally to the here applied standard Fmoc protocol, which is termed three-dimensional orthogonal strategy.[195] The allyl group is especially suitable as it is stable against common acidic and basic conditions. For example, allyl carboxylates are readily removed in the presence of a soluble palladium catalyst (typically $Pd(PPh_3)_4$) while the allyl group is scavenged by a nucleophile.[196] After assembling the linear precursor on the solid phase, the protecting groups at the *C*- and *N*-termini were removed; the peptide sequence was then cyclised in a head-to-tail manner and the product was finally cleaved from the solid support. Although a "pseudo-dilution effect"[197] is described for reactions on solid phase, a resin

with especially low loading was chosen to avoid the formation of oligomers.[198] We introduced a small ethylene glycol spacer into the cyclic tripeptides (Scheme 13, n = 2) to reduce the ring strain, also enabling a regulation of the ring size. Furthermore, previous results showed an enhancement of activity of PEGylated peptides, (see chapter 10.1). The linker might also increase solubility and stability of the peptide. In addition to tripeptides, cyclic derivatives of the sequences FHWH and FHWRYP, also highly potent MIA inhibitors, were synthesised (Figure 6). The coupling reagent propane phosphonic acid anhydride (®T3P) was used for the crucial cyclisation step.[199] T3P is a mild and non-toxic reagent which is easy to handle. Amide bond formation proceeds with high yields and low epimerisation.[200] The best results were obtained applying the method patented by Mollenkopf (T3P, DIPEA, 2 d, rt).[201]

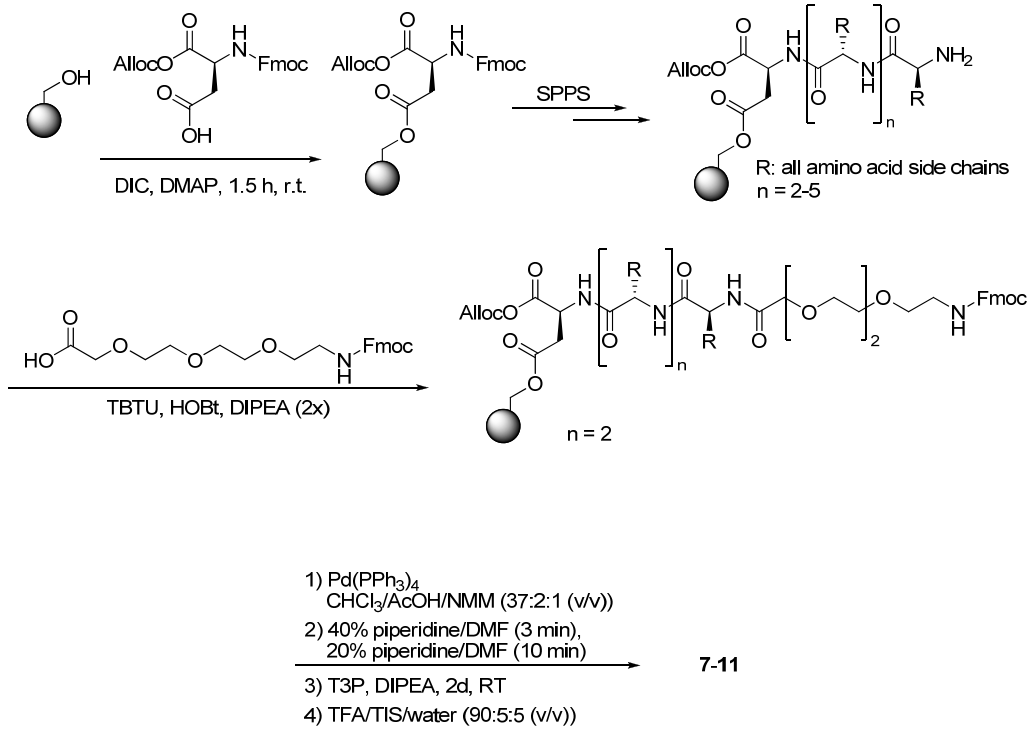

Scheme 13 Synthesis of cyclic peptides 7-11 on solid phase using Fmoc-Asp-OAlloc as trifunctional anchor. Into cyclic peptides derived from tripeptide sequences WHW, FWH, and WWW (n = 2), an ethylene glycol linker was introduced. For deprotection, ring closure, and cleavage the same procedures were used.

All steps of synthesis are depicted in Scheme 13. Initially, the Fmoc-Asp-OAlloc was anchored to the solid phase. Subsequently, the amino acids were coupled by standard Fmoc protocol. When only three amino acids were attached to the anchor, an ethylene

glycol linker was introduced by a double coupling step. After that step, the same conditions were used for all peptides. Before ring closure, first the Alloc group, then the Fmoc group at the amino terminus were removed. Lastly, the completed peptides **7**-**11** were cleaved from the solid support (Figure 6).

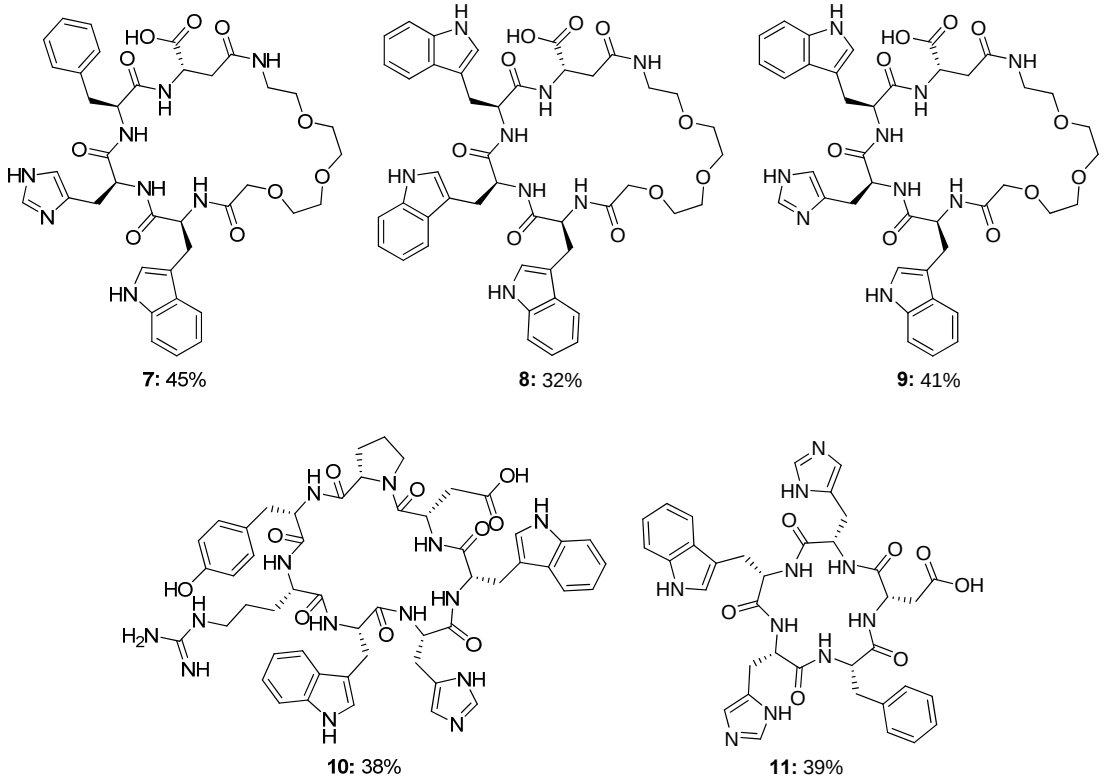

Figure 6 Structures and yields of synthesised cyclic peptides **7**-**11**. **7**-**9**: derived from tripeptides containing an ethylene glycol spacer, **10**-**11**: cyclic derivatives of tetra- and hexapeptides FHWH and FHWRYP, respectively.

9.4 A fast screening process was applied to find potential drug candidates

Novel active compounds were assessed using different reliable methods. In the screening process, three assays were performed in successive order:

1) Heterogeneous Transition Metal-based Fluorescence Polarization (HTFP) Assay
2) Western Blot Analysis
3) Boyden Chamber Invasion Assay

The subsequent tests were only performed if the tested compound was significantly potent in the previous test. Using the HTFP assay, the activity was determined in relation to the original peptide AR71 which serves as reference, and to the blank value (MIA bound the well surface). Therefore, the most important information we obtained from this assay was, whether the inhibitory performance of the newly synthesised compounds was increased or reduced in comparison to AR71 (or the blank value). In some cases the compounds were auto-fluorescent and interfering with the HTFP assay; in these cases, the Western Blot was used instead.

As the HTFP assay was especially developed by Riechers *et al*. to efficiently screen the biological activity of large libraries of potent MIA inhibitors, and most of the testing results are based on the outcome of the HTFP screening, the concept and the experimental setup will be outlined succinctly (Figure 7).[202]

Biotinylated MIA protein is immobilised on a streptavidin-coated well plate. This protein binds the $Ru(bpy)_3$-labelled MIA protein and forms dimers. In the absence of a competitive inhibitor $Ru(bpy)_3$-labelled MIA protein is tethered to the well's surface, dramatically increasing its apparent mass and slowing down rotational motion. This reduced molecular rotation results in an increase in fluorescence polarisation indicated by high values. In the presence of an inhibitor, the MIA protein is displaced from the immobilised MIA protein; the MIA dimers are cleaved. The newly formed inhibitor-MIA protein complex can now freely rotate in solution and the polarisation P is decreased. Physically possible values for P are ranging from -⅓ to ½.[203] Polarisation values are reported relative (P/P_0) to the value of free $Ru(bpy)_3$-labelled MIA in solution (P_0 (in a well not treated with MIA-biotin).

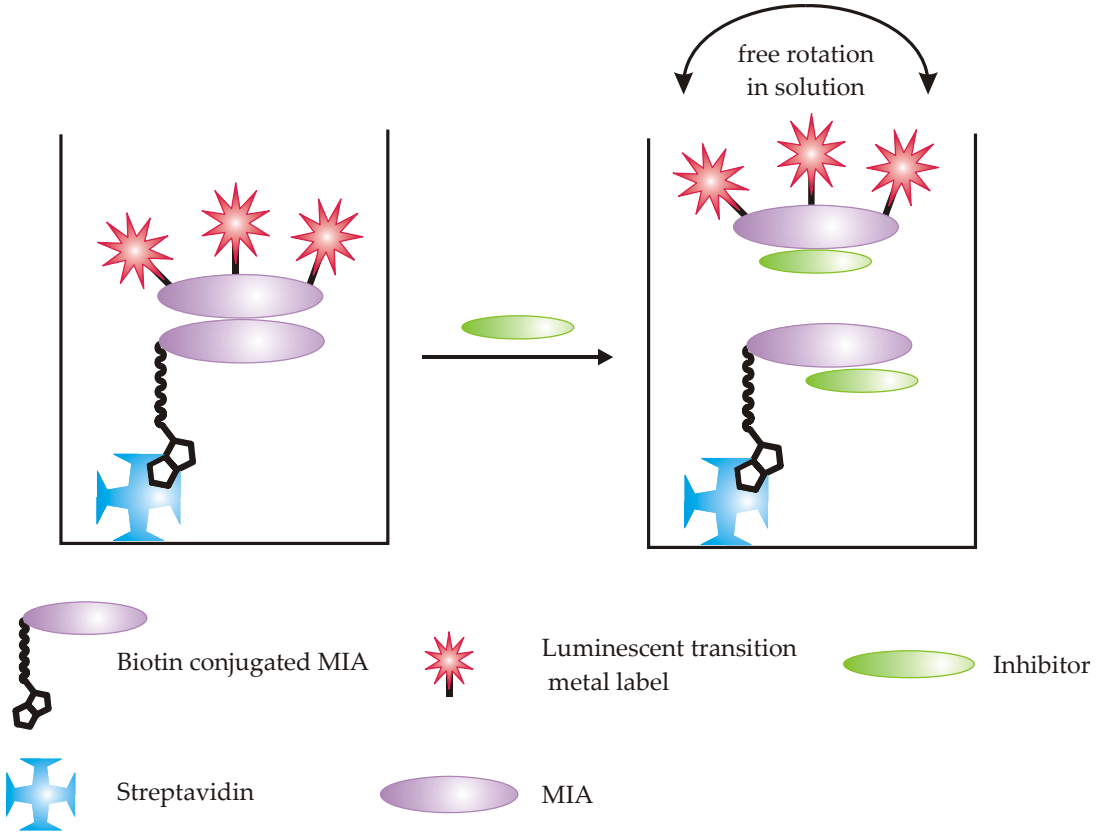

Figure 7 Concept of HTFP Assay: The biotin conjugated MIA protein is immobilised on a streptavidin coated well plate. MIA binds the Ru(bpy)$_3$-labelled MIA protein, forming dimers. In the absence of a competitive inhibitor Ru(bpy)$_3$-labelled MIA protein is tethered to the well's surface, dramatically increasing its apparent mass and slowing down rotational motion (left). In the presence of an inhibitor, the MIA protein is competitively displaced from the immobilised MIA (right). The newly formed inhibitor-MIA protein complex can now freely rotate in solution and the polarisation is decreased.

Western Blot analysis

For Western Blot analysis, MIA protein was pre-incubated with the potential inhibitors, before gel electrophoresis, blotting and immunodetection. In the presence of active compounds a dissociation of the MIA protein dimer was observed: the dimer bands were remarkably reduced compared to the control lane.

N-Methylation of peptide backbone

Although *N*-methylation seemed a very promising strategy, the first screening step, the HTFP assay, showed that all methylated peptides **1**-**3** were less active than the reference AR71. The polarisation values are higher than those of AR71, comparable to the blank without inhibitor (Figure 8).

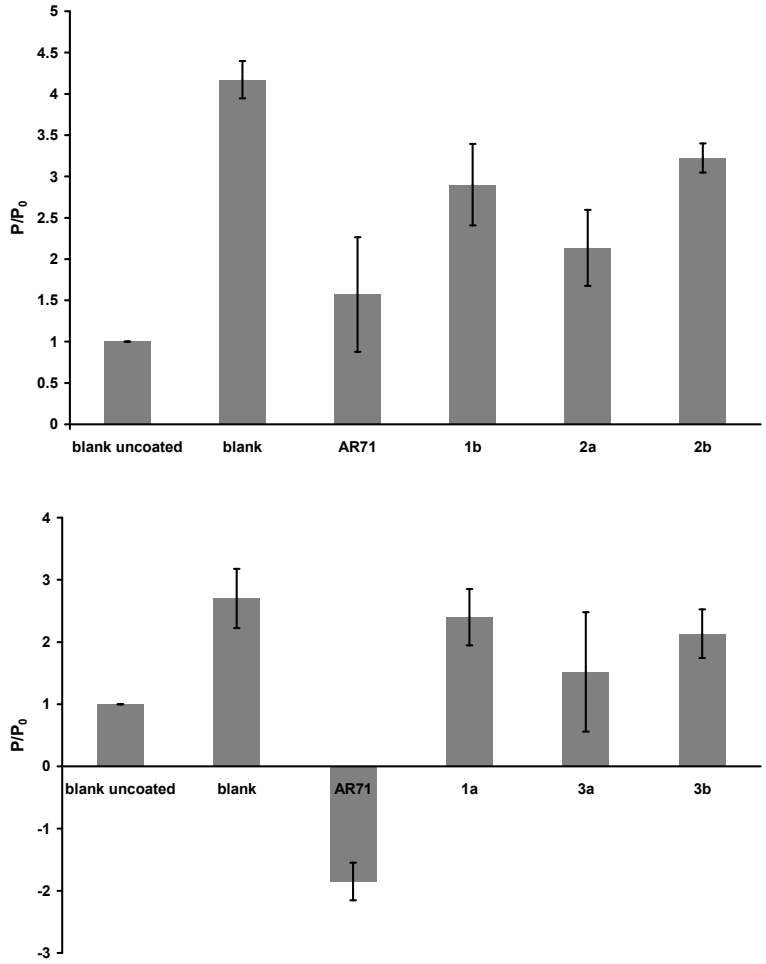

Figure 8 Results of the HTFP assay of *N*-methylated peptides **1-3**. The compounds were less effective inhibitors than AR71; there is only a small difference from the blank value. Blank uncoated: free MIA $Ru(bpy)_3$ protein in solution; Blank: MIA bound to another MIA protein on the surface.

Due to the low solubility of compounds **1b**, **2a**, and **2b**, the used concentration was ⅕ of the usual concentration (1.6 μM instead of 7.8 μM). Consequently, different polarisation values were measured for AR71 in both assays.

As the performance of the *N*-methylated peptides was mediocre, further testings were not carried out.

Peptoids

All *N*-alkylated glycines **4**-**6** were auto-fluorescent and therefore interfering with the HTFP assay. For this reason, this compound class was only investigated by Western Blot analysis. MIA protein dimers with a molecular weight of about 22 kDa were not significantly reduced; they also show an intensity which is comparable to the control lane containing only MIA protein without inhibitor (Figure 9).

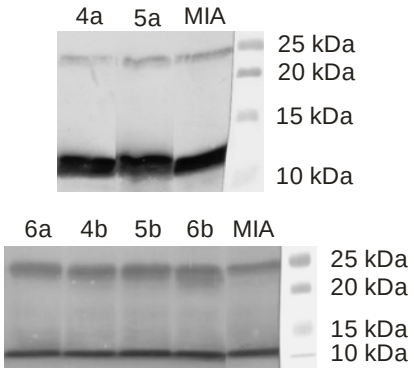

Figure 9 Results of the Western Blot analysis for the peptoids **4**-**6**. MIA dimers (22 kDa, right lane) are still formed in the presence of the compounds **4**-**6**.

Cyclic peptides

The HTFP assay showed that also the cyclic peptides **7**-**11** were less potent than AR71 (Figure 10A) HTFP assay **7**-**9** (Figure 10B). Heptapeptide **11** could not be tested with this method as it was auto-fluorescent. The HTFP assay showed that the polarisation was comparable to the blank value without any inhibitor. These results were also confirmed by the Western Blot: the amount of dimers was similar to the untreated MIA protein (right).

A

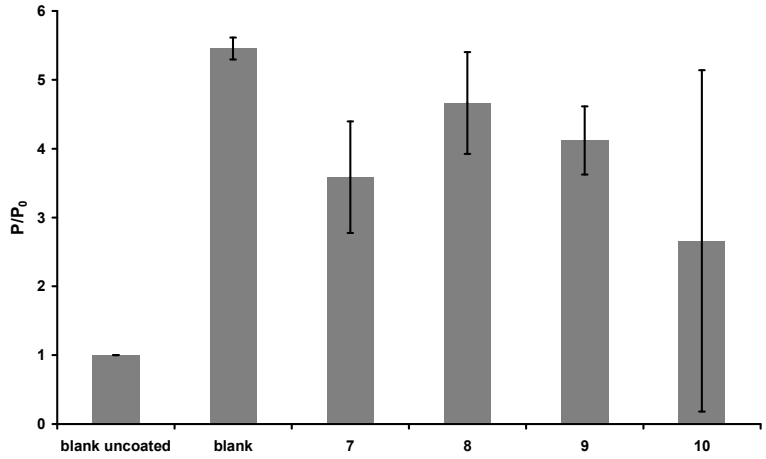

B

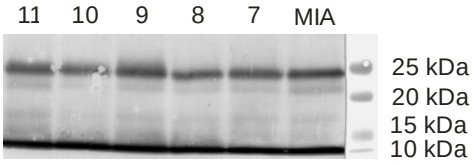

Figure 10 Results of **A)** HTFP assay **7**-**9** (**11** was auto-fluorescent and could not be measured) and **B)** Western Blot analysis of cyclic peptides **7**-**11**. The compounds were less effective inhibitors than AR71; there is only a small difference from the blank value. MIA dimers (22 kDa, right lane) are still formed in the presence of the compounds **7**-**11**.

Truncated and mutated peptide sequences derived from AR71 with up to twelve amino acids were discovered to inhibit the dimerisation of MIA protein, an important factor in metastasis of malignant melanoma. What kind of picture does literature give to imagine these protein-protein interactions between two (or more) MIA protein monomers on a molecular level? Such homodimers interact *via* their surface amino acids. So-called hot spots stabilise the dimeric complex by contributing most of the binding energy and are crucial for the affinity of the interaction.[204, 205] These hot spots are clustered regions buried in the centre of the protein.[204] Another characteristic feature of dimer protein-protein interfaces is that they expose structural properties of both, interior and exterior protein surfaces, but more similar to the exterior.[206] The area of the interface contains, similar to other proteins, mostly non-polar side chains which are buried in the interior of the interface and polar and charged groups are prevalently found in the exterior.[206, 207] Statistically, the amino acid composition in protein-protein interaction sites is enriched in tryptophane (21%), arginine (13.3%) and tyrosine (12.3%), while it is less likely to find leucine, methionine, serine, threonine and valine residues (less than 3%).[208] In contrast to protein monomers, polar and charged residues play a significant role in the stabilisation of the protein assemblies by hydrogen bonds and salt bridges (larger percentage than in monomers).[209]

With regard to MIA protein, NMR titration of MIA with AR71 revealed that the residues C17, S18, Y47, G66, D67, L76, W102, D103 and C106 of MIA protein are clearly involved in the binding at the interface. The interacting amino acids in the binding sites of MIA protein are mainly composed of hydrophobic and aromatic residues, followed by acidic and neutral residues, reflecting the above described picture of the possible binding mode. Another aspect underpinning this concept is that hydrophobic and aromatic amino acids predominate in the small peptidic inhibitors and seem to be crucial for the binding interaction.

All synthesised candidates were less active than the parent compound AR71 and the unmodified peptides (showed a diminished activity compared to) which was shown in the initial screening test, the HTFP assay and the Western Blot analysis.

Certainly, the structural modifications altered the interaction with the target structure. A change of the ligand conformation might impede that the compound binds to the interacting area of the MIA dimers.

Conformational changes are to be expected for *N*-methylated and cyclised peptides. Methyl groups are bulkier than an *H*-atom. They impose the side chain residues to adopt a certain conformation, preferably trans conformation, and also rigidify the molecule.[177] Similarly, ring formation introduces conformational restraints and reduces the number of possible conformations. The cyclic peptides with a strongly restricted conformation did obviously not match the bioactive conformation.

Possibly, the *H*-atom at the amide nitrogen plays an important role in peptide-MIA protein interactions, e.g. *via* hydrogen bonds, as both *N*-methyl and peptoids lack that moiety and both are less potent MIA protein inhibitors than the native parent peptides.

Unexpectedly, ethylene glycol spacers did not improve solubility; on the contrary, the hydrophobicity of the molecules was increased.

Conclusion

Backbone modifications of known MIA inhibitory peptides were synthesised and tested for their ability to inhibit MIA dimerisation. *N*-methylation, cyclisation, and transformation to peptoids might have resulted in the desired enhanced metabolic stability, but also reduced the potency in comparison to the original inhibitors.

We conclude that change of conformation and loss of an *H*-bond donor are the reasons for the mediocre activity. Although we gained more information on the structure activity relationship of the MIA inhibitors, a promising candidate was not found. The synthesis of more modified derivatives to find an active compound might be supplemented by computer-assisted methods, like docking studies.

Experimental

General. Commercial reagents and starting materials were purchased from Aldrich, Fluka or Acros and used without further purification. Fmoc-protected amino acids were acquired from Iris Biotech GmbH; coupling reagents and resins from NovaBiochem (Darmstadt, Germany). The coupling agent T3P was a kind gift of Archimica, (Frankfurt/M, Germany). Mass spectra were recorded on a ThermoQuest Finnigan TSQ 7000 LC/MS spectrometer (low resolution), high resolution spectra (HRMS) on an Agilent Tech 6540 UHD Accurate Mass Q-TOF LC/MS and with Finnigan MAT TSQ 7000 (ESI) spectrometer.

Analytical HPLC

Column: Phenomenex Luna 3 um C18 (2) 100 A, 150 mm x 2.00 mm,

Agilent 1100/1; G1312A Bin Pump, G1313A ALS; G1316A COLCOM, G1315B DAD, G1379 DEGASSER, G1321A FLD; software: ChemStation for LC 3D Systems Rev B.04.02 SP1; column temperature: 25 °C, FLD-A, ELS; Column temperature: 25 °C, FLD-A, ELS; UV detection at 220 nm, fluorescence detection: zero-order. Gradient: from 3% MeCN/H_2O (0.0059% TFA) to 98% MeCN/H_2O (0.0059% TFA) within 30 min. Flow rate: 0.3 mL/min, injection volume: 1 μL;

Preparative HPLC

Column: Phenomenex Luna 10 um C18(2) 100 A, 250 x 21.1 mm

Agilent 1100 Series; Software: Chemstation for LC 3D Systems Rev. B03.02

Peptidomimetics

Sequence: H-W-H-W(Me)-NH_2 (1a)

TFA: 0.059 %

Yield: 8.1 mg, 52%

HPLC (analytic): R_t = 12.135 min (DAD), 12.271 min (ELSD); LC/MS (ESI): m/z = 541.2 (MH^+) (R_t = 12.89 min, 100%); ESI: m/z = 291.5 $(M+2H)^{2+}$ + MeCN (R_t = 9.77 min, 100%), 541.1 (MH^+)(83%); HPLC (preparative): Gradient (t (min), % B: (0, 3), (12, 37), (15, 95), (25, 95), R_t = 10.72 min; Empirical formula: $C_{29}H_{32}N_8O_3$, MW = 540.62

Sequence: H-W-H(Me)-W-NH_2 (1b)

Yield: 6.3 mg, 42%

HPLC (analytic): R_t = 8.122 min (DAD), 8.213 min (ELSD); LC/MS (ESI): m/z = 291.6 $(M+2H)^{2+}$ + MeCN (R_t = 6.90 min, 100 %), 541.2 (MH^+) (39 %); ESI: m/z = 291.6 $(M+2H)^{2+}$ + MeCN (R_t = 4.17 min, 100 %), 541.1 (MH^+)(23 %); HPLC (preparative): Gradient (t (min), % B: (0, 5), (12, 60), (14, 98), (22, 98), R_t = 6.61 min Empirical formula: $C_{29}H_{32}N_8O_3$, MW = 540.62

Sequence: H-W-H-F(Me)-NH_2 (2a)

Yield: 5.9 mg, 41%

HPLC (analytic): R_t = 8.067 min (DAD), 8.145 (ELSD) min; LC/MS (ESI): m/z = 502.1 (MH^+) (R_t = 5.73 min, 100%); ESI: m/z = 272.0 $(M+2H)^{2+}$ + MeCN (R_t = 4.05 min, 100%), 502.2 (MH^+)(46%); HPLC (preparative): Gradient (t (min), % B: (0, 5), (12, 60), (14, 98), (22, 98), R_t = 6.61 min; Empirical formula: $C_{27}H_{31}N_7O_3$, MW = 501.58

Sequence: H-W-H(Me)-F-NH_2 (2b)

Yield: 5.0 mg, 35%

HPLC (analytic): R_t = 8.126 min (DAD), 8.213 (ELSD) min; LC/MS (ESI): m/z = 272.0 $(M+2H)^{2+}$ + MeCN (R_t = 6.14 min, 100%), 502.1 (MH^+)(74%); ESI: m/z = 272.0 $(M+2H)^{2+}$ + MeCN (R_t = 4.27 min, 100%), 502.2 (MH^+)(20%); HPLC (preparative): Gradient (t (min), % B: (0, 5), (12, 60), (14, 98), (22, 98), R_t = 6.61 min; Empirical formula: $C_{27}H_{31}N_7O_3$, MW= 501.58

Sequence: H-W-W-W(Me)-NH_2 (3a)

Yield: 3.4 mg, 21%

HPLC (analytic): R_t = 13.581 min (DAD), 13.649 min (ELSD); LC/MS (ESI): m/z = 590.2 (MH^+) (R_t = 12.90 min, 100%); ESI: m/z = 590.1 (MH^+) (R_t = 13.88 min, 100%); HPLC (preparative): Gradient (t (min), % B: (0, 3), (13, 44), (15, 98), (25, 98), R_t = 12.215 min; Empirical formula: $C_{34}H_{35}N_7O_3$, MW = 589.69

Sequence: H-W-W(Me)-W-NH_2 (3b)

Yield: 4.5 mg, 27%

HPLC (analytic): R_t = 13.896 min (DAD), 13.966 min (ELSD); LC/MS (ESI): m/z = 590.2 (MH^+) (R_t = 13.19 min, 100%); ESI: m/z = 590.1 (MH^+) (R_t = 14.14 min, 100%); HPLC (preparative): Gradient (t (min), % B: (0, 3), (13, 44), (15, 98), (25, 98), R_t = 12.505 min; Empirical formula: $C_{34}H_{35}N_7O_3$, MW = 589.69

Sequence: H-nW-nH-nF-NH_2 (4a)

Yield: 1.5 mg, 25%

HPLC (analytic): R_t = 10.125 min (DAD), 10.256 min (ELSD); LC/MS (ESI): m/z = 530.1 (MH^+) (R_t = 9.78 min, 100%); ESI: m/z = 285.9 $(M+2H)^{2+}$ + MeCN (R_t = 4.17 min, 100%), 530.1 (MH^+)(58%); HPLC (preparative): Gradient (t (min), % B: (0, 3), (12, 41), (15, 98), (25, 98), R_t = 8.32 min; Empirical formula: $C_{29}H_{35}N_7O_3$, MW = 529.63

Sequence: Ac-nW-nH-nF-NH_2 (4b)

Yield: 1.0 mg, 5%

HPLC (analytic): R_t =12.623 min (DAD), 12.709 min (ELSD); LC/MS (ESI): m/z = 572.2989 (MH^+) (R_t = 9.493 min, 100%); ESI: m/z = 572.2 (MH^+) (R_t = 4.94 min, 100%); HPLC (preparative): Gradient (t (min), % B: ((0, 3), (15, 50), (17, 98), (25, 98), R_t = 11.172 min; Empirical formula: $C_{31}H_{37}N_7O_4$, MW = 571.67

Sequence: H-nW-nH-nW-NH_2 (5a)

Yield: 1.5 mg, 10%

HPLC (analytic): R_t = 10.118 min (DAD), 10.218 min (ELSD); LC/MS (ESI): m/z = 569.1 (MH^+) (R_t = 10.0 min, 100%); ESI: m/z = 305.4 $(M+2H)^{2+}$ + MeCN

(R_t = 4.20 min, 100%), 569.1 (MH^+)(74%); HPLC (preparative): Gradient (t (min), %B: (0, 3), (12, 41), (15, 98), (25, 98), R_t = 8.360 min; Empirical formula: $C_{31}H_{36}N_8O_3$, MW = 568.67

Sequence: Ac-nW-nH-nW-NH_2 (5b)

Yield: 0.6 mg, 4%

HPLC (analytic): R_t = 12.722 min (DAD), 12.797 min (ELSD); LC/MS (ESI): m/z = 611.3098 (MH^+) (R_t = 9.545 min, 100%); ESI: m/z = 611.2 (MH^+) (R_t = 4.95 min, 100%); HPLC (preparative): Gradient (t (min), % B: (0, 3), (15, 50), (17, 98), (25, 98), R_t = 11.178 min; Empirical formula: $C_{33}H_{38}N_8O_4$, MW = 610.71

Sequence: H-nW-nW-nW-NH_2 (6a)

Yield: 0.3 mg, 2%

HPLC (analytic): R_t = 15.104 min (DAD), 15.174 min (ELSD); LC/MS (ESI): m/z = 618.3 (MH^+) (R_t = 15.1 min, 100%); ESI: m/z = 618.3 (MH^+) (R_t = 5.58 min, 100%); HPLC (preparative): Gradient (t (min), % B: (0, 3), (15, 50), (18, 98), (25, 98), R_t = 13.681 min; Empirical formula: $C_{36}H_{39}N_7O_3$, MW = 617.74

Sequence: Ac-nW-nW-nW-NH_2 (6b)

Yield: 0.7 mg, 4%

HPLC (analytic): R_t = 19.361 min (DAD), 19.427 min (ELSD); LC/MS (ESI): m/z = 660.3302 (MH^+) (R_t = 16.225 min, 100%); ESI: m/z = 660.3 (MH^+) (R_t = 6.65 min, 100%); HPLC (preparative): Gradient (t (min), % B: (0, 3), (19, 63), (21, 98), (25, 98), R_t = 18.539 min; Empirical formula: $C_{38}H_{41}N_7O_4$, MW = 659.78

Sequence: D-F-H-W-PEG (7)

Yield: 14.1 mg, 45%

HPLC (analytic): R_t = 12.175 min (DAD), 12.245 min (ELSD); LC/MS (ESI): m/z = 775.3409 (MH^+) (R_t = 8.314 min, 100%);

Empirical formula: $C_{38}H_{46}N_8O_{10}$, MW = 774.82

Sequence: **D-W-W-W-PEG (8)**

Yield: 11.2 mg, 32%

HPLC (analytic): R_t = 18.187 min (DAD), 18.258 min (ELSD); LC/MS (ESI): m/z = 863.5 (MH^+) (R_t = 18.04 min, 100%);

Empirical formula: $C_{45}H_{50}N_8O_{10}$, MW = 862.93

Sequence: **D-W-H-W-PEG (9)**

Yield: 13.3 mg, 41%

HPLC (analytic): R_t = 12.514 min (DAD), 12.590 min (ELSD); LC/MS (ESI): m/z = 814.4 (MH^+) (R_t = 12.53 min, 100%);

Empirical formula: $C_{40}H_{47}N_9O_{10}$, MW = 813.86

Sequence: **D-W-H-W-R-Y-P (10)**

Yield: 15.9 mg, 38%

HPLC (analytic): R_t = 10.574 min (DAD), 10.650 min (ELSD); LC/MS (ESI): m/z = 521.4 $(M+2H^+)^{2+}$ (R_t = 10.43 min, 100%);

Empirical formula: $C_{52}H_{60}N_{14}O_{10}$, MW = 1041.12

Sequence: D-H-W-H-F (11)

Yield: 11.0 mg, 39%

HPLC (analytic): R_t = 9.253 min (DAD), 9.341 min (ELSD); LC/MS (ESI): m/z = 382.5 ($M+2H^+$ + MeCN) (R_t = 9.04 min, 100%), 723.3 (MH^+, 30%); ESI: m/z = 382.6 ($M+2H^+$ + MeCN) (R_t = 3.82 min, 100%), 723.5 (MH^+, 42%); HPLC (preparative): Gradient (t (min), % B: (0, 3), (9, 31), (12, 98), (22, 98), R_t = 7.277 min

Empirical formula: $C_{36}H_{38}N10O_7$, MW = 722.75

Solid Phase Peptide Synthesis

General procedure

All peptides were prepared manually on 50 mg of Rink amide MBHA resin (loading 0.56 mmol g^{-1}) using Fmoc chemistry in BD discardit II syringes. Solvents and soluble reagents were removed by suction. The following side-chain protections were applied: tBu (Tyr), Boc (Trp), Mtt (His) and Pbf (Arg). Rink amide MBHA resin was weighed in a syringe equipped with a frit and swollen in DMF for 30 min. Afterwards, the corresponding Fmoc protected amino acid (5 eq) in NMP and the coupling reagents HOBt/TBTU/DIPEA (5:4.5:10 eq) in DMF were added.

A single coupling procedure (45 min) was sufficient as the peptide sequences were short. Fmoc removal followed with piperidine in DMF (80:20, v/v) for 3 min plus 10 min (20% base in DMF). After completion, the resin was washed with DMF, MeOH, DCM and Et_2O (5 times each).

The *N*-terminal acetylation is recommended for the preparation of protein fragments, as the *N*-acetyl group and the amide group better resemble the native situation and avoid the presence of positive and negative charges not present in a protein backbone. For *N*-terminal acetylation acetic anhydride (10 eq), DIPEA (10 eq) and DMF were added to the preswelled peptidyl-resin and the reaction was allowed to run for 30 min. Final cleavage of the peptides from the resin and simultaneous side-chain deprotection was achieved by treatment of the peptidyl resin with 1.5 mL of a TFA/TIS/water (90:5:5 (v/v)) mixture for 3 h. The TFA solution was collected in a Falcon tube and reduced in volume to about 0.5 mL. The peptide was precipitated with cold Et_2O and the suspension was centrifuged at -4 °C for 10 min. The supernatant was discarded and the precipitate was washed again with ice-cold ether. This procedure was repeated five times to remove most of the scavengers. Finally, the precipitate was dried under vacuum.

General procedure for the synthesis of *N*-methylated Peptides 1-3

Peptide chain elongation was performed by the general procedure described above. *N*-Methylation was achieved by the three-step procedure optimised by Biron *et al*.[181] Briefly, the free terminal amino group was protected with a solution of *o*-NBS-Cl (4 eq) and collidine (10 eq) in NMP. The mixture was shaken for 15 min at room temperature and the resin was washed with NMP (5×). Then, a solution of DBU (3 eq) in NMP was added to the resin bound *o*-NBS-protected peptides and shaken for 3 min. After addition of a solution of dimethylsulfate (10 eq) in NMP the reaction mixture was shaken for 2 min. The solution was drained and the resin was washed once with NMP. The *N*-methylation procedure was repeated once more and the resin was washed with NMP (5×). Mitsunobu conditions were applied to avoid the side chain *N*-methylation of His (Trt). The resin-bound *o*-NBS-protected peptides were treated with a solution of triphenylphosphine (5 eq) and MeOH (10 eq) in dry THF for 1 min. A solution of DEAD (5 eq) in dry THF was then added portionwise to the reaction mixture and

shaken for 10 min at room temperature. The resin was washed with NMP (5×). Finally, the o-NBS group was cleaved by shaking the resin bound N^{α}-methyl-N^{α}-*o*-NBS-peptides with mercaptoethanol (10 eq) and DBU (5 eq) in NMP for 5 min. The deprotection procedure was repeated once more and the resin was washed with NMP (5×). The coupling of the next amino acid to the resin-bound N^{α}-methylamine free peptide was accomplished by shaking it with a solution of Fmoc-amino acid (3 eq), HATU (3 eq), HOAt (3 eq), DIEA (6 eq) in NMP for 2 h at room temperature. The coupling was repeated once more and the resin was washed with NMP (5×). Final cleavage of the peptides from the resin and simultaneous side-chain deprotection was achieved by treatment of the peptidyl resin with 1.5 mL of a TFA/TIS/water (90:5:5 (v/v)) mixture for 3 h.

General procedure for the synthesis of peptoids 4-6

Peptoids were synthesised according to a solid-phase submonomer method published by Quintanar-Audelo *et al*.[210]

Preswelling of the Rink Amide MBHA resin in DMF and deprotection of the Fmoc group was followed by acylation. A solution of chloroacetic acid (6 eq) and DIC (3 eq) in DMF was added to the resin, shaken for 1 h at room temperature and washed with DMF. For amination, a solution of amine (4 eq) and triethylamine (4 eq) in DMF was added to the resin and shaken for 4 h. Acylation and amination steps were successively repeated for chain assembly. *N*-terminal acetylation was achieved by shaking the resin with acetic anhydride (10 eq) and DIPEA (10 eq) in DMF for 30 min. The peptoids were cleaved by adding a mixture 2.0 mL of a TFA/DCM/anisole (49:49:2 (v/v)) solution for 1 h. Alternatively, 2.0 mL of a TFA/DCE/water (49:49:2 (v/v)) mixture can be used.

General procedure for the synthesis of cyclised peptides 7-11

All peptides were prepared manually on 100 mg of Wang resin LL preloaded with Fmoc-Asp-OAlloc (loading 0.4 mmol g^{-1}) using Fmoc chemistry in BD discardit II syringes.

Preloading of Wang resin with Fmoc-Asp-OAlloc (according to Alcaro *et al.*)[198]

1.5 g of a low loading Wang resin (0.44 mmol g^{-1}) were preswelled in DMF for 30 min. DIC (153 µL, 124 mg, 1.5 eq) was added to a solution of Fmoc-Asp-OAll (784 mg, 3 eq)

in dry DCM (10 mL) and the mixture was stirred at 0 °C under N_2 for 20 min. Then, the solution was concentrated and the residue dissolved in DMF (5 mL) (1). A second solution, containing DMAP (6.5 mg, 0.8 eq, 0.5 eq referred to DIC) in DMF (0.5 mL), was prepared (2). Both solutions (1+2) were added to the preswelled Wang resin and were shaken for 1 h. The resin was washed with DMF (3×2 min) and DCM (2×2 min). After endcapping with acetic anhydride (1.2 mL, 20 eq) and NMM (2.5 mL, 20 eq) in DCM (5 mL) for 1.5 h, the resin was washed with DCM (2×2 min), DMF (2×2 min) and DCM (2×2 min) and was dried under vacuum. The resin loading (0.4 mmol g^{-1}) was determined from the Fmoc release monitored by UV absorption at 290 nm.

Amino acids were assembled according to the standard Fmoc protocol. A double coupling step was performed for Fmoc-protected amino-PEG-acid spacer which were synthesized by Florian Schmidt.[211]

Removal of allyl protecting group (according to Kates *et al.*)[195]

The peptidyl resin was placed in a dry reaction tube and dried under high vacuum. A mixture of $CHCl_3$/AcOH/NMM (37:2:1 (v/v), 4 mL) was added and degassed using 4-5 freeze-pump-thaw cycles. After addition of $Pd(PPh_3)_4$ (3 eq), the reaction mixture was left to stand for 2 h in the dark with occasional gentle agitation. The resin was washed with DMF, a solution of 0.5% DIPEA in DMF (2×2 min), a solution of 0.5% sodium diethyldithiocarbamate in DMF (3×15 min), and finally with DMF, MeOH, DCM, and Et_2O (5×2 mL each). The free carboxyl group was confirmed by the malachite green test.[212] The Fmoc deprotected peptide was cyclised on the solid phase by a method published by Mollenkopf *et al*.[201] A solution of DIPEA (6 eq) and T3P (6 eq) in ethyl acetate (50 % (w/w)) in DMF was added to the resin and shaken for 48 h at room temperature. After washing with DMF, MeOH, DCM, and Et_2O (5×2 mL each), the peptide was cleaved from the resin with 1.5 mL of a TFA/TIS/water (90:5:5 (v/v)) mixture for 3 h.

Coating of well plates with MIA-biotin, HTFP assay setup, and Protein analysis in vitro (Western Blotting) were performed according to literature.[166]

10. Evaluation of different devices for the delivery of melanoma inhibitory activity (MIA) protein inhibitors

MIA protein is an important factor in the formation of metastases of the malignant melanoma. Highly potent MIA inhibitors would be a powerful tool in the treatment of this kind of skin cancer. Small peptidic molecules are known to inhibit the functional activity of MIA protein. However, administration of peptides and proteins requires an efficient protection against enzymatic degradation or extreme pH values. As therapeutic proteins are generally readily degraded, they only exhibit a low plasma concentration. To reduce the injection frequency, various drug delivery systems were investigated, including agents with covalently attached poly(ethylene glycol) (PEG) chains, a lipid implant, and injectable PEG hydrogels.

All *in vitro* release studies were carried out by C. Ruß. The lipid implant was kindly produced by Angelika Berié, Department of Pharmaceutical Technology, University of Regensburg. The technology and precursors for poly(ethylene glycol) hydrogels were provided by the Department of Pharmaceutical Technology, University of Regensburg. All test assays of the biological activity were performed by Dr. Alexander Riechers, Institute of Molecular Pathology, Regensburg.

Introduction

The challenging task to deliver therapeutic proteins efficiently to their biological target is impeded by their lack of stability, immunogenicity, and short half-life, resulting in a low bioavailability. We focused on two approaches to overcome these obstacles: the change of the molecular structure of the lead compounds and the change in formulation under retention of the original molecular structure. As we could see from our previous results (chapter 9), the modification of the chemical structure of the lead compound is often connected with the risk of losing or diminishing the functional activity at the target. For this reason, we also pursued the strategy to deliver the unchanged drug candidate by an appropriate drug delivery system. According to Jain, a drug delivery system is defined as " a formulation or a device that enables the introduction of a therapeutic substance in the body and improves its efficacy and safety by controlling the rate, time, and place of release of drugs in the body."[171] Furthermore, the drug delivery system protects the embedded drug from detrimental effects of the environment catalysing the degradation of the protein, like extreme pH values and high temperatures. By administering the drug *via* different anatomical routes, e.g. transdermal, nasal, pulmonary, oral, intravenous, and subcutaneous, some of these barriers can be circumvented. Furthermore, various formulations or devices can be applied such as tablets, emulsions, liposomes, polymers, implants or implanted pumps.[171]

The goal of this study was to find a device that gradually releases the incorporated therapeutic agent. As a prerequisite, the device has to be small enough to be applicable in animal models, specifically in mice. To this end, various drug delivery systems were investigated, including agents with covalently attached poly(ethylene glycol) (PEG) chains (chapter 10.1), a lipid implant (chapter 10.2), and injectable PEG hydrogels (chapter 10.3).

10.1 Conjugation of poly(ethylene glycol) to melanoma inhibitory activity (MIA) inhibitors and biological evaluation

Introduction

One example, which will be illustrated in the following, is the covalent attachment of macromolecules to the therapeutic agent. Hence, the change of physico-chemical properties alters the pharmacodynamic and pharmacokinetic profile. The conjugation of poly(ethylene glycol) (PEG) to an active compound (PEGylation) is meanwhile a common method (in protein delivery) and has resulted in several clinically approved products.[213]

In literature, many reviews summarised the effects of PEGylation, only a small selection of synthetic strategies of PEGylation is shown here.[214-216] The most prominent features of PEG are now recapitulated.

Linear and branched PEGs are accessible in a wide range of molecular weights. From the chemical point of view, PEGs are inexpensive, non-toxic, chemically stable, highly soluble in water and in many organic solvents and are available with a low polydispersity index (PDI); many reactions are established for derivatisation and they are approved for human use by the FDA (U.S. Food and Drug Administration).[213] The most salient features of PEGylated drugs are a prolonged blood circulation time, an increase in stability against metabolic enzymes, and a reduced immunogenicity.[217-219] Attachment of PEG increases the size and the molecular weight of the original compound, and also its hydrophilicity. One effect is a decreased rate of (size-dependent) kidney clearance. The PEG moiety also forms a kind of shell around the molecule, thus protecting it against uptake and clearance by the reticuloendothelial system (RES). This shell also masks antigenic sites and consequently the formation of neutralising antibodies is reduced. But this is only one side of the coin. PEGylation can change the conformation and electrostatic binding properties of the derivatised compound. Furthermore, the PEG shield often creates steric hindrance which results in a reduction of biological activity and binding affinity to the target structure. Nevertheless, many studies proved that the favourable features of this method often prevail over the disadvantages.[217]

The aim of this study was to evaluate if PEGylation of MIA inhibiting tripeptides would be a successful strategy to achieve higher plasma levels and to improve pharmacokinetics.

Results and Discussion

As simple conjugation with an activated PEG derivative to the MIA inhibitory peptides failed and synthesis - most reasonably by a liquid-phase peptide synthesis[220] - from scratch is tedious and time-consuming, two tripeptides (WHF and WWW) were purchased with an *N*-terminal attached PEG chain of 2000 Da and subjected to the standard tests (see chapter 9.4).

The HTFP assay showed that the PEG derivatives of the short peptide sequences were highly active: they effectively dissociate MIA protein from the surface which is inferred from the high change in polarisation (Figure 11A). It can be clearly seen that the tested compounds are superior (PEG-WWW) or similar (PEG-WHF) to the standard peptide AR71. Due to these promising results, the substances were directly tested *in vitro* by the Boyden Chamber Invasion Assay described below.

Here, the invasion of cells of the melanoma cell line Mel Im was significantly reduced about 40% to 50% compared to untreated control cells after external treatment with MIA (Figure 11B). Pre-incubation of MIA with inhibitory compounds like AR71 or the PEGylated tripeptide completely neutralised the effect caused by MIA protein: the number of invaded cells was comparable to the number of the control cell line. Similarly, control lanes incubated only with the inhibitory compounds and without extra MIA protein (two columns on the right) confirmed that the drug candidates alone did not influence the migratory behaviour.

A

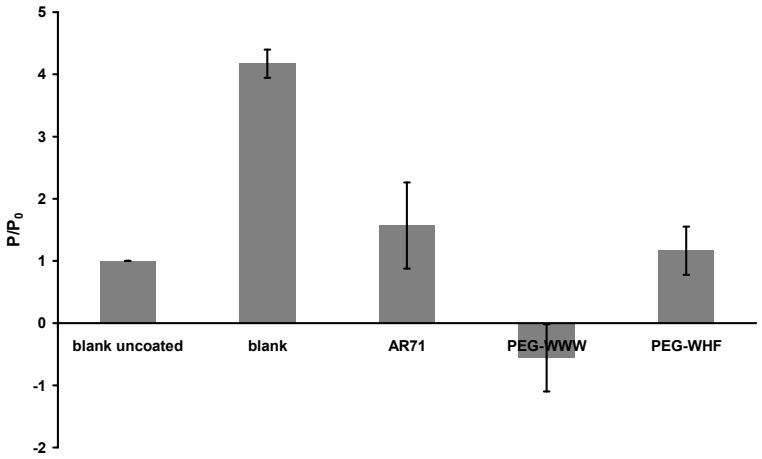

B

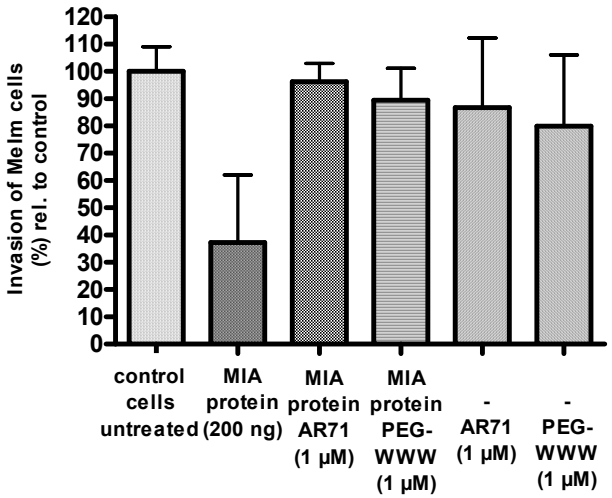

Figure 11 Results of **A)** the HTFP assay and **B)** Boyden chamber invasion assay of *N*-terminal PEGylated tripeptides.

A) Displacement of MIA protein by the PEGylated compounds reduces the polarisation remarkably, implying a high inhibitory activity.

B) The invasion of cells of the melanoma cell line Mel Im is significantly reduced by about 40%to 50% compared to untreated control cells after external treatment with MIA. Pre-incubation of MIA with inhibitory compounds like AR71 or the PEGylated tripeptide completely neutralised the effect caused by MIA protein: the number of invaded cells is comparable to the number of the control cells.

Boyden Chamber Invasion Assay

This assay (Figure 12) measures the invasive or metastatic potential of tumor cells. To establish distant metastases, tumor cells must first cross the basement membrane, a thin extracellular matrix (ECM). Boyden Chambers consist of two compartments separated by a filter coated with matrigel. Matrigel is a commercialised cell culture matrix, primarily consisting of the ECM molecules laminin, collagen IV, and enactin.[221] Thus, the 3-D *in vivo* environment is mimicked and furthermore the matrix is considered as a reconstituted basement membrane preparation.[221] Basically, melanoma cells are placed in the upper compartment of the Boyden chamber and the second chamber contains a chemoattractant. In this assay, only metastatic cells are able to penetrate through the matrix on the filter and attach to its surface, while non-metastatic tumor cells cannot cross the barrier.[222, 223] After a certain time of incubation, tumor cells are counted on the lower surface of the membrane. Albini *et al.* postulated that tumor cells first attach to the basement membrane *via* cell surface receptor, then secrete enzymes to degrade the adjacent membrane, and finally migrate into the target tissue in response to chemotactic stimuli.[222] In 2003, Bosserhoff *et al*. used the Boyden chamber assay to reveal that MIA protein inhibits also the interaction of melanoma cells with matrigel. As a consequence, the tumor cells cannot attach to the matrix and thus, do not invade in this *in vitro* model.[224]

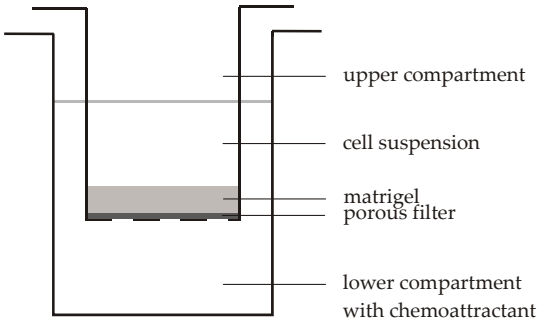

Figure 12 General principle of Boyden Chamber Invasion Assay which measures the invasive potential of tumor cells. Boyden Chambers consist of two compartments separated by a filter coated with matrigel. Melanoma cells are placed in the upper compartment of the Boyden chamber and the second chamber contains a chemoattractant. In this assay, only metastatic cells are able penetrate through the matrix on the filter and attach to its surface, while non-metastatic tumor cells cannot cross the barrier. After a certain time of incubation, tumor cells are counted on the lower surface of the membrane.

Frequently, PEGylation of proteins results in a loss of activity due to steric interference of the polymer chains with the biological target.[218] Both *in vitro* assays clearly showed that PEGylation did not affect the biological activity of the tripeptides whose activity is comparable to the control peptide AR71.

The good potency of the derivatives could be explained by a stabilising influence of PEG on the drug molecules: the polymer could mask sensitive amino acids and prevent the chemical degradation of the residues by oxidation or hydrolysis.[225] Aromatic amino acids, like tryptophane and histidine, predominate in the short MIA inhibitors and are particularly prone to oxidation; oxidation can change the physico-chemical properties of a protein and cause aggregation or fragmentation.[226] Aggregation of proteins is a common problem and associated with a decreased bioactivity, reduced solubility, and an increased immunogenicity.[227] The high content of hydrophobic amino acids in the MIA inhibitors may also trigger aggregation, as the hydrophobic effect is considered to be the major driving force in this process.[227] Conjugation of lipophilic drugs with hydrophilic polymers like PEG usually reduce the formation of aggregates and might overcome the above mentioned limitations. So far, the conducted experiments give

only information about how PEGylation influences the physical properties of the peptide. For a future application, detailed data about pharmacokinetics and *in vivo* half-life are essential and need to be collected.

Conclusion

Simple conjugation of a hydrophilic polymer to a drug prolongs the plasma circulation time and protects the therapeutic compound against metabolic degradation. The experiments showed that PEGylation of the potential drug candidates retained their affinity and resulted in a superior binding affinity and biological activity in comparison to the reference AR71. Due to their excellent *in vitro* performance, the PEGylated derivatives of MIA inhibitors were included in a patent held by Bosserhoff *et al.*[165] In the future, *in vivo* studies are planned to obtain detailed pharmacokinetic information of the PEGylated peptides.

Experimental

General. The tripeptides PEG-WWW and PEG-WHF, PEGlyated at the *N*-terminus with an mPEG2000, were purchased from GL Brioche (Shanghai) Ltd., China.

Coating of well plates with MIA-biotin, HTFP assay, conditions for cell lines and cell culture, and Boyden Chamber Invasion Assay were performed according to literature.[166]

10.2 Lipid implants as potential controlled release system for melanoma inhibitory activity (MIA) protein inhibitors

Introduction

Currently, daily *i.v.* injections of MIA inhibitory compounds are required to prevent or reduce the formation of metastases in mouse melanoma models. This frequency of application is caused by the short *in vivo* half-life of the peptidic inhibitors, and would be painful for the treated patients, resulting in a reduced compliance. One solution to this problem might be the implementation devices which release the drug at a predetermined rate. The goal of such sustained release formulations is to prolong the duration of action of the drug, to reduce the frequency of dosing, to minimise the fluctuations in plasma level, to improve drug utilisation, and to diminish adverse effects.[171] Shortly, by releasing the drug constantly at the site of action, the therapy becomes more efficient, costs and the risk of toxic side effects can be reduced.[228]

Lipid carriers are highly biocompatible as only naturally occurring materials are used as matrices, e.g. triglycerides, phospholipids, and cholesterol. Their main advantages are the simple manufacture of the devices by compression or moulding, the lower susceptibility to erosion phenomena, and their slower water uptake. Major drawbacks of these devices are drug degradation during preparation, especially when the commonly used high pressure homogenisation is applied. Due to crystallisation of the lipids in polymorphic forms, unpredictable release profiles and low drug loading might be the result.[228] Upon degradation or erosion the drug is exposed to a constantly changing microenvironment which might damage the peptide or protein.[228] Lipid based carriers for proteins and peptides were summarised by Rawat *et al*. in 2008.[228] Some examples for the formulations of physiological triglycerides as microparticles and cylindrical matrices are given in reference [229].

The aim of this study was to find a drug carrier that releases the therapeutic agent continuously over 30 days and is also small enough to be applied in animal models. Ideally, 50 to 100 μg of peptide would be released per day.

Results and Discussion

In our study, we used lipid implants as long-term release system based on the research of Koennings *et al*.[230] They introduced an improved method for the preparation of lipid implants. To achieve a homogeneous protein distribution in the lipid cylinders, a PEG-co-lyophilisation method was applied. The developed carriers contained 2 weight% of brain-derived neurotrophic factor (BDNF) and 60% of the total protein loading were continuously released over one month.

To prove the feasibility of this system as sustained-release carrier, somatostatin was used as model substance. Somatostatin is a cyclic tetradecapeptide (AGCKNFFWKTFTSC) (Figure 13) with an internal disulfide bridge and a molecular weight of 1638 g/mol. It is a multi-functional peptide hormone regulating a great variety of biological processes, e.g. growth, metabolism, and development.[231] In comparison, the dodecapeptide AR71 (Ac-FHWRYPLPLPGQ-NH_2) (Figure 13) has a similar molecular weight of 1552 g/mol. Both peptides are mainly composed of hydrophobic and neutral, and a few basic amino acids.

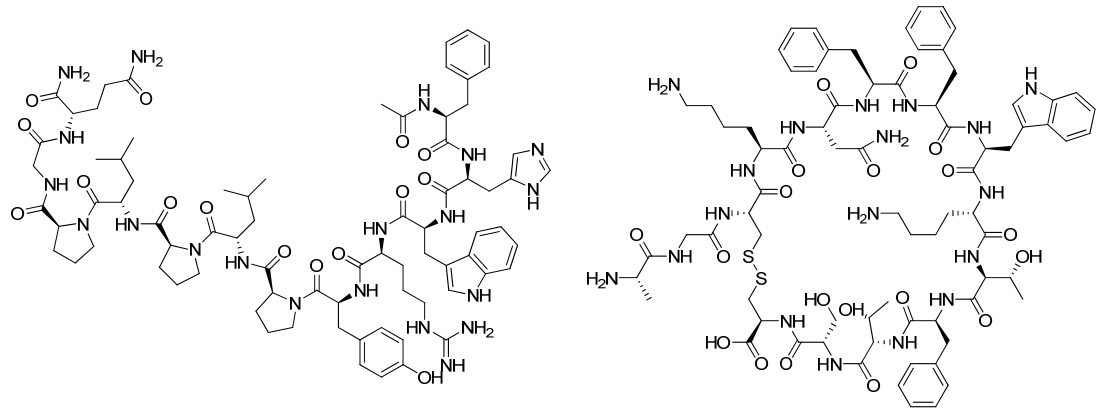

Figure 13 Molecular structures of AR71 (left) and somatostatin (right).

As the size of the implant needed to be small enough in order to be applicable in mice, the drug content in the carrier was raised to 10 weight% of the lipid matrix. At a release rate of 50 µg/day, the laboratory animals could be supplied with peptide over 36 days. This means that 1.8 mg of peptide were incorporated into the lipid matrix with a total weight of 18 mg and a diameter of 3 mm. To achieve higher loading, the implant was formulated without PEG. Furthermore, PEG is often applied as porogen. As a consequence, water intrudes into the interconnected pore network, facilitates

dissolution and diffusion of the incorporated drug, finally resulting in a faster drug release.[232] The implant was compressed and release behaviour was assessed at 37 °C.

A

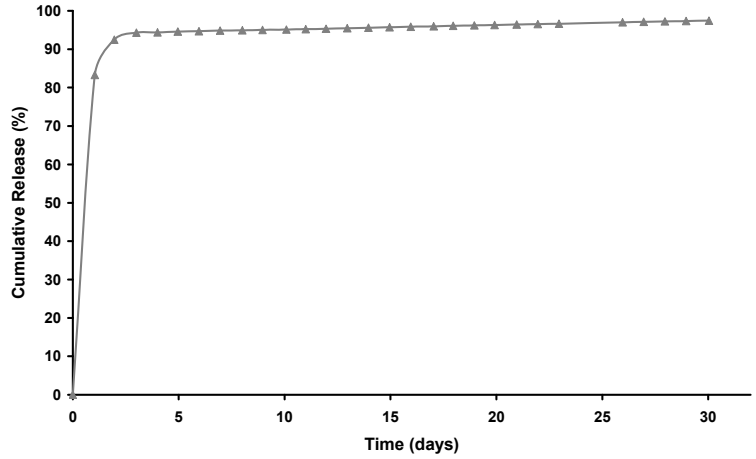

B

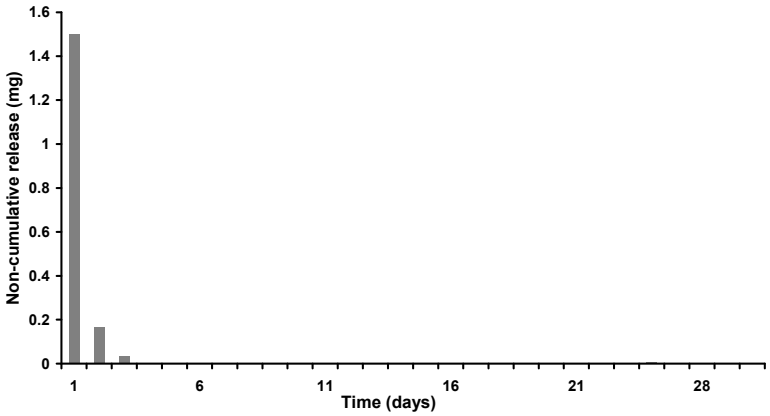

Figure 14 *In vitro* release of somatostatin from glyceryl tripalmitate matrices incubated in phosphate buffer pH7.4 at 37 °C depicted as **A)** cumulative amount in %, and **B)** mg released per day. Most of the peptide is already released after 24 hours.

Our study showed that 83% of the peptide was released after 24 hours, as shown in Figure 14. After the initial burst, no significant amounts of peptide were found over the following weeks. This burst release effect is a common problem observed for controlled release systems. Thereby, a large amount of drug is immediately released upon placement in the release medium before the release profile reaches a stable profile.[233] Generally, to release drugs in aqueous medium, they need first to be dissolved and then diffuse through the porous structures of the matrix into the solution. The high initial release can be explained by a heterogeneous drug distribution in the matrix, either caused by the manufacturing method or due to the material properties. If the protein is mostly enriched in the surface, especially in the case of high drug loading, release will be extremely fast. An increased porosity of the matrix would also support a faster diffusion of the drug through the cracks, channels, and pores. The high drug loading of the carrier might also contribute to the mentioned effects.

Apart from a different formulation and higher loading, the embedded drugs differ in molecular weight by one order of magnitude: BDNF has a molecular weight of 13.6 kDa and somatostatin of 1.6 kDa. Diffusion of the smaller somatostatin may be less restricted by the matrix, resulting in the high initial burst.

Conclusion

Biologically occurring and biocompatible triglycerides are interesting materials for sustained release formulations. A new formulation of a lipid implant was developed as a potential carrier and reservoir for MIA inhibitors. An *in vitro* release study revealed that a small lipid implant, which was loaded with a model compound, released the drug almost completely after 24 hours. For this reason, this carrier will not be optimised and the focus will be laid on systems that fulfil the requirement of a controlled long-term release.

Experimental

General. All chemicals were purchased from Aldrich, Fluka or Acros and used without further purification. Glyceryl tripalmitate (Dyanasan®116) was a gift from Sasol (Witten, Germany). Somatostatin Curamed ® ampoules containing 3 mg somatostatinacetate were from CuraMEDPharma GmbH.

Preparation method of lipid microparticles

3 mg of protein were dissolved in 1 mL of double-distilled water. After freezing in liquid nitrogen, the mixture was lyophilized at 6 °C and 0.12 mbar for 30 hours in a benchtop freeze-dryer (Beta 2-16 with LMC-2 system control, Christ, Osterode, Germany). When vacuum was removed, 1.5 mL THF were immediately added to the lyophilisate, resulting in a suspension of solid protein particles. Glyceryl tripalmitate (Dynasan 114®, 27 mg) was dissolved in the suspension with the help of sonication for 5 seconds. Afterwards, the mixture was again frozen in liquid nitrogen.

The organic solvent was removed from the frozen formulation under a vacuum of 6×10^{-3} mbar and cooling (two stage High vacuum Pump E2M5, Edwards, Crawley, UK). The resulting dry powder was ground in an agate mortar.

For all formulations, cylindrical matrices of 3 mm diameter, 5 mm height and 18 mg weight were prepared form the protein-loaded lipid powder by manual compression in a custom-designed compression tool made of hardened steel. Compression force was controlled at 560 N for 10 seconds by a Perkin-Elmer hydraulic press (Perkin-Elmer, Ueberlingen, Germany). Matrices were weighed on an analytical balance to determine their exact weight prior to release studies.

In vitro protein release behaviour

All vials were treated with Sigmacote® prior to use to prevent adsorption of protein. The matrix was incubated in 0.5 mL of the release medium (50 mM phosphate buffer pH 7.4) in a water bath at 37 °C. Buffer was replaced completely after each sampling interval, the samples stored at -20 °C and thawed before analysis.

Determination of drug release *via* HPLC measurements

The amount of somatostatin released at 37 °C was determined using the following HPLC method.

Column: Supelcosil LC318, Shimadzu LC-10AT autosampler, SIL-10 AD autoinjector, FCV-10AL pump, CTO-10ASvp oven, SCL-10Avp controller, RF-10Axl fluorescence detector, SPC 10Avp UV detector; Software: Class VP, Version 6.12, Shimadzu; Column temperature: 35 °C; Solvent A: water: MeCN = 90 : 10 + 0.1% TFA; solvent B: H_2O: MeCN = 10 : 90 + 0.1% TFA; gradient: from 15% B to 50% B within 20 min. Flow rate: 1 mL/min, injection volume: 50 µL; UV detection at 210 and 280 nm, fluorescence detection λ_{ex}= 280 nm, λ_{em}= 356 nm. The retention time of somatostatin under these conditions was approximately 12.3 min. Peptide solutions of known concentrations (0.1 – 1.0 µg/mL) were used to generate calibration curves.

10.3 Poly(ethylene glycol) based hydrogels for sustained delivery of melanoma inhibitory activity (MIA) protein inhibitors

Introduction

The rapid development of biotechnology entailed the discovery of a magnitude of potential protein drugs. Biopharmaceuticals are a rapidly growing field in pharmaceutical industry; currently, more than 25% of all substances are produced by biotechnological methods.[234] Meanwhile, a considerable number of newly developed biotechnology drugs are proteins or peptides. However, the successful delivery of therapeutic proteins is still a challenge for the pharmaceutical scientist.[235] Application of suitable drug delivery systems would result in optimised pharmacokinetics, reduction of degradation, avoidance of detrimental systemic side effects, increase of bioavailability and reduction of the frequency of injection. A commonly investigated method in protein delivery is to entrap or encapsulate the therapeutic agents in polymeric carriers.[235]

Hydrogels are highly biocompatible and widely used in the biomedical sector.[236] They consist of physically or covalently cross-linked hydrophilic polymers which swell in aqueous media due to the uptake of water, but are not dissolved by the medium.[237, 238] Their high water content and soft consistency resembles the native extracellular matrix resulting in high biocompatibility.[238] Drugs can be embedded in the gel matrix and their release rate is mostly diffusion controlled.[237, 238] However, the applicability of hydrogels in sustained release systems is still limited: incorporated compounds are rapidly released in a few hours to a few days due the high water content and the large pore size of most gels.[238] To slow down the release rate, different strategies have been applied. First, the microstructure of the hydrogel can be altered to increase the diffusive barrier. This can be achieved by using interpenetrating polymer networks.[238] To do this, a second second hydrogel network is polymerised within a pre-polymerised hydrogel. Thus not only the mechanical properties can be changed, but also mesh size or pH responsitivity of the hydrogel can be tuned. Other methods to increase the diffusive barrier include the grafting a second polymer film onto the surface or entrapping microparticles into the gels to form composite hydrogels.[238] In addition, the

interactions between drug and the hydrogel network can be strengthened by electrostatic interactions or by covalent conjugation (the polymer-drug bond is subsequently cleaved chemically or enzymatically).[238]

The goal of this study was to design a drug reservoir based on PEG hydrogels that releases peptidic MIA inhibitor AR60I constantly over a predetermined time.

Results and Discussion

The high biocompatibility of the PEG hydrogels make them an interesting biomaterial with multiple applications, especially in biomedical science.[239] The peptide AR60I, used here as a model compound for the release study, is a known MIA inhibitor with the sequence H-NSLLVSFQPPRAR-NH_2 (Figure 15).

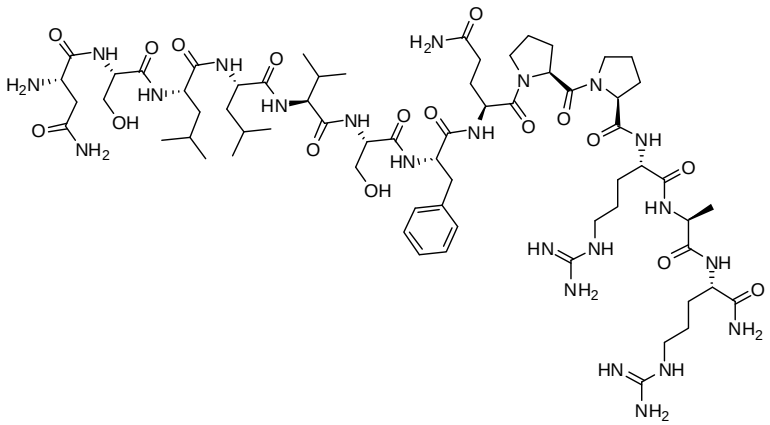

Figure 15 Chemical structure of peptidic MIA inhibitor AR60I.

In this study, hydrogels based on branched PEG succinimidyl carbonates and branched PEG amines, both with 10 kDa molecular weight, were used; gel formation occurs *in situ* upon chemical reaction of these macromers (Figure 16).[240, 241]

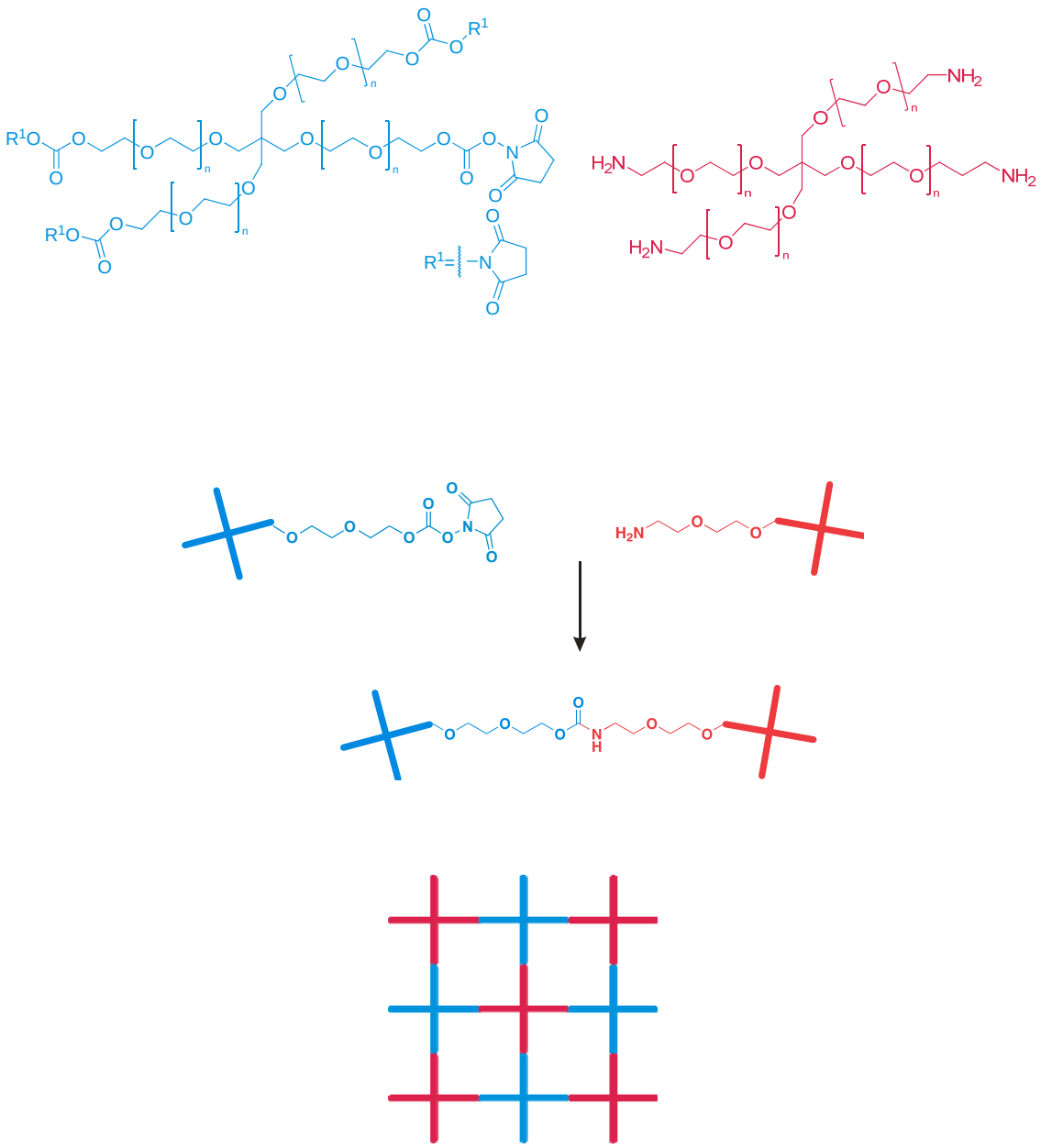

Figure 16 Principle of the *in situ* forming of PEG hydrogels. The *N*-hydroxysuccinimide activated PEG (left) is conjugated to the second amine functionalised PEG component (right) under formation of an amide bond. Directly after mixing the precursor solutions, a highly elastic polymer network (bottom) is formed.

The drug was embedded into an *in situ* polymerising PEG hydrogel. The compounds were added to the gel forming polymer solutions and entrapped during the *in situ* cross-linking process. Usually, good nucleophiles like free amine groups of lysine residues can also react with the activated PEG monomer and are covalently bound to the polymer. Here, we do not expect such kind of interference with peptide AR60I as no nucleophilic residues are present. After incubation at 37 °C, the released peptide was determined by HPLC. Unfortunately, the HPLC measurements showed that the peptide was not stable in solution, indicated by numerous smaller peaks at similar retention time. Therefore, we evaluated the area under the curve of the UV signal at 210 nm of a constantly recurring fragment (also confirmed by LC-MS) to acquire qualitative information. The diagram obtained by this method showed that the amount of released peptide decreases gradually (Figure 17). Apparently, the active compound is released within five days. These data must be interpreted with caution because it could not be determined if the total amount of the incorporated agent was released into solution or if the hydrogel still contained residual drug.

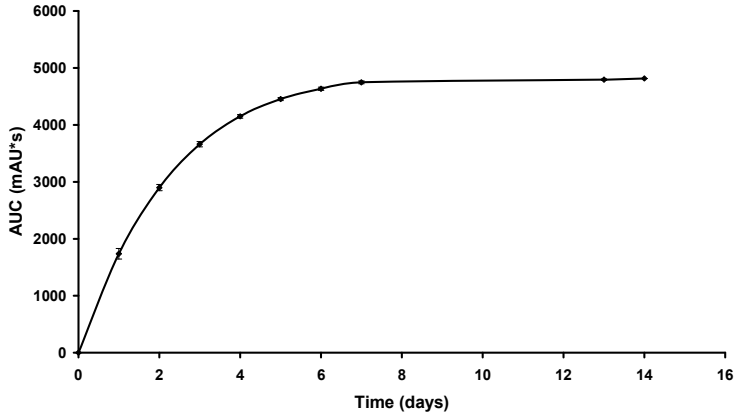

Figure 17 In vitro release of AR60I showing the cumulative area under the curve of a recurring fragment of the used peptide. The incorporated tridecapeptide is released over five days.

In general, hydrophilic compounds like peptides are suitable candidates to be embedded into a hydrophilic polymer network. Due to the high water content of the hydrogels, the peptide remains dissolved. However, the hydrogel has no significant diffusion barrier for the hydrophilic peptide resulting in a rapid release. As the drug release is diffusion controlled, prolonged drug release might be achieved by increasing of the hydrodynamic radius of the incorporated compound, reducing the mesh size or by increasing the polymer content of the hydrogel.

Conclusion

In summary, we applied biocompatible PEG hydrogels as drug delivery vehicles for small MIA protein inhibiting peptides and determined their drug release profile *in vitro*. The drug was encapsulated during the *in situ* cross-linking process. It was demonstrated that the used PEG hydrogel networks release the incorporated peptide within five days. However, the current results encourage us to further optimise the PEG carrier system in order to achieve sustained release in the future.

Experimental

General. 4-armPEG10k-succinimidyl carbonate and of 4-armPEG10k-amine were synthesised according to Brandl *et al*.[241] Alginate Pronova UP LVM was purchased from Nova Matrix, Norway. AR60I was previously synthesised by solid phase synthesis.

Preparation of PEG hydrogels loaded with peptide AR60I (H-NSLLVSFQPPRAR-NH_2)

For the release studies, accurately weighed amounts of the 4-armPEG10k-amine component were dissolved in peptide in aqueous solution and in 50 mM phosphate buffer, pH7.4 (control). Each of the solutions was added to a solution of 4-armPEG10k-succinimidyl carbonate in 50 mM phosphate buffer. The stoichiometric ratio between succinimidyl carbonate and amino groups was balanced, and the overall polymer concentration was 5% (w/v) for all gels. After vortexing, 350 µL of the respective solutions were cast into cylindrical glass molds (7 mm inner diameter) and allowed to gel for 2 h. The gel cylinders were incubated in 3 mL of 50 mM phosphate buffer pH7.4 (containing 0.1% NaN_3) at 37 °C in a shaking water bath. Every day, samples of 1 mL were collected and replaced by the same volume of buffer.

Determination of drug release *via* HPLC measurements

The amount of released AR60I at 37 °C was determined using the following HPLC method.

Column: Phenomenex Luna 3 um C18 (2) 100 A, 150 mm x 2.00 mm,

Agilent 1100/1; G1312A Bin Pump, G1313A COLCOM, G131B DAD, G1379 DEGASSER, G1321A FLD; software: ChemStation for LC 3D Systems Rev B.04.02 SP1; column temperature: 25 °C, FLD-A, ELS; UV detection at 210 and 220 nm, fluorescence detection λ_{ex}= 280 nm, λ_{em}= 350 nm. Gradient: from 3% MeCN/H_2O (0.0059% TFA) to 98% MeCN/H_2O (0.0059% TFA) within 30 min. Flow rate: 0.3 mL/min, injection volume: 30 µL. The retention time of AR60I under these conditions was approximately 10.2 min.

11. Summary

Aggressive growth accompanied by rapid metastasis makes the malignant melanoma a kind of cancer with a low rate of survival in an advanced stage. The melanoma inhibitory activity (MIA) protein reduces the cell contacts to the extracellular matrix and facilitates metastasis. Remarkably, MIA protein is exclusively expressed in malignant melanoma cells and chondrocytes. In comparison to other chemotherapeutic agents, anti metastatic agents (substances which inhibit the functional activity of MIA protein) would thus prevent the spreading of these cells and reduce the side effects of systemic chemotherapy dramatically. MIA protein is functionally active after formation of dimers. Small compounds which prevent this assembly would be very interesting drugs in the treatment of cancer. Short peptides consisting of three to eighteen amino acids were assessed in a screening process to inhibit the dimerisation of MIA protein *in vitro* and *in vivo*. The major drawback of proteins and peptides as drugs is their poor *in vivo* stability and the resulting low plasma concentration which is often below the effective dose. Currently, the poor pharmacokinetic properties of proteins often require daily injections which entail high costs and are a burden to the treated patients. Therefore, the aim of this thesis was to increase the *in vivo* stability of MIA inhibiting peptides and thus to achieve adequate drug levels in plasma.

It was attempted to achieve this goal by simple modifications of the molecular structure of the known inhibitors, with the focus on modifications of the peptide backbone. The synthesised peptide mimetics were methylated at the nitrogen atom of the amide bond of the peptide chain, transformed to N-substituted glycines (peptoids), or cyclised in a head-to-tail fashion. Subsequent *in vitro* tests (HTFP assay, Western Blot analysis) of the derivatives showed that their activity was significantly reduced in comparison to the original compounds. This was attributed to a conformational change of the mimics due to variations in the chemical structure. The results implicate that their conformation differs strongly from the bioactive conformation, thus reducing the potency. As the structural variation of lead compounds is often connected with the risk of losing activity, a second approach was pursued. By applying drug delivery systems the molecular structure can be retained. Furthermore, these devices should ideally release a drug selectively at the site of action over a predetermined period of time.

Consequently, a constant plasma concentration might be maintained leading to a reduced frequency of application and overall in an improved therapy.

Covalent attachment of polymers like poly(ethylene glycol) is a convenient method to increase the circulation time by reducing the rate of renal and hepatic clearance and metabolic degradation of the drugs. PEGylation of small MIA inhibitors led to highly active compounds, as *in vitro* tests showed. Future experiments will have to elucidate their pharmacokinetic properties.

Sustained release devices are also suitable alternatives to reduce the drug administration frequency. A new formulation of biocompatible triglyceride implants released the incorporated peptide almost completely within 24 hours which provided no improvement over the current application method. For this reason, highly biocompatible PEG hydrogels were applied as slow-releasing matrices. The applicability of hydrogels in sustained release systems is still limited as incorporated compounds are rapidly released. It was observed that the incorporated model peptide was released within five days from PEG hydrogels.

In conclusion, first steps to increase the *in vivo* stability of MIA inhibitors by different approaches have been made within the scope of this thesis. Certainly, many experiments will still be necessary in order to obtain a marketable product for the treatment of malignant melanoma. First steps have been made in the challenging field of peptide delivery. The knowledge attained in this work contributes significantly to future work of optimising the molecular structure of the drug or the drug carrier system

12. Zusammenfassung

Aggressives Wachstum mit schneller Metastasierung macht das maligne Melanom zu einer Krebsart mit einer sehr niedrigen Überlebensrate im fortgeschrittenen Stadium. Das Protein MIA ermöglicht es den Krebszellen sich aus der extrazellulären Matrix zu lösen und erleichtert so die Metastasenbildung. Das Besondere am MIA Protein ist, das es ausschließlich in malignen Melanomzellen und Chondrocyten exprimiert wird. Antimetastasische Wirkstoffe, die die Funktion des MIA Proteins unterbinden, würden somit nur die Verbreitung dieser Zellen verhindern und so Nebenwirkungen im Vergleich zu anderen Chemotherapeutika drastisch reduzieren.

Das Melanoma Inhibitory Activity (MIA) Protein erfüllt erst dann seine biologische Funktion, wenn es Dimere gebildet hat. Einfache Verbindungen, die diese Dimerisierung verhindern bzw. die aktiven Dimere dissoziieren, wären deshalb sehr interessante Therapeutika. In einem Screening Verfahren wurden kurze Peptide mit drei bis achtzehn Aminosäuren entdeckt, die die Dimerbildung des MIA Proteins *in vitro* und *in vivo* inhibieren.

Der große Nachteil von Proteinen und Peptiden als Wirkstoffe ist deren geringe *in vivo* Stabilität und die daraus resultierende niedrige Plasmakonzentration, oftmals unterhalb der wirksamen Dosis. Derzeit erfordern die schlechten pharmakologischen Eigenschaften von Proteinen und Peptiden regelmäßige Injektionen, die mit einem hohen Kostenaufwand und auch einer Belastung für die Patienten verbunden sind.

Das Ziel dieser Arbeit war es deshalb, die *in vivo* Stabilität der MIA inhibierenden Peptide zu erhöhen und damit ausreichende Wirkstoffspiegel im Plasma zu erreichen.

Zunächst sollte die dieses Ziel durch einfache Veränderungen der chemischen Struktur, speziell am Peptidrückgrat, der bekannten Inhibitoren bewirkt werden. Die synthetisierten Peptidmimetika wurden am Stickstoffatom der Amidbindung in der Peptidkette methyliert, zu *N*-substituierten Glycinen (Peptoide) umgewandelt oder zu einem Ring mit einer Kopf-Schwanz-Struktur verknüpft. In den nachfolgenden *in vitro* Funktionstests (HTFP assay, Western Blot Analyse) der Derivate zeigte sich, dass sich die biologische Aktivität durch Strukturänderungen, im Vergleich zu den Originalsequenzen deutlich verringert hatte. Dies wurde auf eine Konformationsänderung der Mimetika zurückgeführt, so dass deren Konformation

stark von der bioaktiven Konformation abweicht und somit zu einer Verringerung der Wirkung führt.

Aus diesem Grund wurde eine zweite Strategie verfolgt bei der die ursprüngliche Molekülstruktur beibehalten werden kann. Indem der Wirkstoff gezielt am Wirkort und über einen festgelegten Zeitraum freigesetzt wird, kann die Häufigkeit der Anwendung reduziert werden und gleichzeitig konstante Plasmaspiegel und damit eine Verbesserung der Therapie erreicht werden.

Eine dafür geeignete Methode ist die kovalente Anknüpfung von Polymeren wie Poly(ethylen glykol) (PEG). Durch PEGylierung kann die Zirkulationsdauer erhöht werden, indem die renale und hepatische Clearance und auch der metabolische Abbau der Wirkstoffe verringert wird. Wie in *in vitro* Tests gezeigt wurde, führte die PEGylierung von kleinen MIA Inhibitoren zu hochaktiven Verbindungen. Zukünftige Experimente werden sich mit der Aufklärung der pharmakinetischen Eigenschaften befassen. Sustained release Formulierungen sind ebenfalls geeignete Alternativen, um die Häufigkeit der Injektionen herabzusetzen. Eine neue Formulierung eines Implantats basierend auf biokompatiblen Triglyceriden setzte das eingebettete Modellpeptid fast vollständig innerhalb von 24 Stunden frei; im Vergleich zur bisherigen Anwendungsweise stellt diese Methode keine Verbesserung dar. Deshalb wurden biokompatible PEG Hydrogele als langsam freisetzende Matrices eingesetzt. Die Anwendbarkeit von Hydrogelen als sustained release Systeme ist immer noch begrenzt, da die eingeschlossenen Verbindungen schnell freigesetzt werden. Es wurde beobachtet, dass das eingebettete Modellpeptid innerhalb von fünf Tagen freigesetzt wurde. Zusammenfassend wurde im Rahmen dieser Arbeit erste Schritte gemacht, die *in vivo* Stabilität von MIA Inhibitoren durch verschiedenartige Ansätze zu erhöhen. Obwohl sicherlich noch viele Experimente notwenig sein werden, um ein marktfähiges Produkt für die Behandlung des malignen Melanoms zu bekommen, wurden mit dieser Arbeit grundlegende Erkenntnisse gewonnen, die zur Entwicklung eines verbesserten Wirkstoffes bzw. eines Wirkstoffträgersystems maßgeblich beitragen werden.

13. Bibliography

1. L. Moity, M. Durand, A. Benazzouz, C. Pierlot, V. Molinier and J.-M. Aubry, *Green Chem.*, 2012, **14**, 1132-1145.
2. D. Reinhardt, F. Ilgen, D. Kralisch, B. Konig and G. Kreisel, *Green Chem.*, 2008, **10**, 1170-1181.
3. P. Wasserscheid and T. Welton, *Ionic Liquids in Synthesis*, Wiley-VCH Verlag GmbH & Co. KGaA, 2003.
4. S. Stolte, J. Arning and J. Thöming, *Chem. Ing. Tech.*, 2011, **83**, 1454-1467.
5. M. Petkovic, K. R. Seddon, L. P. N. Rebelo and C. Silva Pereira, *Chem. Soc. Rev.*, 2011, **40**, 1383-1403.
6. C. Atwater, in *Ullmann's Encyclopedia of Industrial Chemistry*, Wiley-VCH Verlag GmbH & Co. KGaA, 2000.
7. A. P. Abbott, G. Capper, D. L. Davies, R. K. Rasheed and V. Tambyrajah, *Chem. Commun.*, 2003, 70-71.
8. A. P. Abbott, R. C. Harris, K. S. Ryder, C. D'Agostino, L. F. Gladden and M. D. Mantle, *Green Chem.*, 2011, **13**, 82-90.
9. A. P. Abbott, D. Boothby, G. Capper, D. L. Davies and R. K. Rasheed, *J. Am. Chem. Soc.*, 2004, **126**, 9142-9147.
10. A. P. Abbott, G. Capper and S. Gray, *ChemPhysChem*, 2006, **7**, 803-806.
11. A. P. Abbott, R. C. Harris and K. S. Ryder, *J. Phys. Chem. B*, 2007, **111**, 4910-4913.
12. Z. Maugeri and P. D. de Maria, *RSC Adv.*, 2012, **2**, 421-425.
13. P. Nockemann, B. Thijs, K. Driesen, C. R. Janssen, K. Van Hecke, L. Van Meervelt, S. Kossmann, B. Kirchner and K. Binnemans, *J. Phys. Chem. B*, 2007, **111**, 5254-5263.
14. Y. Fukaya, Y. Iizuka, K. Sekikawa and H. Ohno, *Green Chem.*, 2007, **9**, 1155-1157.
15. M. Petkovic, J. L. Ferguson, H. Q. N. Gunaratne, R. Ferreira, M. C. Leitao, K. R. Seddon, L. P. N. Rebelo and C. S. Pereira, *Green Chem.*, 2010, **12**, 643-649.
16. Q.-P. Liu, X.-D. Hou, N. Li and M.-H. Zong, *Green Chem.*, 2012, **14**, 304-307.
17. G. Imperato, E. Eibler, J. Niedermaier and B. Konig, *Chem. Commun.*, 2005, 1170-1172.

18. G. Imperato, S. Hoger, D. Lenoir and B. Konig, *Green Chem.*, 2006, **8**, 1051-1055.

19. G. Imperato, R. Vasold and B. König, *Adv. Synth. Catal.*, 2006, **348**, 2243-2247.

20. Y. H. Choi, J. van Spronsen, Y. T. Dai, M. Verberne, F. Hollmann, I. Arends, G. J. Witkamp and R. Verpoorte, *Plant Physiol.*, 2011, **156**, 1701-1705.

21. WO 02/26701 (A2), 2002.

22. F. Ilgen and B. Konig, *Green Chem.*, 2009, **11**, 848-854.

23. H.-j. Lu, Y.-x. Hua, Y. Li and X.-y. Zhang, *Kunming Ligong Daxue Xuebao, Ligongban*, 2010, **35**, 11-14.

24. K. D. O. Vigier, A. Benguerba, J. Barrault and F. Jerome, *Green Chem.*, 2012, **14**, 285-289.

25. C. Russ, F. Ilgen, C. Reil, C. Luff, A. Haji Begli and B. Koenig, *Green Chem.*, 2011, **13**, 156-161.

26. C. Reichardt, *Solvent Effects on the Rates of Homogeneous Chemical Reactions*, Wiley-VCH Verlag GmbH & Co. KGaA, 2004.

27. C. Reichardt, *Chem. Rev.*, 1994, **94**, 2319-2358.

28. Y. Wu, T. Sasaki, K. Kazushi, T. Seo and K. Sakurai, *J. Phys. Chem. B*, 2008, **112**, 7530-7536.

29. J. T. Gorke, F. Srienc and R. J. Kazlauskas, *Chem. Commun.*, 2008, 1235-1237.

30. C. Reichardt, *Green Chem.*, 2005, **7**, 339-351.

31. D. Lide, *CRC Handbook of Chemistry and Physics, 88th Edition (CRC Handbook of Chemistry & Physics)*, CRC Press, 2007.

32. J. Pernak, N. Borucka, F. Walkiewicz, B. Markiewicz, P. Fochtman, S. Stolte, S. Steudte and P. Stepnowski, *Green Chem.*, 2011, **13**, 2901-2910.

33. Z. Yu, H. Gao, H. Wang and L. Chen, *J. Solution Chem.*, 2012, **41**, 173-186.

34. N. Muhammad, Z. B. Man, M. A. Bustam, M. I. A. Mutalib, C. D. Wilfred and S. Rafiq, *J. Chem. Eng. Data*, 2011, **56**, 3157-3162.

35. A. S. Nagare and A. Kumar, *Indian J. Chem.*, 2011, **50A**, 788-792.

36. J. Restolho, J. L. Mata and B. Saramago, *Fluid Phase Equilib.*, 2012, **322–323**, 142-147.

37. C. D'Agostino, R. C. Harris, A. P. Abbott, L. F. Gladden and M. D. Mantle, *Phys. Chem. Chem. Phys.*, 2011, **13**, 21383-21391.

38. R. B. Leron and M.-H. Li, *Thermochim. Acta*, 2012, **530**, 52-57.

39. G. García-Miaja, J. Troncoso and L. Romaní, *J. Chem. Thermodyn.*, 2009, **41**, 161-166.

40. S. J. Zhang, N. Sun, X. Z. He, X. M. Lu and X. P. Zhang, *J. Phys. Chem. Ref. Data*, 2006, **35**, 1475-1517.

41. J. L. Anthony, J. F. Brennecke, J. D. Holbrey, E. J. Maginn, R. A. Mantz, R. D. Rogers, P. C. Trulove, A. E. Visser and T. Welton, in *Ionic Liquids in Synthesis*, Wiley-VCH Verlag GmbH & Co. KGaA, 2003, pp. 41-126.

42. Y. H. You, C. D. Gu, X. L. Wang and J. P. Tu, *Surf. Coat. Technol.*, 2012, **206**, 3632-3638.

43. A. H. Whitehead, M. Polzler and B. Gollas, *J. Electrochem. Soc.*, 2010, **157**, D328-D334.

44. L. Wei, Y.-J. Fan, N. Tian, Z.-Y. Zhou, X.-Q. Zhao, B.-W. Mao and S.-G. Sun, *J. Phys. Chem. C*, 2011, **116**, 2040-2044.

45. M. Steichen, M. Thomassey, S. Siebentritt and P. J. Dale, *Phys. Chem. Chem. Phys.*, 2011, **13**, 4292-4302.

46. G. Saravanan and S. Mohan, *J. Alloys Compd.*, 2012, **522**, 162-166.

47. A.-M. Popescu, V. Constantin, A. Cojocaru and M. Olteanu, *Rev. Chim. (Bucharest, Rom.)*, 2011, **62**, 206-211.

48. B. G. Pollet, J.-Y. Hihn and T. J. Mason, *Electrochim. Acta*, 2008, **53**, 4248-4256.

49. P. Martis, V. S. Dilimon, J. Delhalle and Z. Mekhalif, *Electrochim. Acta*, 2010, **55**, 5407-5410.

50. K. Haerens, E. Matthijs, A. Chmielarz and d. B. B. Van, *J. Environ. Manage.*, 2009, **90**, 3245-3252.

51. P. Guillamat, M. Cortes, E. Valles and E. Gomez, *Surf. Coat. Technol.*, Ahead of Print.

52. C.-D. Gu and J.-P. Tu, *Langmuir*, 2011, **27**, 10132-10140.

53. E. Gomez, P. Cojocaru, L. Magagnin and E. Valles, *J. Electroanal. Chem.*, 2011, **658**, 18-24.

54. P. Cojocaru, L. Magagnin, E. Gomez and E. Valles, *Mater. Lett.*, 2011, **65**, 3597-3600.

55. A. P. Abbott, T. K. El, G. Frisch, K. S. Ryder and D. Weston, *Phys. Chem. Chem. Phys.*, 2012, **14**, 2443-2449.

56. A. P. Abbott, T. K. El, G. Frisch, K. J. McKenzie and K. S. Ryder, *Phys. Chem. Chem. Phys.*, 2009, **11**, 4269-4277.

57. A. P. Abbott, G. Capper, K. J. McKenzie and K. S. Ryder, *J. Electroanal. Chem.*, 2007, **599**, 288-294.

58. A. P. Abbott, J. C. Barron, G. Frisch, K. S. Ryder and A. F. Silva, *Electrochim. Acta*, 2011, **56**, 5272-5279.

59. A. P. Abbott, J. C. Barron, G. Frisch, S. Gurman, K. S. Ryder and S. A. Fernando, *Phys. Chem. Chem. Phys.*, 2011, **13**, 10224-10231.

60. S. B. Phadtare and G. S. Shankarling, *Green Chem.*, 2010, **12**, 458-462.

61. P. M. Pawar, K. J. Jarag and G. S. Shankarling, *Green Chem.*, 2011, **13**, 2130-2134.

62. H. N. Harishkumar, K. M. Mahadevan, K. H. C. Kiran and N. D. Satyanarayan, *Org. Commun.*, 2011, **4**, 26-32.

63. N. Azizi, E. Batebi, S. Bagherpour and H. Ghafuri, *RSC Adv.*, 2012, **2**, 2289-2293.

64. C. Chiappe, M. Malvaldi and C. S. Pomelli, *Green Chem.*, 2010, **12**, 1330-1339.

65. Z.-H. Zhang, X.-N. Zhang, L.-P. Mo, Y.-X. Li and F.-P. Ma, *Green Chem.*, 2012.

66. S. Q. Hu, Z. F. Zhang, Y. X. Zhou, B. X. Han, H. L. Fan, W. J. Li, J. L. Song and Y. Xie, *Green Chem.*, 2008, **10**, 1280-1283.

67. F. Ilgen, D. Ott, D. Kralisch, C. Reil, A. Palmberger and B. Koenig, *Green Chem.*, 2009, **11**, 1948-1954.

68. C. Russ, C. Luff, A. Haji Begli and B. Koenig, *Synth. Commun.*, 2011, **42**, 1- 5.

69. S. Gore, S. Baskaran and B. Koenig, *Green Chem.*, 2011, **13**, 1009-1013.

70. K. Faber, in *Biotransformations in Organic Chemistry*, Springer Berlin Heidelberg, 6th Edition edn., 2011, pp. 1-30.

71. Z. Yang and W. Pan, *Enzyme and Microbial Technology*, 2005, **37**, 19-28.

72. F. van Rantwijk and R. A. Sheldon, *Chem. Rev.*, 2007, **107**, 2757-2785.

73. S. Klembt, S. Dreyer, M. Eckstein and U. Kragl, in *Ionic Liquids in Synthesis*, Wiley-VCH Verlag GmbH & Co. KGaA, 2008, pp. 641-661.

74. H. Weingartner, C. Cabrele and C. Herrmann, *Phys. Chem. Chem. Phys.*, 2012, **14**, 415-426.

75. D. Lindberg, M. de la Fuente Revenga and M. Widersten, *J. Biotechnol.*, 2010, **147**, 169-171.

76. H. Zhao, G. A. Baker and S. Holmes, *J. Mol. Catal. B: Enzym.*, 2011, **72**, 163-167.

77. H. Zhao, G. A. Baker and S. Holmes, *Org. Biomol. Chem.*, 2011, **9**, 1908-1916.

78. B. N. Borse, V. S. Borude and S. R. Shukla, *Curr. Chem. Lett.*, 2012, **1**, 47 – 58.

79. H. G. Morrison, C. C. Sun and S. Neervannan, *Int. J. Pharm.*, 2009, **378**, 136-139.

80. E. R. Parnham, E. A. Drylie, P. S. Wheatley, A. M. Z. Slawin and R. E. Morris, *Angew. Chem., Int. Ed.*, 2006, **45**, 4962-4966.

81. C.-Y. Sheu, S.-F. Lee and K.-H. Lii, *Inorg. Chem.*, 2006, **45**, 1891-1893.

82. A. C. Martins, R. Fernandez-Felisbino and L. A. M. Ruotolo, *Microporous Mesoporous Mater.*, 2012, **149**, 55-59.

83. J.-H. Liao, P.-C. Wu and Y.-H. Bai, *Inorg. Chem. Commun.*, 2005, **8**, 390-392.

84. C.-P. Tsao, C.-Y. Sheu, N. Nguyen and K.-H. Lii, *Inorg. Chem.*, 2006, **45**, 6361-6364.

85. S.-M. Wang, W.-L. Chen, E.-B. Wang, Y.-G. Li, X.-J. Feng and L. Liu, *Inorg. Chem. Commun.*, 2010, **13**, 972-975.

86. E. R. Cooper, C. D. Andrews, P. S. Wheatley, P. B. Webb, P. Wormald and R. E. Morris, *Nature*, 2004, **430**, 1012-1016.

87. J. Zhang, T. Wu, S. M. Chen, P. Y. Feng and X. H. Bu, *Angew. Chem., Int. Ed.*, 2009, **48**, 3486-3490.

88. I. Mamajanov, A. E. Engelhart, H. D. Bean and N. V. Hud, *Angew. Chem., Int. Ed.*, 2010, **49**, 6310-6314.

89. Q. Zhang, M. Benoit, K. De Oliveira Vigier, J. Barrault and F. Jérôme, *Chem. Eur. J.*, 2012, **18**, 1043-1046.

90. H. Garcia, R. Ferreira, M. Petkovic, J. L. Ferguson, M. C. Leitao, H. Q. N. Gunaratne, K. R. Seddon, L. P. N. Rebelo and C. S. Pereira, *Green Chem.*, 2010, **12**, 367-369.

91. Y. Roman-Leshkov, C. J. Barrett, Z. Y. Liu and J. A. Dumesic, *Nature*, 2007, **447**, 982-985.

92. Y. Roman-Leshkov, J. N. Chheda and J. A. Dumesic, *Science*, 2006, **312**, 1933-1937.

93. D. Peters, *Chem. Ing. Tech.*, 2006, **78**, 229-238.

94. R. R. Schmidt and W. Kinzy, in *Adv. Carbohydr. Chem. Biochem.*, ed. H. Derek, Academic Press, 1994, vol. Volume 50, pp. 21-123.

95. J. D. Wander and D. Horton, in *Adv. Carbohydr. Chem. Biochem.*, ed. R. S. Tipson, Academic Press, 1976, vol. Volume 32, pp. 15-123.

96. M. D. Lewis, J. K. Cha and Y. Kishi, *J. Am. Chem. Soc.*, 1982, **104**, 4976-4978.

97. I. Paterson and L. E. Keown, *Tetrahedron Lett.*, 1997, **38**, 5727-5730.

98. W. Pigman, D. Horton and A. Herp, *The Carbohydrates: chemistry and biochemistry*, Academic Press, New York :, 1970.

99. R. F. Helm, J. J. Karchesy and D. F. Barofsky, *Carbohydr. Res.*, 1989, **189**, 103-112.

100. T. Naito, M. Hirata, T. Kawakami and M. Sano, *Chem. Pharm. Bull.*, 1961, **9**, 703-708.

101. *JP Pat.*, 2002-64466, 2003261591, 2003.

102. *JP Pat.*, 2003-413746, 2004203870, 2004.

103. L. Somsak, K. Czifrak, M. Toth, E. Bokor, E. D. Chrysina, K. M. Alexacou, J. M. Hayes, C. Tiraidis, E. Lazoura, D. D. Leonidas, S. E. Zographos and N. G. Oikonomakos, *Curr. Med. Chem.*, 2008, **15**, 2933-2983.

104. L. Somsák, N. Felföldi, B. Kónya, C. Hüse, K. Telepó, É. Bokor and K. Czifrák, *Carbohyd. Res.*, 2008, **343**, 2083-2093.

105. N. Felföldi, M. Tóth, E. D. Chrysina, M.-D. Charavgi, K.-M. Alexacou and L. Somsák, *Carbohydr. Res.*, 2010, **345**, 208-213.

106. N. Schoorl, *Rec. trav. chim. Pays-Bas*, 1901, **19**, 398-400.

107. N. Schoorl, *Rec. trav. chim. Pays-Bas*, 1903, **22**, 31-77.

108. M. H. Benn and A. S. Jones, *J. Chem. Soc.*, 1960, 3837-3841.

109. P. Spanu and F. Ulgheri, *Curr. Org. Chem.*, 2008, **12**, 1071-1092.

110. A. Bianchi, D. Ferrario and A. Bernardi, *Carbohydr. Res.*, 2006, **341**, 1438-1446.

111. G. Imperato, B. König and C. Chiappe, *Eur. J. Org. Chem.*, 2007, **2007**, 1049-1058.

112. D. Reinhardt, F. Ilgen, D. Kralisch, B. Konig and G. Kreisel, *Green Chem.*, 2008, **10**, 1170-1181.

113. J. P. Praly and R. U. Lemieux, *Can. J. Chem.*, 1987, **65**, 213-223.

114. E. A. M. Badawi, A. S. Jones and M. Stacey, *Tetrahedron*, 1966, **22**, 281-285.

115. M. Okahara, J. Goto and S. Komori, *Kogyo Kagaku Zasshi*, 1963, **66**, 948-952.

116. J. G. Erickson, *J. Am. Chem. Soc.*, 1954, **76**, 3977-3978.

117. D. Plusquellec, F. Roulleau, M. Lefeuvre and E. Brown, *Tetrahedron*, 1990, **46**, 465-474.

118. D. Wells and C. J. Drummond, *Langmuir*, 1999, **15**, 4713-4721.

119. D. Wells, C. Fong and C. J. Drummond, *J. Phys. Chem. B*, 2006, **110**, 12660-12665.

120. B. Helferich and W. Portz, *Chem. Ber.*, 1953, **86**, 604-612.

121. A. G. Sarap and S. P. Deshmukh, *Int. J. Chem. Sci.*, 2009, **7**, 2389-2397.

122. B. B. Kehm and C. W. Whitehead, *Org. Synth.*, 1957, **37**, 52.

123. F. W. Lichtenthaler and S. Mondel, *Pure Appl. Chem.*, 1997, **69**, 1853-1866.

124. J. N. Chheda, G. W. Huber and J. A. Dumesic, *Angew. Chem. Int. Ed.*, 2007, **46**, 7164-7183.

125. J. J. Bozell and G. R. Petersen, *Green Chem.*, 2010, **12**, 539-554.

126. M. J. Antal, W. S. L. Mok and G. N. Richards, *Carbohydr. Res.*, 1990, **199**, 91-109.

127. *EP 1062941 A2 Pat.*, 2000-112968, 1062941, 2000.

128. A. S. Lin, K. Qian, Y. Usami, L. Lin, H. Itokawa, C. Hsu, S. L. Morris-Natschke and K. H. Lee, *J. Nat. Med.*, 2008, **62**, 164-167.

129. D. P. Adhikari, R. E. Schutzki, D. L. DeWitt and M. G. Nair, *Food Chem.*, 2006, **97**, 56-64.

130. T. Urashima, K. Suyama and S. Adachi, *Food Chem.*, 1988, **29**, 7-17.

131. F. W. Lichtenthaler, D. Martin, T. Weber and H. Schiweck, *Liebigs Ann. Chem.*, 1993, **1993**, 967-974.

132. *Germany Pat.*, EP 0 426 176 A2, 1991.

133. H. Schiweck, M. Munir, K. M. Rapp, B. Schneider and M. Vogel, *Zuckerind. (Berlin)*, 1990, **115**, 555-565.

134. M. Avalos, R. Babiano, P. Cintas, J. L. Jiménez and J. C. Palacios, *Angew. Chem. Int. Ed.*, 2006, **45**, 3904-3908.

135. C. Russ, F. Ilgen, C. Reil, C. Luff, A. Haji Begli and B. Koenig, *Green Chem.*, 2011, **13**, 156- 161.

136. S. Hu, Z. Zhang, Y. Zhou, J. Song, H. Fan and B. Han, *Green Chem.*, 2009, **11**, 873-877.

137. B. F. M. Kuster, *Starch - Stärke*, 1990, **42**, 314-321.

138. F. W. Lichtenthaler and S. Ronninger, *J. Chem. Soc., Perkin Trans. 2*, 1990.

139. I. Zebiri, S. Balieu, A. Guilleret, R. Reynaud and A. Haudrechy, *Eur. J. Org. Chem.*, 2011, 2905-2910.

140. F. W. Lichtenthaler, *Carbohydr. Res.*, 1998, **313**, 69-89.

141. S. J. Angyal, *Adv. Carbohydr. Chem. Biochem.*, 1984, **42**, 15-68.

142. B. Schneider, F. W. Lichtenthaler, G. Steinle and H. Schiweck, *Liebigs Ann. Chem.*, 1985, **1985**, 2443-2453.

143. K. Tokuyama and M. Katsuhara, *Bull. Chem. Soc. Jpn.*, 1966, **39**, 2728-2733.

144. GB600871, 1948.

145. K. Seri, Y. Inoue and H. Ishida, *Chem. Lett.*, 2000, 22-23.

146. F. Salak Asghari and H. Yoshida, *Ind. Eng. Chem. Res.*, 2006, **45**, 2163-2173.

147. A. A. Rosatella, S. P. Simeonov, R. F. M. Frade and C. A. M. Afonso, *Green Chem.*, 2011, **13**, 754-793.

148. X. Tong, Y. Ma and Y. Li, *Appl. Catal. A-Gen.*, 2010, **385**, 1-13.

149. C. Carlini, P. Patrono, A. M. R. Galletti and G. Sbrana, *Appl. Catal. A-Gen.*, 2004, **275**, 111-118.

150. B. König, W. Kunz and O. Reiser, *Blick in die Wissenschaft*, 2011, **23**, 39-46.

151. S. Gore, S. Baskaran and B. Koenig, *Green Chem.*, 2011, **13**, 1009-1013.

152. G. M. Boyle, *Expert Rev. Anticanc.*, **11**, 725-737.

153. R. Abe, Y. Fujita and S.-i. Yamagishi, *Mini Rev. Med. Chem.*, 2007, **7**, 649-661.

154. A. K. Bosserhoff, *Pigm. Cell. Res.*, 2005, **18**, 411-416.

155. A.-K. Bosserhoff, eds. V. J. Hearing and S. P. L. Leong, Humana Press, 2006, pp. 475-487.

156. A. K. Bosserhoff, M. Kaufmann, B. Kaluza, I. Bartke, H. Zirngibl, R. Hein, W. Stolz and R. Buettner, *Cancer Res.*, 1997, **57**, 3149-3153.

157. A. Blesch, A. K. Bosserhoff, R. Apfel, C. Behl, B. Hessdoerfer, A. Schmitt, P. Jachimczak, F. Lottspeich, R. Buettner and U. Bogdahn, *Cancer Res.*, 1994, **54**, 5695-5701.

158. R. Bauer, M. Humphries, R. Fässler, A. Winklmeier, S. E. Craig and A.-K. Bosserhoff, *J. Biol. Chem.*, 2006, **281**, 11669-11677.

159. A.-K. Bosserhoff and V. J. Hearing, *From Melanocytes to Melanoma: The Progression to Malignancy*, 2006, 475-487.

160. R. Stoll, C. Renner, M. Zweckstetter, M. Brüggert, D. Ambrosius, S. Palme, R. A. Engh, M. Golob, I. Breibach, R. Buettner, W. Voelter, T. A. Holak and A.-K. Bosserhoff, *EMBO J.*, 2001, **20**, 340-349.

161. R. Stoll, C. Renner, R. Buettner, W. Voelter, A. K. Bosserhoff and T. A. Holak, *Protein Sci.*, 2003, **12**, 510-519.

162. R. Stoll and A. Bosserhoff, *Curr. Protein Pept. Sci.*, 2008, **9**, 221-226.

163. R. Stoll, C. Renner, D. Ambrosius, M. Golob, W. Voelter, R. Buettner, A. K. Bosserhoff and T. A. Holak, *J. Biomol. NMR*, 2000, **17**, 87-88.

164. J. C. Lougheed, J. M. Holton, T. Alber, J. F. Bazan and T. M. Handel, *P. Natl. Acad. Sci.*, 2001, **98**, 5515-5520.

165. WO 2011113604 (A1), 2011.

166. J. Schmidt, A. Riechers, R. Stoll, T. Amann, F. Fink, T. Spruss, W. Gronwald, B. Koenig, C. Hellerbrand and A. K. Bosserhoff, *PLoS ONE*, 2012, **7**, 37941.

167. A. Riechers, PhD Thesis, University of Regensburg 2010.

168. J. Schmidt, PhD Thesis, University of Regensburg 2010.

169. Z. Xin Hua, *J. Controlled Release*, 1994, **29**, 239-252.

170. V. R. Sinha and A. Trehan, *J. Controlled Release*, 2003, **90**, 261-280.

171. K. K. Jain, in *Methods in Molecular Biology*, ed. K. K. Jain, Humana Press Inc, 999 Riverview Dr, Ste 208, Totowa, Nj 07512-1165 USA, 2008, vol. 437, pp. 1-50.

172. L. R. Brown, *Expert Opin. Drug Del.*, 2005, **2**, 29-42.

173. J. Gante, *Angew. Chem. Int. Ed. Engl.*, 1994, **33**, 1699-1720.

174. A. Giannis and T. Kolter, *Angew. Chem.*, 1993, **105**, 1303-1326.

175. P. Cudic and M. Stawikowski, in *Methods in Molecular Biology*, ed. L. Otvos, Humana Press Inc, 2008, pp. 223-246.

176. A. F. M. Goodman, L. Moroder, C. Toniolo, *Synthesis of Peptides and Peptidomimetics*, Thieme Verlag, Stuttgart, New York, 2003.

177. J. Chatterjee, C. Gilon, A. Hoffman and H. Kessler, *Acc. Chem. Res.*, 2008, **41**, 1331-1342.

178. M. Teixidó, F. Albericio and E. Giralt, *The Journal of Peptide Research*, 2005, **65**, 153-166.

179. H. Kessler, *Angew. Chem. Int. Ed. Engl.*, 1970, **9**, 219-235.

180. K. Eller, E. Henkes, R. Rossbacher and H. Höke, in *Ullmann's Encyclopedia of Industrial Chemistry*, Wiley-VCH Verlag GmbH & Co. KGaA, 2000.

181. E. Biron, J. Chatterjee and H. Kessler, *J. Pept. Sci.*, 2006, **12**, 213-219.

182. S. C. Miller and T. S. Scanlan, *J. Am. Chem. Soc.*, 1997, **119**, 2301-2302.

183. R. N. Zuckermann, J. M. Kerr, S. B. H. Kent and W. H. Moos, *J. Am. Chem. Soc.*, 1992, **114**, 10646-10647.

184. C. W. Wu, T. J. Sanborn, K. Huang, R. N. Zuckermann and A. E. Barron, *J. Am. Chem. Soc.*, 2001, **123**, 6778-6784.

185. P. A. Wender, D. J. Mitchell, K. Pattabiraman, E. T. Pelkey, L. Steinman and J. B. Rothbard, *P. Natl. Acad. Sci.*, 2000, **97**, 13003-13008.

186. Y.-U. Kwon and T. Kodadek, *J. Am. Chem. Soc.*, 2007, **129**, 1508-1509.

187. S. M. Miller, R. J. Simon, S. Ng, R. N. Zuckermann, J. M. Kerr and W. H. Moos, *Drug Dev. Res.*, 1995, **35**, 20-32.

188. S. M. Miller, R. J. Simon, S. Ng, R. N. Zuckermann, J. M. Kerr and W. H. Moos, *Bioorg. Med. Chem. Lett.*, 1994, **4**, 2657-2662.

189. C. M. Madsen and M. H. Clausen, *Eur. J. Org. Chem.*, 2011, 3107-3115.

190. E. M. Driggers, S. P. Hale, J. Lee and N. K. Terrett, *Nat Rev Drug Discov*, 2008, **7**, 608-624.

191. C. J. White and A. K. Yudin, *Nat. Chem.*, 2011, **3**, 509-524.

192. O. Demmer, A. O. Frank and H. Kessler, in *Peptide and Protein Design for Biopharmaceutical Applications*, John Wiley & Sons, Ltd, 2009, pp. 133-176.

193. C. A. Lipinski, F. Lombardo, B. W. Dominy and P. J. Feeney, *Adv. Drug Deliv. Rev.*, 2001, **46**, 3-26.

194. M. Katsara, T. Tselios, S. Deraos, G. Deraos, M. T. Matsoukas, E. Lazoura, J. Matsoukas and V. Apostolopoulos, *Curr. Med. Chem.*, 2006, **13**, 2221-2232.

195. S. A. Kates, N. A. Solé, C. R. Johnson, D. Hudson, G. Barany and F. Albericio, *Tetrahedron Lett.*, 1993, **34**, 1549-1552.

196. M. Dessolin, M. G. Guillerez, N. Thieriet, F. Guibe and A. Loffet, *Tetrahedron Lett.*, 1995, **36**, 5741-5744.

197. R. Shi, F. Wang and B. Yan, *Int. J. Pept. Res. Ther.*, 2007, **13**, 213-219.

198. M. C. Alcaro, G. Sabatino, J. Uziel, M. Chelli, M. Ginanneschi, P. Rovero and A. M. Papini, *J. Pept. Sci.*, 2004, **10**, 218-228.

199. H. Wissmann and H.-J. Kleiner, *Angew. Chem. Int. Ed. Engl.*, 1980, **19**, 133-134.

200. J. R. Dunetz, Y. Xiang, A. Baldwin and J. Ringling, *Org. Lett.*, 2011, **13**, 5048-5051.

201. EP962465A1, 1999.

202. A. Riechers, J. Schmidt, B. Koenig and A. K. Bosserhoff, *BioTechniques*, 2009, **47**, 837-838, 840, 842, 844.

203. J. R. Lakowicz, ed. J. R. Lakowicz, Springer US, 2006, pp. 353-382.

204. O. Keskin, B. Ma and R. Nussinov, *J. Mol. Biol.*, 2005, **345**, 1281-1294.

205. M. R. Arkin and J. A. Wells, *Nat Rev Drug Discov*, 2004, **3**, 301-317.

206. S. Jones and J. M. Thornton, *Prog. Biophys. Mol. Biol.*, 1995, **63**, 31-65.

207. C.-J. Tsai, S. L. Lin, H. J. Wolfson and R. Nussinov, *Protein Sci.*, 1997, **6**, 53-64.

208. A. A. Bogan and K. S. Thorn, *J. Mol. Biol.*, 1998, **280**, 1-9.

209. D. Xu, C. J. Tsai and R. Nussinov, *Protein Eng.*, 1997, **10**, 999-1012.

210. M. Quintanar-Audelo, A. Fernández-Carvajal, W. Van Den Nest, C. Carreño, A. Ferrer-Montiel and F. Albericio, *J. Med. Chem.*, 2007, **50**, 6133-6143.

211. F. Schmidt, I. C. Rosnizeck, M. Spoerner, H. R. Kalbitzer and B. König, *Inorg. Chim. Acta*, 2011, **365**, 38-48.

212. M. E. Attardi, G. Porcu and M. Taddei, *Tetrahedron Lett.*, 2000, **41**, 7391-7394.

213. R. B. Greenwald, *J. Controlled Release*, 2001, **74**, 159-171.

214. F. M. Veronese, *Biomaterials*, 2001, **22**, 405-417.

215. S. Zalipsky, *Adv. Drug Deliv. Rev.*, 1995, **16**, 157-182.

216. M. J. Roberts, M. D. Bentley and J. M. Harris, *Adv. Drug Deliv. Rev.*, 2002, **54**, 459-476.

217. F. M. Veronese and G. Pasut, *Drug Discovery Today*, 2005, **10**, 1451-1458.

218. D. S. Pisal, M. P. Kosloski and S. V. Balu-Iyer, *J. Pharm. Sci.*, 2010, **99**, 2557-2575.

219. C. S. Fishburn, *J. Pharm. Sci.*, 2008, **97**, 4167-4183.

220. M. Mutter, R. Uhmann and E. Bayer, *Liebigs Ann. Chem.*, 1975, 901-915.

221. C. S. Hughes, L. M. Postovit and G. A. Lajoie, *Proteomics*, 2010, **10**, 1886-1890.

222. A. Albini, Y. Iwamoto, H. K. Kleinman, G. R. Martin, S. A. Aaronson, J. M. Kozlowski and R. N. McEwan, *Cancer Res.*, 1987, **47**, 3239-3245.

223. V. P. Terranova, E. S. Hujanen, D. M. Loeb, G. R. Martin, L. Thornburg and V. Glushko, *P. Natl. Acad. Sci.*, 1986, **83**, 465-469.

224. A.-K. Bosserhoff, R. Stoll, J. P. Sleeman, F. Bataille, R. Buettner and T. A. Holak, *Lab Invest*, 2003, **83**, 1583-1594.

225. F. M. Veronese, A. Mero and G. Pasut, ed. F. M. Veronese, Birkhäuser Basel, 2009, pp. 11-31.

226. M. C. Manning, K. Patel and R. T. Borchardt, *Pharm. Res.*, 1989, **6**, 903-918.

227. W. Wei, *Int. J. Pharm.*, 1999, **185**, 129-188.

228. M. Rawat, D. Singh and S. Saraf, *Yakugaku Zasshi-J. Pharm. Soc. Jpn.*, 2008, **128**, 269-280.

229. A. Zaky, A. Elbakry, A. Ehmer, M. Breunig and A. Goepferich, *J. Controlled Release*, 2010, **147**, 202-210.

230. S. Koennings, A. Sapin, T. Blunk, P. Menei and A. Goepferich, *J. Controlled Release*, 2007, **119**, 163-172.

231. M. A. Sheridan, J. D. Kittilson and B. J. Slagter, *Am. Zool.*, 2000, **40**, 269-286.

232. S. Herrmann, S. Mohl, F. Siepmann, J. Siepmann and G. Winter, *Pharm. Res.*, 2007, **24**, 1527-1537.

233. X. Huang and C. S. Brazel, *J. Controlled Release*, 2001, **73**, 121-136.

234. S. Gaisser and M. Nusser, *Zeitschrift fur Evidenz, Fortbildung und Qualitat im Gesundheitswesen*, 2010, **104**, 732-737.

235. S. Frokjaer and D. E. Otzen, *Nat Rev Drug Discov*, 2005, **4**, 298-306.

236. N. A. Peppas, P. Bures, W. Leobandung and H. Ichikawa, *Eur. J. Pharm. Biopharm.*, 2000, **50**, 27-46.

237. F. Ganji and E. Vasheghani-Farahani, *Iran. Polym. J.*, 2009, **18**, 63-88.

238. T. R. Hoare and D. S. Kohane, *Polymer*, 2008, **49**, 1993-2007.

239. K. Y. Lee and D. J. Mooney, *Prog. Polym. Sci.*, 2012, **37**, 106-126.

240. F. Brandl, F. Kastner, R. M. Gschwind, T. Blunk, J. Tessmar and A. Gopferich, *J. Controlled Release*, 2010, **142**, 221-228.

241. F. Brandl, M. Henke, S. Rothschenk, R. Gschwind, M. Breunig, T. Blunk, J. Tessmar and A. Gopferich, *Adv. Eng. Mater.*, 2007, **9**, 1141-1149.

III. APPENDIX

14. Abbreviations

Ac	acetyl
AcOH	acetic acid
Ac_2O	acetic anhydride
AS	ammonium salt
ATR	attenuated total reflectance
BCIP	5-bromo-4-chloro-3-indolyl phosphate
BDNF	brain-derived neurotrophic factor
[Bmim]	1-butyl-3-methylimidazolium
[BMmorf]	4-benzyl-4-methylmorpholinium
Boc	t-butyloxycarbonyl
bpy	2,2′-bipyridine
BSA	bovine serum albumine
c	speed of light
Ch	choline
ChCl	choline chloride
cP	centiPoise
C_p	molar heat capacity
DAD	diode array detector
DCM	dichloromethane
DEAD	diethyl azodicarboxylate
DES	deep eutectic solvent
DIC	*N*,*N*'-diisopropylcarbodiimide
DIPEA	diisopropylethylamine
DMAP	dimethylaminopyridine
DMEM	dulbecco's modified eagle medium
DMF	dimethylformamid
DMSO	dimethylsulfoxide
DMU	1,3-dimethylurea
DPBS	dulbecco's phosphate buffered saline

ECM	extracellular matrix
[Emim]	1-ethyl-3-methylimidazolium
ELSD	evaporative light scattering detector
Et_2O	diethylether
EtOAc	ethylacetate
Eq	equivalent
Eqn	equation
EtOH	ethanol
ESI	electronic spray ionisation
FCS	fetal calf serum
FDA	U.S. food and drug administration
FLD	fluorescence detector
Fmoc	fluorenylmethoxycarbonyl
FT	fourier transformed
GMF	5-(α-D-glucosyloxymethyl)furfural
h	Planck's constant
HATU	2-(7-aza-1*H*-benzotriazole-1-yl)-1,1,3,3-tetramethyluronium hexafluorophosphate
HBD	hydrogen bond donor
HBTU	2-(1*H*-benzotriazole-1-yl)-1,1,3,3-tetramethyluronium hexafluorophosphate
HMF	5-hydroxymethylfurfural
HOAt	1-hydroxy-7-azabenzotriazole
HOBt	hydroxybenzotriazole
HPLC	high performance liquid chromatography
HTFP	heterogeneous transition metal-based fluorescence polarization
IL	ionic liquid
IR	infrared spectroscopy
i.v.	intravenous
J	coupling constant
LC/MS	liquid chromatography/mass spectrometry

LSI/MS	liquid secondary ion mass spectrometry
MBHA	4-methylbenzhydrylamine
Me	methyl
MeCN	acetonitrile
MeOH	methanol
MIA	melanoma inhibitory activity
MP	melting point
MS	mass spectrometry
Mtt	4-metyltrityl
ν_{max}	wave number of absorption maximum
N_A	Avogadro's constant
NBT	nitro blue tetrazolium
NBS	nitrobenzenesulfonyl chloride
NEt_3	triethylamine
NMM	*N*-methylmorpholine
NMP	*N*-methyl-2-pyrrolidone
NMR	nuclear magnetic resonance
NOE	nuclear overhauser effect
NOESY	nuclear overhauser effect spectroscopy
NR	nile red
OAll	allyl ether
Pbf	2,2,4,6,7- pentamethyldihydrobenzofuran-5-sulfonyl
PBS	phosphate buffered saline
PDI	polydispersity index
PE	petroleum ether
PEG	poly(ethylene glycol)
PVDF	polyvinylidene fluoride
p-TsOH	para-toluene sulfonic acid
ϱ	density
RES	reticuloendothelial system
rt	room temperature

R_t	retention time
SDS-PAGE	sodium dodecylsulfate polyacrylamide gel electrophoresis
σ	conductivity
TBTU	*O*-(benzotriazole-1-yl)-*N*,*N*,*N*′,*N*′-tetramethyluronium tetrafluoroborate
tBu	tert.-butyl
T_f	freezing point/temperature
T_g	glass transition temperature
THF	tetrahydrofurane
TIS	triisopropylsilane
TFA	trifluoroacetic acid
TLC	thin layer chromatography
T_m	melting point/temperature
TOF	time of flight
UV	ultraviolet
wt%	weight percent

Amino acids

A	Ala	Alanine	M	Met	Methionine
C	Cys	Cysteine	N	Asn	Asparagine
D	Asp	Aspartic acid	P	Pro	Proline
E	Glu	Glutamic acid	Q	Gln	Glutamine
F	Phe	Phenylalanine	R	Arg	Arginine
G	Gly	Glycine	S	Ser	Serine
H	His	Histidine	T	Thr	Threonine
I	Ile	Isoleucine	V	Val	Valine
K	Lys	Lysine	W	Trp	Tryptophan
L	Leu	Leucine	Y	Tyr	Tyrosine

15. List of Publications

Poster Presentations

C. Ruß, F. Ilgen, B. König, B. "Sweet Solvents – Sustainable Carbohydrate Melts as Non-toxic Reaction Media", 3rd EuCheMS Chemistry Congress, Nürnberg 2010

C. Ruß, F. Ilgen, B. König, B. "Sweet Solvents – Sustainable Carbohydrate Melts as Non-toxic Reaction Media", EUCHEM Conference on Molten Salts and Ionic Liquids, Bamberg 2010

C. Ruß, F. Ilgen, B. König, B. "Chemically catalyzed conversion of carbohydrates in solvent-free systems", GDCh Wissenschaftsforum Chemie, Frankfurt/Main 2009

Oral Presentations

C. Ruß, F. Ilgen, B. König, B. „Sweet Chemistry – Conversion of Carbohydrates in Sustainable Melts", GDCh Wissenschaftsforum Chemie, Bremen 2011.

Publications

C. Ruß, F. Ilgen, C. Reil, C. Luff, A. Haji Begli, B. König

"Efficient preparation of β-D-glucosyl and β-D-mannosyl ureas and other *N*-glucosides in carbohydrate melts" *Green Chem.*, **2011**, *13*, 156-161.

C. Ruß, C. Luff, A. Haji Begli, B. König

"Solvent-free preparation of 5-(α-D-glucosyloxymethyl)furfural from isomaltulose - choline chloride melts" *Synth. Commun.*, **2012**, *42*, 1-5.

C. Ruß, B. König

„Süße Chemie zum Dahinschmelzen", GIT Labor Fachz., **2011**, *55*, (12), 836-837.

C. Ruß, B. König

„Low melting mixtures – the „greener" ionic liquids?" invited review, *Green Chem.*, **2012**, *submitted*.

C. Ruß, A. Haji Begli, B. König

"Condensation and dehydration reactions of L-sorbose in eco-friendly melt systems" *Synth. Commun.*, **2012,** *accepted.*

16. Curriculum Vitae

Carolin Ruß

*15.08.1983, Schweinfurt

Education

06/2008-07/2012	Dissertation „ Conversion of Carbohydrates in Low Melting Mixtures and Melanoma Inhibitory Activity (MIA) Protein Inhibitors for the Treatment of Malignant Melanoma “, University of Regensburg
04/2007-03/2008	Diploma Thesis „Biodegradable Polyethyleneglycol-Polyethylenimine Copolymers for Gene Delivery”, University of Regensburg
10/2005-03/2008	Studies of Medicinal Chemistry, University of Regensburg (Diploma in Chemistry)
10/2002-09/2005	Studies of Molecular Life Sciences, University of Erlangen-Nuremberg Bachelor Thesis “Synthese und Rezeptorbindungsstudien von N-(4-(4-(Pyrimidin-2-yl)piperazin-1-yl)butyl)benzo[*b*]thiophen-3-carboxamid als potentieller 5-HT_{1A}-Ligand“ (B. Sc.)

Teaching Experience

2008-2012	Teaching assistant in laboratory courses for chemistry, biology and biochemistry, supervisor of teaching students during the final thesis.

17. Danksagung

An dieser Stelle möchte ich mich bei allen bedanken, die direkt und indirekt zum Gelingen dieser Arbeit beigetragen haben.

Ich danke meinem Betreuer Herrn Prof. Dr. Burkhard König für die Bereitstellung der spannenden und vielseitigen Themen. Seine hilfreichen Tipps und Anregungen, sowie zahlreiche Diskussionen haben maßgeblichen Anteil an dieser Arbeit.

Weiterhin danke ich Herrn Prof. Dr. Achim Göpferich für die freundliche Übernahme des Amts des Zweitgutachters und die Unterstützung und Expertise bei der Entwicklung von Trägersystemen von Arzneistoffen.

Der Südzucker AG danke ich für die Finanzierung des Zuckprojekts und für die Bereitstellung von Chemikalien. Mein spezieller Dank geht an meinen Ansprechpartner dort, Herrn Dr. Alireza Haji Begli, für gute Ideen, die schnelle Begutachtung der Publikationen und die sehr angenehme und unkomplizierte Arbeitsatmosphäre.

Großen Dank schulde ich meinen Kooperationspartnern am Institut für Molekulare Pathologie in Regensburg, Frau Prof. Dr. Anja Katrin Boßerhoff und Dr. Alexander Riechers für die gute Zusammenarbeit im MIA Projekt. Ganz besonders möchte ich mich hiermit bei Dr. Alexander Riechers bedanken, der sehr viel zum Verlauf des Projektes beigetragen hat und der mich geduldig an das komplexe Thema herangeführt hat. Außerdem sage ich danke für die sehr schnelle Testung der Verbindungen (HTFP, Western Blot usw) und für die Bereitstellung von Peptiden für die Freisetzungsversuche.

Mein Dank gilt Dr. Rudolf Vasold für zahlreiche HPLC-Analysen, Simone Strauß für die zeitintensive Aufreinigung verschiedener Verbindungen mittels präparativer HPLC.

Den Mitarbeitern der zentralen Analytik danke ich für schnelle und zuverlässige Durchführung der analytischen Messungen: Fritz Kastner, Annette Schramm, Georgine Stühler und Dr. Thomas Burgemeister für die Aufnahme von NMR-Spektren

und Josef Kiermeier, Wolfgang Söllner und Carola Prockl für die Messung und Auswertung von Massenspektren und hilfreiche Diskussionen.
Am Lehrstuhl für Pharmazeutische Technologie möchte ich mich bei Angelika Berié für die Herstellung des Implantats und Susanne Kirchhof für die reibungslose Kooperation bei den Freisetzungsversuchen bedanken. Außerdem sage ich Danke für die Benutzung der HPLC und den Status als assoziierte Ehemalige.

Dem Arbeitskreis von Prof. Dr. Oliver Reiser und seinen Mitarbeitern danke ich für die Möglichkeit, das IR-Spektrometer und das Polarimeter zu nutzen.

Bei Britta Badziura, Regina Hoheisel, Ernst Lautenschlager, Elisabeth Liebl und Anke-Susanne Schulze und bedanke ich mich für ihre Unterstützung bei der Chemikalienbestellung und organisatorischen Angelegenheiten.

Meinem Forschungspraktikanten Roland Linhardt und Claudia Luff danke ich für die Mitarbeit und Unterstützung in den Projekten.

Ich danke den Mitarbeitern des AK König:
- dem zauberhaften Dr. Florian Ilgen für die Einarbeitung ins Zuckerthema, Überlassung der Glucosylharnstoffe und inspirirende Gespräche außerhalb der Chemie.
- meinen Laborkollegen Agnes Palmberger, Dr. Muruganantham Rajendran, Peter Raster, Peter Schroll, Sangram Gore, Claudia Luff, Natascha Kuzmanović, Andreas Müller, Manuel Bause für die unzähligen gemeinsamen Stunden im Labor, die sie durch ihre Anwesenheit aufgewertet und erheitert haben.

Mein besonderer Dank geht an Andi Müller für „frängische Momende“, aufrichtiges und geduldiges Zuhören, wertvolle Ratschläge und das richtige Maß an Ordnung; Manuel Bause für das Organisieren von Papern und die angenehme Zeit im KombiChem Praktikum; Peter Raster für seine etwas andere Sicht auf die Welt.
- allen Teilnehmern an Tagungen (Carolin Fischer., Dr. Robert „Robbl“ Lechner, Benjamin „Benno“ Gruber, Josef Herrmann, Natascha Kuzmanović, Susanne Kümmel, Andreas Hohenleutner, Susanna Schmidbauer, Cristian Ochoa-Puentes) für unvergessliche Momente und die schöne gemeinsame Zeit in Frankfurt, Nürnberg und Bremen.

- allen ehemaligen und aktuellen Mitarbeitern während der letzten vier Jahre, die beim Skifahren dabei waren, viele „Kabinenparties“, Hüttenabende, eine fantastische Königsseewanderung, Friday Lunch, Feiern an der Uni, gemütliches Kaffee und Bier trinken oder einen kurzen Plausch auf dem Gang.
Danke für ein äußerst kollegiales Arbeitsklima zum Wohlfühlen! Ihr seid die Besten!

- allen, denen ich auch über die Arbeit hinaus im Herzen verbunden bin, für Dampfablassen, gegenseitiges Zuhören und Motivieren: Sanne ,Tascha, Andi H., Susa, Josef, Benno, Michl, Andi M., Caro, Robbl, Flo Schmidt.

- der ursprünglichen Mittagsgruppe: Dr. Christopher „Günni“ Rose, Dr. Dominik „Gregor“ Grögel und Dr. Carolin Fischer für eine erfrischende Mittagspause. Ebenso der „neuen“ Mittagsgruppe: Manuel Achatz, Thomas „Horst“ Lang, Dr. Beatriz López, Dr. Stefanie Michaelis und Dr. Judith Stolwijk.

Ich danke meinen Korrekturlesern Dr. Ferdinand Brandl, Natascha Kuzmanović, Andreas Müller und Dr. Alexander Riechers für Adleraugen und hilfreiche Verbesserungsvorschläge.

Dr. Ferdinand Brandl für alles!

Allen meinen Freunden und Kollegen, die hier nicht namentlich erwähnt sind, die mich während des Studiums und der Doktorarbeit begleitet und unterstützt haben und mich das Leben außerhalb der Arbeit nicht haben vergessen lassen.

Meiner Familie, meinen Eltern und Geschwistern, für bedingungslosen Rückhalt, unterstützende und aufbauende Worte während der letzten, sehr anstrengenden Jahre. Danke, dass ihr immer für mich da wart (und seid) und für einen Ort zum Entspannen und Energie tanken.